2012

Ambient Geochemical and Isotopic Variations in Groundwaters Across an Area of Accelerating Shale Gas Development

Michon L. Mulder
West Virginia University

Ambient Geochemical and Isotopic Variations in Groundwaters Across an Area of Accelerating Shale Gas Development

Michon L. Mulder

Thesis submitted to the Eberly College of Arts and Sciences
at West Virginia University
in partial fulfillment of the requirements
for the degree of

Master of Science
in
Geology

Shikha Sharma, Ph.D., Chair
Tim Carr, Ph.D.
Doug Chambers

Department of Geology & Geography

Morgantown, West Virginia
2012

Keywords: Isotope; Geochemistry; Groundwater; West Virginia

ABSTRACT

Ambient Geochemical and Isotopic Variations in Groundwaters Across an Area of Accelerating Shale Gas Development

Michon L. Mulder

One of the main challenges associated with Marcellus Formation shale gas development is to ensure proper management and disposal of flowback water produced as a result of hydraulic fracturing of gas wells. The flowback water consists of a mixture of returned frac'ing fluids and highly saline formation brines. As a result, improper management or disposal of this flowback can potentially contaminate the fresh surface waters and groundwaters of the area. To better assess any detrimental effect on water quality, there is need to understand the natural geochemical variations prior to the rapid expansion of gas drilling in the area.

This study focuses on documenting the baseline geochemical characteristics of groundwaters in different formations lying stratigraphically above the Marcellus Formation. 41 groundwater well sites in north central West Virginia were sampled with the USGS Water Science Center of West Virginia. These private and public sampling locations were chosen from within the United States Geological Survey database and represent different formation aquifers with differing well depths. Geochemical data was obtained for major cations and anions, dissolved gas concentrations of methane, oxygen and hydrogen isotopic compositions of water ($\delta^{18}O_{H2O}$ and $\delta^{2}H_{H2O}$), carbon isotopic compositions of dissolved inorganic carbon ($\delta^{13}C_{DIC}$), sulfur and oxygen isotope compositions of dissolved sulfate ($\delta^{34}S_{SO4}$ and $\delta^{18}O_{SO4}$) and carbon and hydrogen isotope compositions of dissolved methane ($\delta^{13}C_{CH4}$ and $\delta^{2}H_{CH4}$). Field parameters of temperature, conductivity, pH, dissolved oxygen, turbidity, and oxidation reduction potential were also collected. I hypothesize that the baseline variations of stable isotopes can be used in conjunction with other geochemical parameters to identify groundwater aquifers that have received significant contribution from frac flowback waters.

ACKNOWLEDGMENTS

I would like to thank my thesis advisor, Dr. Sharma, whose background and past research, in conjunction with her patience and commitment, made this study conceivable. I would also like to thank the members of my thesis committee, Dr. Tim Carr and Doug Chambers, whose diverse backgrounds provided valuable comments and expertise throughout this study. This research was funded through the USGS 104b grant provided to Dr. Sharma through the West Virginia Water Research Institute.

Over 8 weeks of field work was necessary to accomplish this research, across many miles and hours of waiting for wells to purge. Thankfully, this was not only the most fun and entertaining time I've spent in the field, but a beneficial and knowledgeable experience. This was through the collaboration with Jeremy White and Katherine Paybins of the USGS West Virginia Water Science Center. Their cooperation and resources in field sampling and site access aided this research invaluably.

Lastly, completing this work and analysis and receiving my M.S. within 2 years was only possible through the support of my family and friends across 1000+ miles. Additionally, my priceless friendship with Andrea Sack, established through months of stress and countless hours in lab and the office together, was the necessary support to finish my bold endeavors.

Trust me – it's not as easy as it looks.

Michon L. Mulder

West Virginia University

April, 2012

TABLE OF CONTENTS

LIST OF FIGURES

LIST OF TABLES

LIST OF MAJOR EQUATIONS

1.0 – Study Introduction and Objectives

1.1 – The Marcellus Formation and Natural Gas

Natural gas accounts for 25% of the total energy consumed within the United States and is rapidly increasing; half of that came from new wells drilled within the last 3.5 years (DOE, 2009). The gas reserves can be classified as conventional or unconventional. Gas underlying impermeable rock layers in conventional reserves is released through vertical drilling, where pore migration allows the gas to travel to the surface. Unconventional gas reserves are formations where the rock unit is not permeable enough for the gas to escape readily. These reserves include tight sand gases, coalbed methane, methane hydrates, and shale gas. The difference between the natural gas usage and availability is estimated to be 9 trillion cubic feet (tcf) by 2025, (DOE, 2009). As a result, focus has begun to shift away from the current conventional gas reserves and towards exploration within the onshore unconventional reserves (Figure 1). Within the last ten years, the production demand for natural gas from unconventional reserves has grown 65%, with nearly a 50% reduction from conventional reserves (Arthur et al., 2008). The current and forthcoming shale gas plays include the Antrim, Barnett, Fayetteville, Haynesville/Bossier, Marcellus Formation, and New Albany Shale.

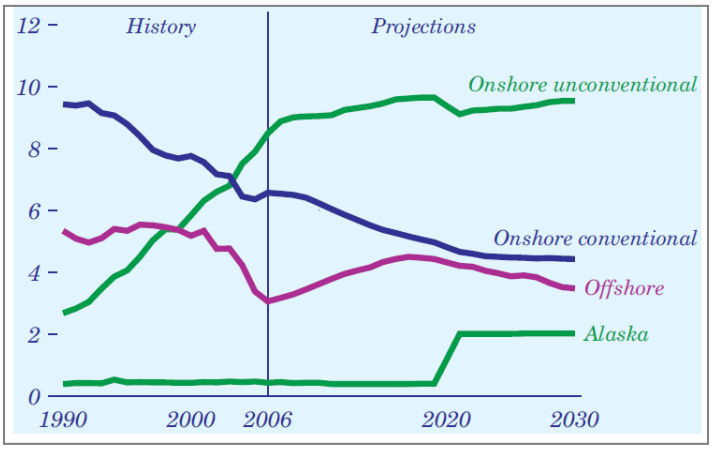

Figure 1: Projected rise of unconventional natural gas (DOE, 2008)

One of the largest natural gas reserves is the Marcellus Formation, covering an area of over 24,000 square kilometers over six states in the northeastern part of the country (Figure 2). This shale has depths ranging from 4,000 to 8,500 feet with thicknesses between 50 and 200 feet (Andrews et al., 2009). The natural gas within the 350 million year old, organic-rich black shale is the result of compression, high temperatures, and time (E&P, 2009; Soeder et al, 2011). The low permeability and 10% porosity requires unconventional methods to access the natural gas and allow it to migrate (DOE, 2009, Hazen and Sawyer, 2009).

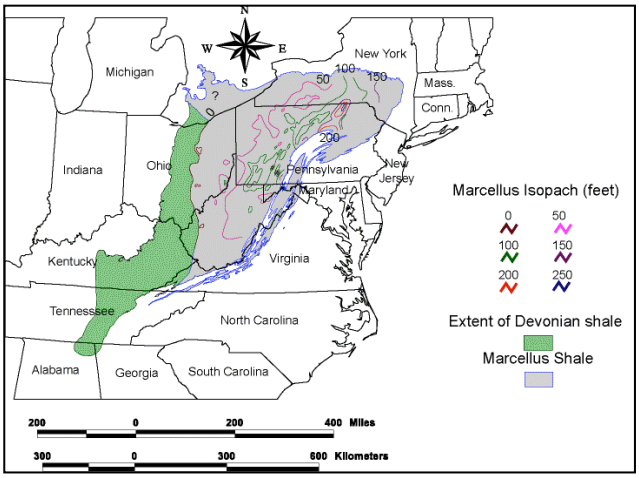

Figure 2: Marcellus Formation isopach boundaries (DOE et al, 2009)

Unconventional drilling through hydraulic fracturing could recover an estimated 363 tcf of natural gas, enough to supply the United States for 15 years according to current usage rates (Soeder et al., 2011).

The horizontal drilling process for hydraulic fracturing was previously developed for the purpose of offshore drilling and is actively used within Marcellus Formation gas exploration. The initial process involves drilling with a rotating bit, lubricated with drilling fluids to drill a bore hole and withdraw rock cuttings. To ensure the wellbore is completely confined, several steel casings are cemented in throughout the entire wellbore. A “special oil-well cement” is used that expands to plug the area between the casing and wellbore (Andrews et al., 2009). The series of casings decreases in diameter until the depth of the Marcellus Formation is reached (Figure 3). The well continues horizontally, to increase the surface area and wellbore length and allow gas to

flow through to the well. Fracturing fluids, water, and sand are then pumped through the well at pressures high enough to stimulate fractures within the Marcellus Formation. The sand acts as the proppant within the mixture, which "props" the fractures to stay open, allowing the gas to freely migrate to the well, also known as stimulation (Soeder et al., 2009). The high pressure creates the fracture and forces the fluid into the pores of the shale, maintained through sequences of continuous fluid pumping. The water carrying sand keeps the fractures open which allows the natural gas to readily migrate through the bore hole and up to the surface. These horizontal fractures are the main difference between horizontal drilling and vertical drilling.

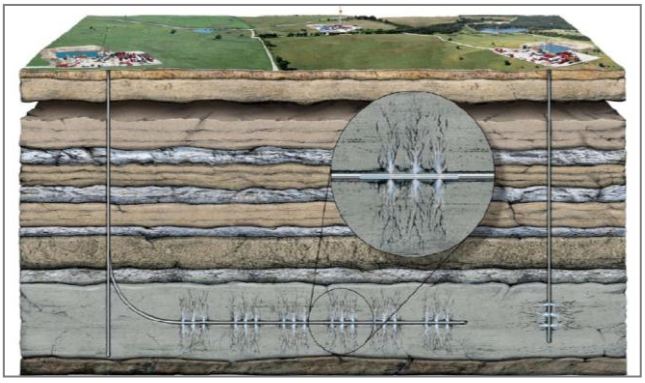

Figure 3: Cross sectional view of vertical and horizontal drilling (Susquehanna, 2008)

The composition of the fluids used varies considerably between different companies and well specifications. Chemicals can make up 0.5-2% of the total fracturing fluid, and may include HCl, biocide, surfactants, friction reducers, scale inhibitors and other chemicals (DOE, 2009). The fracturing fluids are also known as frack fluid or frack water. A large electrical submersible pump is used to pump the fracturing fluid back to the surface when the fracturing is complete, which can take up to several months (Bruner et al., 2001; Eckel, 2010). The resulting waste pumped back up through the well is known as flowback or production brine.

At such depths averaging 6000 feet, the fracturing fluids are exposed to formations which contain brine. This produced brine from the Marcellus Formation is common due to the marine origin of the shale. As a result, the flowback waste becomes a mixture of formation fluids, any

water present originally in the formation, brine, and dissolved minerals from the target, overlying, and/or underlying formations. The produced water can range from fresh to saline; depending on the amount of total dissolved solids (TDS) present as less or greater than 5,000 ppm, respectively (DOE, 2009). The fluids can be reused for future wells, recycled or disposed of at disposal facilities. The percent of recoverable fluid varies significantly based on the pathways available.

The fracturing fluids have potential to be exposed to surrounding formations, which may hinder gas production. This could result from introducing new fractures or lengthening old fractures, extending them into the overlying formation (Andrews et al., 2009). There is also potential for contamination of surface and/or groundwater if returning flowback is not disposed or managed properly. There are three main aquifer systems above the Marcellus Formation. In West Virginia, the valley-and-ridge carbonate rock system exists in the eastern portion of the state, and typically contains drinking water wells that are only several hundred feet deep (Arthur et al., 2008). The causes for such contamination are not likely to be from migration of fracturing fluids to the surface through naturally occurring/induced fractures, where Marcellus Formation depths can reach thousands of feet in depth. There are also several siltstone and shale formations stratigraphically above the Marcellus Formation, acting as confining layers not allowing fluids to migrate vertically (Arthur et al., 2008). Sources of contamination are likely to ensue from improper handling of the fluids or failed well seals (Hazen and Sawyer, 2009). More specifically, these may include over-pressurized wells causing flowback to overflow on the surface, leaking casings, improper seals, and/or leaking storage pits of flowback (Hazen and Sawyer, 2009). There is also the possibility of releasing naturally occurring radioactive materials (NORM) into the environment through drill cuttings or within the flowback (DOE, NETL, 2009). Within the

Marcellus Formation, radium-226 and radon exist at levels above federal environmental limits in some locations in New York (Eckel, 2010). This radioactivity is mainly the result of uranium precipitation in specific anaerobic settings for forming hydrocarbons. In general, black shales have low concentrations of uranium that are (on average) higher than other shales (Arthur et al., 2008). Gas companies are required to use caution signs and assess the radiation levels through OSHA, as well as supply protection gear for employees.

Mainly state laws regulate hydraulic fracturing and shale gas production (Andrews et al., 2009). Hydraulic fracturing is currently unrestricted from the Safe Drinking Water Act, with no current federal laws regulating the chemical injection during hydraulic fracturing (Andrews et al., 2009; Eckel, 2010). The Clean Water Act was extended to contain specific details within oil and gas operations for construction and waste treatment (Eckel, 2010). Drilling within West Virginia is subject to the West Virginia Department of Environmental Protection and the Water Resources Protection Act to register details when more than 750,000 gallons of water per month are withdrawn (Weston, 2008).

1.2– Objectives of Current Study

The Marcellus Formation Play within the 50 foot thickness isopach is the estimated area of highest productivity, predominantly in Pennsylvania and West Virginia (Figure 4). Natural gas is already predicted to have great probability of significantly replacing coal within West Virginia (Figure 5) due to an

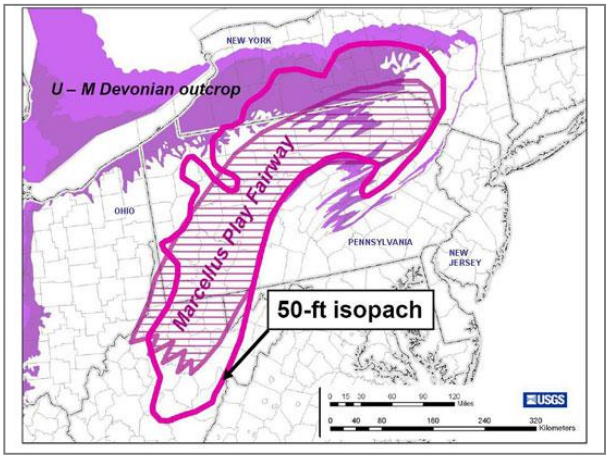

Figure 4: Area of the Marcellus Formation gas play (SSM Group, 2011)

increase in Marcellus Formation gas production (Figure 6). The production within the Marcellus Formation in Pennsylvania is projected to increase through at least year 2020 (Figure 7). With an overall dramatic rise of onshore unconventional natural gas resources, especially in Pennsylvania and West Virginia, it is necessary to acknowledge and recognize the risk and potential sources of contamination within groundwater resources.

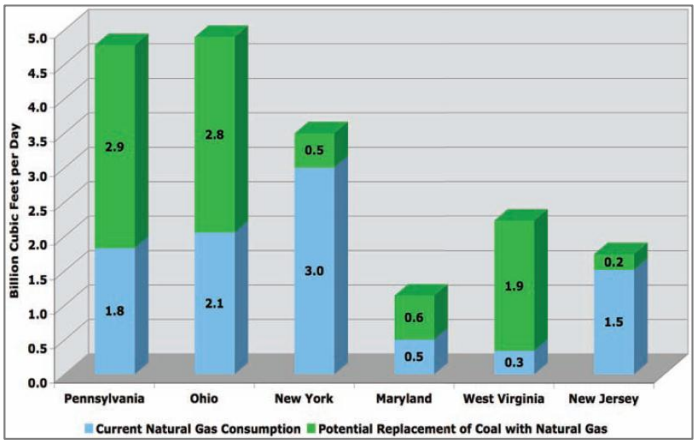

Figure 5: Coal and natural gas energy consumption comparisons across the East coast (Considine et al., 2009)

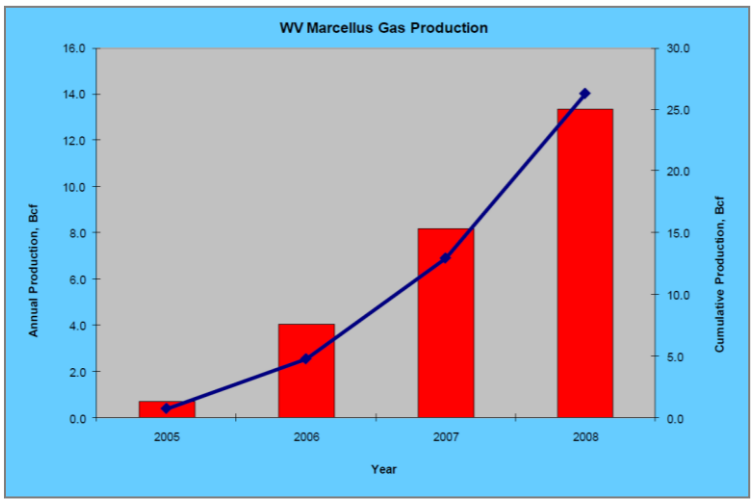

Figure 6: Increase in West Virginia Marcellus Formation production (Avary, WVGES)

This study focuses on the area of the Monongahela river basin of West Virginia, which is within the Marcellus Formation gas play and 50 foot isopach, where Marcellus Formation drilling is expected to expand rapidly. As more permits continue to be issued, the study area is anticipated to be the next focus area for natural gas drilling. The

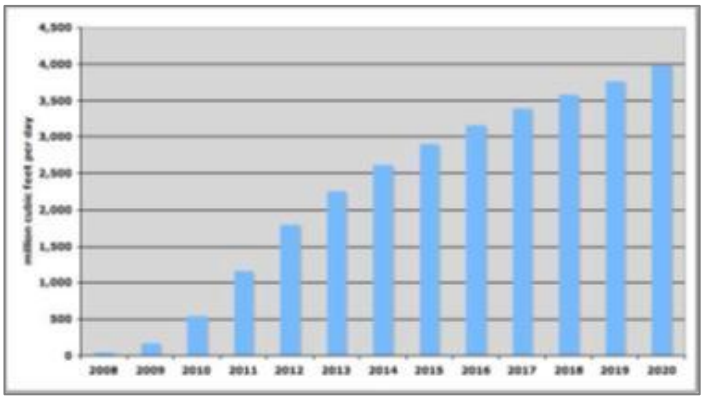

Figure 7: Projected increase in Pennsylvania Marcellus Formation production (Considine et al., 2009)

amount of active wells (shown in red) and issued permits (shown in yellow) in West Virginia is displayed in Figure 8.

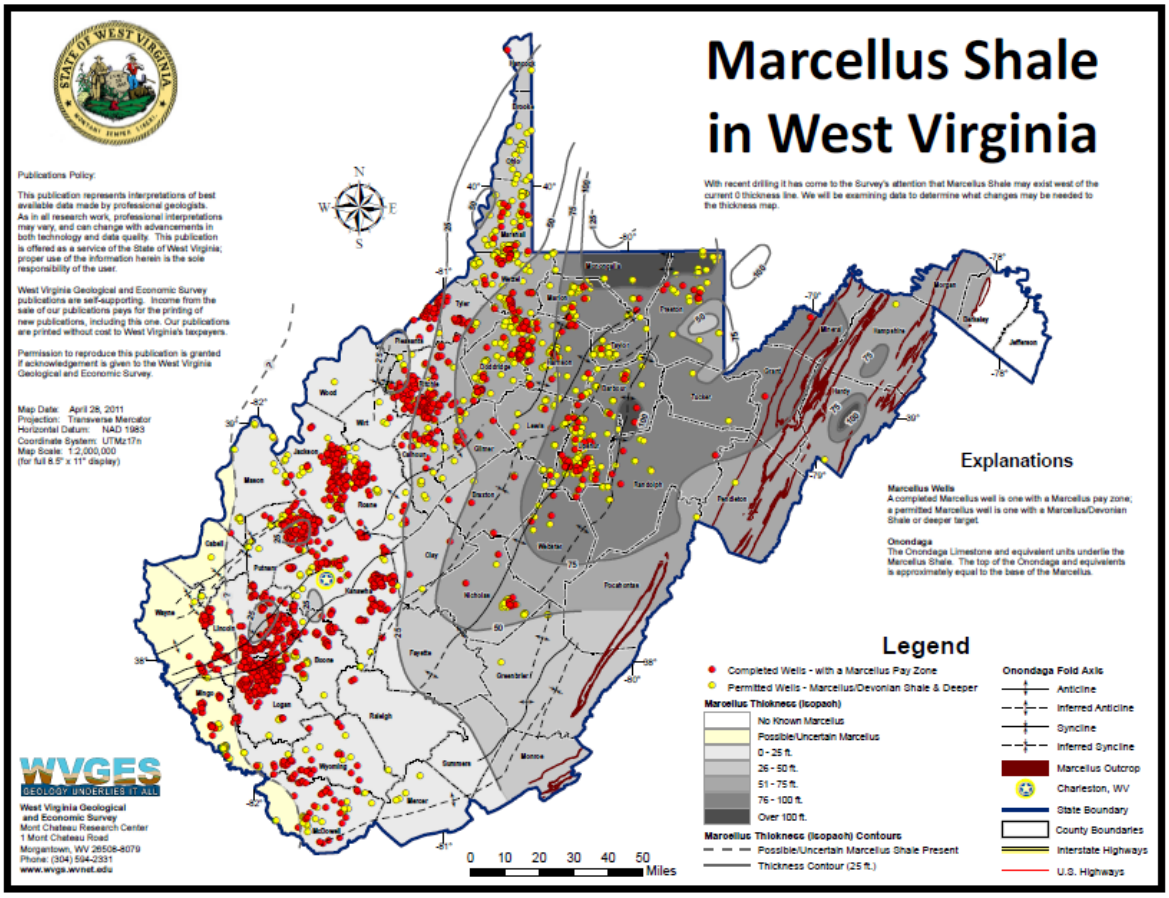

Figure 8: Completed and permitted wells within West Virginia (WV-GES 4/28/2011)

In order to determine if any water contamination is occurring as a result of shale development, ambient conditions prior to drilling are necessary for evaluation. These baseline water conditions can be analyzed through routine geochemistry, but additional environmental impacts can alter the geochemistry of groundwater i.e. coal mine discharge, natural saline groundwater, coal ash leachates, or landfill discharge. As a result, the main focus of this study is to test the feasibility of using stable isotopes, in addition to routine geochemistry, to distinguish and fingerprint the different groundwater sources in the area. We hypothesize that selected stable

isotopes of oxygen and hydrogen in water, carbon in dissolved inorganic carbon, sulfur and oxygen in dissolved sulfate, and carbon and hydrogen in dissolved methane (as well as hydrochemistry) will vary across the study area and between aquifers. These variations may be due to water-rock interactions, formation geochemistry, land use, and water recharge sources. Therefore, the overall objective of this study is to determine the baseline hydrochemistry and isotopic signatures, and to identify the prominent geochemical pathways in groundwaters of the study area.

The specific tasks necessary to complete this project objective include:

1) Obtain hydrochemistry data for 41 groundwater wells (public and private) spanning across the Monongahela river basin in West Virginia. During the summer of 2011, shallow groundwater wells were sampled for temperature, pH, conductivity, and major cations and anions. This data was collected in collaboration with the USGS - Water Science Center of West Virginia.
2) Each groundwater sample was analyzed for isotope signatures of $\delta^{2}H_{H2O}$, $\delta^{18}O_{H2O}$, $\delta^{34}S_{SO4}$, $\delta^{18}O_{SO4}$, and $\delta^{13}C_{DIC}$, with approximately half of the samples analyzed for $\delta^{13}C_{CH4}$ and $\delta^{2}H_{CH4}$. Isotopic analysis was done at the West Virginia University Stable Isotope Laboratory and Isotech Laboratory.

2.0 – Background Literature

2.1 – Regional Geology

The complex structural systems in the Appalachian basin within the study area are mainly due to three distinct orogeny events: the Middle-Late Ordovician Taconic orogeny, Middle Devonian to Lower Mississippian Acadian orogeny, and the Pennsylvanian-Permian Allegheny orogeny (Bruner et al., 2011). The Marcellus Formation underwent widespread structural deformation specifically during the Allegheny Orogeny (Bruner et al., 2011), shown in cross section (Figure 9). Using data from 13 drill holes, the cross section includes the Findlay arch in Ohio through the valley and ridge area in West Virginia including Pennsylvania and Maryland. Structural systems of note are four regional unconformities, central West Virginia anticlines including the Chestnut Ridge anticline, the Valley and Ridge province, numerous faults, basement structures, and multiple thin-skinned structures (Ryder et al, 2009). These tectonic systems introduce fracture systems and fractured bedrock aquifers within the Marcellus Formation fairway, increasing potential for contamination pathways.

Permian and Pennsylvanian rocks stratigraphically cover approximately 75% of the study area with the Mississippian and Devonian systems occurring to the east (Herb, 1981). Nine aquifer formations were sampled through 41 groundwater well sites, all stratigraphically above the Marcellus Formation (Figure 10). These sampled sites include formations covering the Devonian through Permian periods in north central West Virginia (Figure 11).

The oldest sampled formation is the Chemung Group. Deposited during the late Devonian in a marine environment, it consists of mainly siltstone and sandstone, with shale beds throughout (USGS, 2012). In the study area, the unit thickness ranges from 2115-3000 feet (USGS, 2012). The Hampshire Formation was deposited at the end of the Devonian as the

shoreline retreated to the west, resulting in red shale with sands of gas-producing quality (Cardwell, 1975). The thickness is between 1710 and 3350 feet in the northeastern portion of the state and is distinguishable with its red color (USGS, 2012).

The sandstones of the Price Formation (formerly known as the Pocono Group) were deposited in the early Mississippian (Cardwell, 1975). The gray sandstone includes a few layers of shale, siltstone, and coal (Cardwell, 1975). The Price Formation also contains several gas-producing zones: the Berea and Big Injun (Cardwell, 1975). The non-marine deltaic environment of deposition resulted in its detrital composition (Cardwell, 1975), with thicknesses of 570-1030 feet (USGS, 2012). The Greenbrier Formation was deposited mid-Mississippian, during the last main marine environment in West Virginia with a thickness of 400 feet (USGS, 2012). Its lithology is mainly oolitic limestone with a cherty base, with minor sandy layers and calcareous red non-marine shale (Cardwell, 1975; USGS, 2012). Some gas and oil producing areas are present (Cardwell, 1975).

The Pottsville Group, deposited in the early Pennsylvanian, is divided into the Kanawha, New River, and Pocahontas Formations with thicknesses ranging from 360 feet in northeast West Virginia to over 3000 feet in the southeast (USGS, 2012). The environment at this time was swamp lands and prevalent organics prevailed at the low sea level (Cardwell, 1975). It is the result of these conditions that resulted in the majority of the current coal deposits as well as oil and gas reservoirs (Cardwell, 1975). The continuous change in sea level throughout the Pennsylvanian resulted in a repeated depositional sequence of clays, coal, shale, sandstone, and siltstone (Cardwell, 1975). More specifically, the New River Formation has an average thickness of 100 feet in northeast West Virginia of mainly sandstone with minor shale, siltstone, and coal layers (Cardwell, 1975; USGS. 2012). The Kanawha Formation has a thickness of 260 feet in

northeast West Virginia and is also majority sandstone at 50% of the total lithology with the remainder being shale, siltstone and coal (Cardwell, 1975). The same sequential deposition pattern continued for the Allegheny formation but with more even distributions of sandstone, siltstone, shale, limestone, and coal in the lithology. The Upper Freeport coal serves the stratigraphic marker as the top of the ~175 foot Allegheny formation, moving to the Conemaugh Group. The Conemaugh Group is distinguished by the presence of red beds as the accrual of peat lowered. This group has sequences of red and gray shales with siltstone, sandstone with fewer layers of limestone and coal for a total of approximately 750 to 850 feet. Finally, the Pennsylvanian ends with the deposition of the Monongahela Group with the important economic Pittsburgh coal seam up to 10 feet thick. This group continues with sequences of sandstone, siltstone, red and gray shales, limestone and coal in a non-marine setting with a 170 foot thickness (USGS, 2012).

The youngest aquifer formation accessed in the study area is the Dunkard Group during the Permian in an environment similar to the Pennsylvanian. This is seen in the continued cyclic trend of sandstone, siltstone, red and gray shales, limestone, and coal units. In northern West Virginia, more gray shale and sandstone is common with less coal, limestone and calcareous shale. The boundary between the Monongahela and Dunkard Groups and therefore the Pennsylvanian and Permian periods is not of complete certainty (USGS, 2012).

Throughout the stratigraphy of the Devonian to the Permian, the abundance of economical coal and methane has resulted in heavy mining and drilling. Specifically, the top six producing coal beds of the Pennsylvanian are the Fire Clay, Pond Creek and Pocahontas No. 3 of the Pottsville Group, Lower Kittanning and Upper Freeport of the Allegheny Formation, none in the Conemaugh Group, and Pittsburgh of the Monongahela Group (Ruppert and Rice, 2000).

This includes 12 feet in the Allegheny Formation and 3 feet in the Monongahela Group (Herb, 1981). The northern and central Appalachian basins produced a combined 403.4 million short tons of bituminous coal in 1998, spanning 50 coal beds and 1421 mines to make up 40% of the entire US coal production (Ruppert and Rice, 2000). Coal production has been occurring for at least 200 years, producing a total of 32 trillion short tons of bituminous coal (Ruppert and Rice, 2000). Half of that total tonnage was mined during the last 50 years, with over 18.5 trillion produced in the northern Appalachian basin alone (Ruppert and Rice, 2000). Commercial coalbed methane production is present in the lower and mid Pottsville Group in Pocahontas No. 3 and No. 4 coal beds, and the lower Allegheny Formation in the Lower Horsepen, Little Fire Creek, War Creek, Beckley, Lower Seaboard, Sewell, Jawbone, and Iaeger coal beds (Ruppert and Rice, 2000).

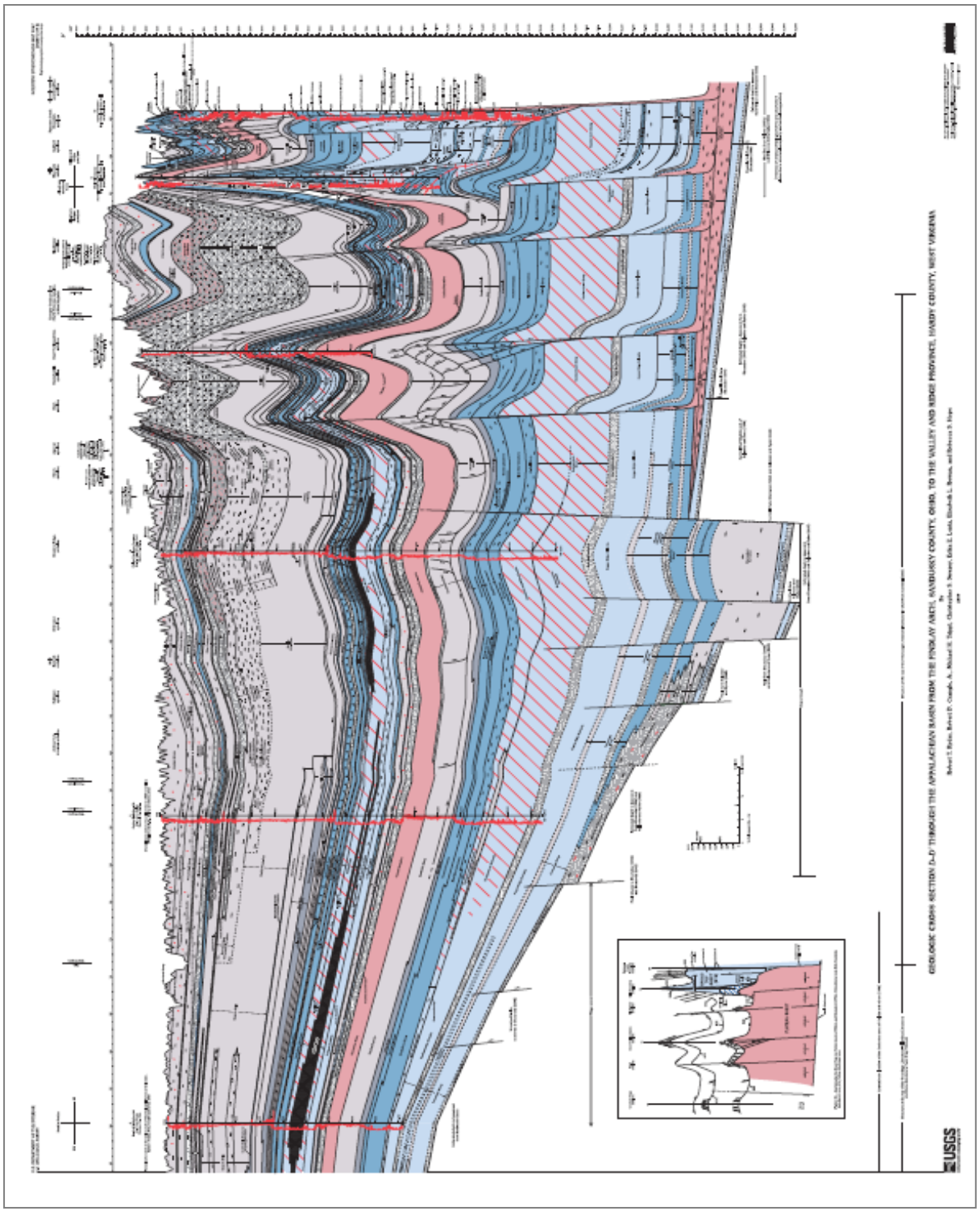

Figure 9: Cross Section from Sandusky County, OH to Hardy County, WV (Ryder et al., 2009)

Age	Geologic Formation		Lithology of Sampled Formations
Permian ?	Dunkard Group		Sequence of ss, slts, sh, ls, coal
Pennsylvanian	Monongahela Group		Sequence of ss, slts, sh, ls, coal (Pittsburgh coal)
	Conemaugh Group		Red beds, sequence of sh, slts, ss, with ls, coal
	Allegheny Formation		Sequence of ss, slts, sh, ls, coal
	Pottsville Group	Kanawha Fm.	Sequence of ss with sh, slts, coal
		New River Fm.	Sequence of ss with sh, slts, coal
		Pocahontas Fm.	--
Mississippian	Mauch Chunk Formation		--
	Greenbrier Formation		Ls
	Maccrady Formation		--
	Price Formation		Ss with sh, slts, coal
Devonian	Hampshire Formation		Sh
	Chemung Group		Slts, ss, sh
	Brallier Formation		--
	Harrell Shale		--
	Mahantango Formation		--
	Marcellus Formation		--
	Onesou Thaw Stage	Tioga Metabentonite Bed	--
		Onondaga Limestone / Hunters-ville Chert / Needmore Shale	--

Figure 10: Simplified stratigraphic column of study area and sampled groundwater formations (modified from Cardwell, 1975)
ss – sandstone; slts – siltstone; sh – shale; ls – limestone; Fm. - Formation

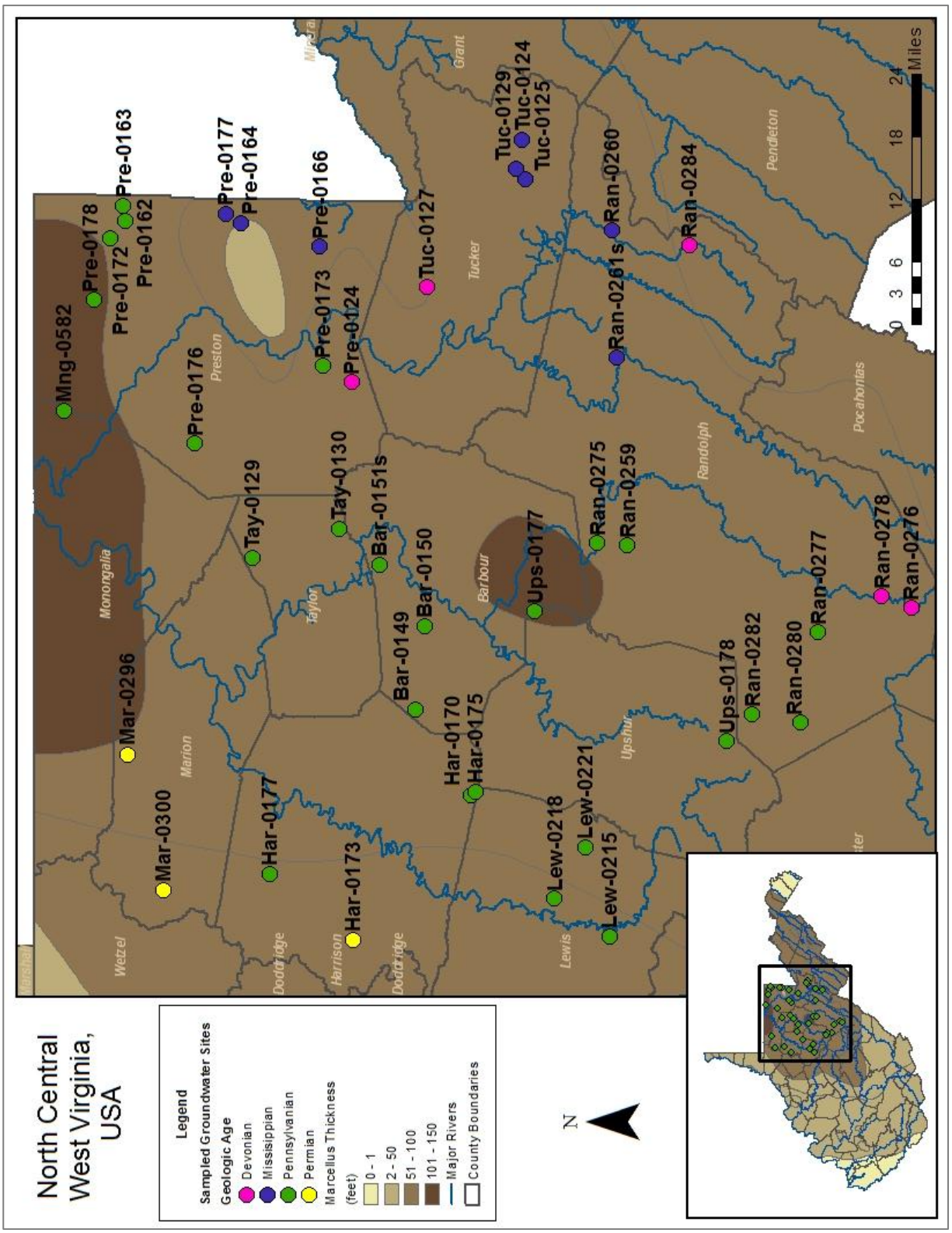

Figure 11: North central West Virginia study area within the Monongahela river basin

2.2 – West Virginia Groundwaters

Covering this study area is the Monongahela river basin, drained completely by the Monongahela river. Its extent ranges from Pittsburgh, Pennsylvania at the mouth of the Monongahela river south to the headwaters of the Tygart Valley river in West Virginia. With a surface area of 7384 square miles, the main tributaries contributing include the Youghiogheny, Cheat, Tygart Valley, and West Fork riverss (Herb et al., 1981).

Numerous aquifer formations and groups are used within the Monongahela river basin and throughout West Virginia. These include the Beekmantown and St. Paul, Catoctin, Conemaugh, Elbrook, Connococheague and Chambersburg, Hampshire, Helderberg, Pottsville, Price, Rockdale Run, Stonehenge, Tonoloway, Wills Creek, and Williamsport (Kozar et al, 2001). Alluvial aquifers are also present from the Ohio and Kanawha rivers.

Sandstone aquifers in West Virginia produce the highest yields of groundwater compared to other coal basins in the Appalachian Plateau, ranging from 5 to 400 gpm (Appendix C, EPA). The presence of fractures and joints within the aquifer system highly influence the productivity and flow of groundwater (Appendix C, EPA). This leads to shallow and deeper groundwater flow along fractures, thrust faults, or bedding plane separations (Kozar et al., 2011). Aquifer characteristics differ greatly in terms of storage coefficients, specific capacity, and transmissivity due to the fracture systems (Kozar et al., 2011). Storage coefficients in bedrock aquifers range from 0.0001 to 0.031 for the Pottsville Group, Price Formation, Hampshire Formation and Conemaugh Group (Kozar et al., 2011). The specific capacity of an aquifer represents maximum yields and can be used for determining pumping rates. Using median values of gpm/ft, the study formations and groups range from 0.31 to 5.09 and include the Pottsville, Price, Hampshire, Chemung, Conemaugh, Dunkard, Monongahela, Allegheny, Kanawha, New River and

Greenbrier (Kozar et al., 2011). The storage coefficients and specific capacities are lower in bedrock aquifers compared to alluvial aquifers in the state due to the fracture systems and low primary porosity (Kozar et al., 2011). Transmissivity values cover the widest range, depending on formation thickness and lithology. These range from 74 to 1300 ft^2/day with the Pottsville, Price, Hampshire, Chemung, Conemaugh, Dunkard, Monongahela, Allegheny, Kanawha, New River and Greenbrier Groups and Formations (Kozar et al., 2011).

Effects of land use and mining on groundwater quality have been studied within the USGS. Dissolved methane was detected in groundwaters in concentrations of 0.00 to 68.50 mg/L in a study conducted between 1997-2005 of 170 wells in West Virginia (White and Mathes, 2006). Concentrations above 28 mg/L were not found in the area of this study out of the previous 170 wells. The hydrogeology of Appalachian coal mines has been studied to map areas of mines, outcrops, associated structures, and discharges (Morris et al., 2008). Herb et al. (1981) evaluated the impact of coal and coal mining on water quality within the Monongahela river basin. 50% of the coal mined within the basin in 1978 was from surface mining. 136 square miles in the Monongahela river basin need remediation from surface mining activities, specifically within Somerset, Fayette, and Westmoreland counties in Pennsylvania. Streams with pH values less than 4.5 were located in and around Preston county and near Elkins, West Virginia. The eastern half of the basin showed acidity superseding alkalinity values. 11 streams showed evidence of acid mine drainage in Preston, Taylor, Tucker, Upshur, and Randolph counties in West Virginia and Greensburg county in Pennsylvania. This evidence was derived from necessary criteria of pH, alkalinity, acidity, with iron, manganese, and dissolved sulfate concentrations. The overall hydrology has also been determined for south central West Virginia and within the Kanawha river basin (Ehlke et al, 1982). The Kanawha river basin has been heavily surface and

underground mined. The indicator used for surface waters affected by mining was specific conductance. The highest values (735 µmhos/cm) were shown to be in mined areas with overall averages between 344-499 µmhos/cm. High sulfate values were also connected to underground mining, with the highest iron and manganese concentrations found in older mined areas.

The water chemistry of the mine discharges and quantifying it with flooding and temporal changes is necessary for applying to changes in stream chemistry in mined/mining areas for AMD (Donovan and Leavitt, 2004; Donovan et al. 2003; Merovich, Jr. et al 2007). Geochemical speciations and cycling has also been studied in the coal mine drainage (Vesper and Smilley, 2010). The Monongahela Basin Mine Pool Project, researched by the West Virginia Water Research Institute and directed by Dr. Paul Ziemkiewicz, examined the effects of underground coal mining. This included the hydrogeology of underground mine pools with their water levels and chemistry as well as changes in stream chemistry over the past several decades. Additionally, modeling of flooding, hydrology, hydrogeology, and geochemistry was conducted to quantify mine discharge and its effects on surface water. Over a dozen mines have also been studied to relate water quality from underground coal mines (Demchak et al., 2000).

The overall water quality within the combined Allegheny and Monongahela river basins was previously established between 1996 and 1998 through the USGS NAWQA program. Sulfate concentrations were five times higher in streams of mined areas compared to streams without mining. It was determined that the primary causes for variation in groundwater quality are from coal mining, use of pesticide and fertilizer, gasoline and oxygenates, and radon concentrations found naturally occurring. Pesticide regulations for drinking water were surpassed in local areas within both basins from both agriculture and urban sources. One pesticide compound was found in 29% of the total samples but not at concentrations above regulation.

92% of the domestic wells had at least one volatile organic compound (VOC) with 28 different types of VOCs detected overall. These were found in low concentrations, but only 20 of the 28 detected VOCs have regulations established for drinking water. These occurrences were thought to be the result of proximity to reclaimed mines or coal lithologies due to gasoline compounds found more concentrated in mining locations. Potential sources could include equipment used in mine operations, fuel spills, or other land uses. Nitrate was detected in 62% of the well sites, with the highest concentration found in an agricultural domestic well. Sulfate concentrations were found to be higher in wells that were within 1000 feet of reclaimed surface mines. Sites in the northern coal field had greater sulfate and calcium concentrations when comparing to unmined areas and the central coal field. Turbidity, specific conductance, and concentrations of iron, manganese, aluminum, and magnesium were higher within 2000 feet of both reclaimed mines and coal fields. These trends could be the result of the use of calcium and magnesium as constituents in chemicals used in the treatments of mines or iron and manganese occurring naturally in native coal bearing rocks.

2.3 – Geochemistry

2.3.1 – Hydrochemistry: Major Cations and Anions

Major ions have been traditionally used as tracers for evaluating groundwater mixing, in combination with trace elements. These include major cations and anions: Ca^{2+}, Mg^{2+}, Na^{+}, K^{+}, SO_4^{2-}, Cl^{-}, HCO_3^{-}, and CO_3^{2-}. Geochemical plots, such as Piper diagrams, are frequently used to distinguish different water types and potential mineral dissolution and saturations through water-rock interactions. Major cations and anions are grouped by percentages on a Piper diagram, which can visually show different trends that may exist between waters. To explain trends or

changes in the hydrochemistry, reactions involving specific ions are examined. Horizontal and vertical changes in total dissolved solids (TDS) values can be interpreted as the result of groundwater mixing. High TDS values can also be used as an indicator for high residence times in conjunction with ratios of $(Ca^{2+}+Mg^{2+})/Na^{+}$ (Atekwana et al., 2004; Bouchaou et al., 2009; Cartwright et al., 2007; Kim et al., 2003; Tweed et al., 2005). In addition to groundwater mixing, rock weathering and mineral dissolution can be evident through geochemical relationships. Dolomite and calcite dissolution can occur through carbonate weathering. An increase of HCO_3^- with an increase of Ca^{2+} in a 2:1 molar ratio indicates dissolution of calcite and dolomite dissolution by a 1:1 molar ratio of Ca^{2+} and Mg^{2+}. An additional trend to signify calcite dissolution is a positive correlation between SO_4^{2-} and Ca^{2+} or alkalinity and SO_4^{2-}. Gypsum dissolution can be accounted for through the 1:1 molar ratio of Ca^{2+} and SO_4^{2-}. Pyrite dissolution from oxidation can be seen in a 2:1 ratio of Fe and SO_4^{2-}. TDS values can also be used to generalize if water-rock interactions are occurring through an increase simultaneous with pH. Studies emphasizing these relationships include those done by Bouchaou et al., 2009; Jiráková et al., 2010; Marfia et al., 2004; Tweed et al., 2005; and Van Donkelaar et al., 1995. The sampled formations potentially include the mentioned minerals through the cyclic depositions in both marine and non-marine settings. Dissolution and weathering may therefore be an important factor for variations in groundwater hydrochemistry in the study area. The different abundance of major cations and anions in groundwaters formations in the study area preliminarily indicates a combination of these different processes is occurring. Shallow brines may be encountered within the formations of the study area, due to the changing sea levels during deposition.

Sources of salinity in groundwater can be determined through Cl^-/Br^- ratios, such as oceanic inputs, plant organics, halite dissolution and/or precipitation, and the effect of

evapotranspiration. These can also be determined through plots of elemental ratios including Cl^-/Br^-, Si^{4+}/Cl, or Ca^{2+}/Cl^- versus Cl^- concentration or K^+/Cl^-, Mg^{2+}/Cl^-, or Ca^{2+} vs. DIC. Ratios of Br^-/Cl^- in comparison to seawater values and high TDS values can be the result of saline groundwater mixing within the aquifer. Na^+/Cl^- ratios can also be compared with seawater ratios to evaluate seawater exposure. Changes in electrical conductivity and therefore ionic charge alterations can decipher specific seawater intrusions. Other correlations to demonstrate saline sources include direct trends of Na^+, Mg^{2+}, and SO_4^{2-} with Cl^-, or Cl^-/HCO_3^- vs. Cl^- for the mixing of fresh and saline waters (Cartwright et al., 2007; Kim et al., 2003; Mondal et al., 2010). These salinity tools may be necessary for determining the potential exposure to the highly saline flowback waters and/or underlying saline formations. Specifically, within deep formations with mixed water origin of meteoric and seawater, the geochemistry can vary in dominant cations and anions from Na^+ and Cl^- or Na^+, Ca^{2+}, and Cl^-. Geochemical reactions that alter these can be mineral dissolution (i.e. halite), water-rock interaction of clays and organics, and diffusion.

2.3.2 Stable Isotope Geochemistry

Routine hydrochemistry can be used to understand basic geochemical patterns, but isotopic analysis allows further interpretations due to their inert and conservative nature. Isotopes, atoms with the same number of protons but different number of neutrons, can be found naturally as stable isotopes within the environment. The specific elements and their isotopes of focus in this study are hydrogen, carbon, oxygen, and sulfur. Isotopes of methane will also be examined. Found in abundance naturally, they can be used as tracers due to light masses and increased differences in mass between the element and its isotope. They can be used as tracers in hydrology, carbon input, nutrient cycles, contaminant transport, groundwater recharge, and

geochemical reactions. Fractionation is the redistribution of isotopes as a result of variations in physiochemical properties and reaction rates between the different isotopes, determined by the fraction of heavy to light isotopes of both phases. These factors affecting fractionation include velocity rates, temperature, and dissociation energy. The fractionation factors lead to discrimination, which is the preference of one isotope to the other (heavy or light). This preference is calculated as the delta value (δ) in units of permil (‰):

$$\delta_{\text{sample}} = \left(\frac{R_{\text{sample}}}{R_{\text{standard}}} - 1\right) * 1000 \qquad \text{(Eqn 1)}$$

Where, R represents the ratio of the heavy to light isotope, multiplied by 1000 to express small relative differences in isotopic ratios. A positive value indicates that the ratio of heavy to light isotopes is higher in the sample compared to the standard and that the sample is "enriched" in heavy isotopes compared to the assigned IAEA standard. The opposite, with negative values, indicate the sample is "depleted" with respect to the standard. Each specific isotope has an assigned international reference standard by the United Nations International Atomic Energy Agency (IAEA), approximately 0‰ each. Oxygen and hydrogen are measured with respect to Vienna Standard Mean Ocean Water (V-SMOW), carbon with respect to Vienna Pee Dee Belemnite (V-PDB), and sulfur with respect to the Cañon Diablo meteorite (CDT). The isotope ratios are determined through mass differences using a gas source stable isotope ratio mass spectrometer.

2.3.3 Oxygen and Hydrogen Isotopes in Water

A detailed overview of oxygen and hydrogen isotope variations can be found in Clark and Fritz (1997). Since oxygen and hydrogen form the water molecule itself they are excellent natural tracers for tracking water sources. Globally, waters show an excellent correlation

between the O and H isotopic composition. This correlation is defined as the global meteoric water line (GMWL), defined by $\delta^2H = 8.13^{18}O+10.8‰$ (Figure 12). This equation is the result of averaging meteoric water lines that vary globally in climate and geography. The isotopic signature begins as the originating vapor mass over large bodies of water, moving inland on continental masses and cooling, with the heavy isotopes to distill out in precipitation. This process is known as Rayleigh distillation, resulting in precipitation from higher latitudes and cooler climates having more depleted O and H isotopic signatures.

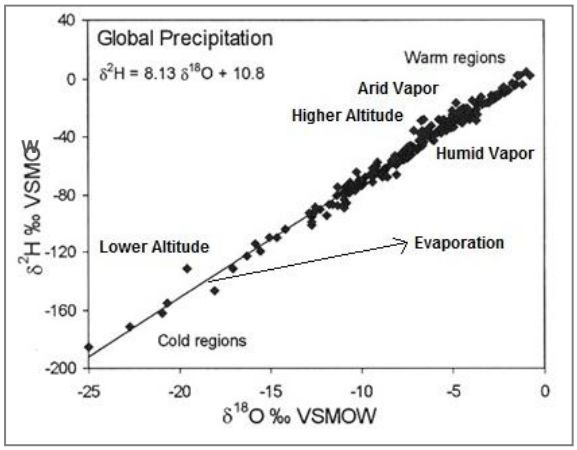

Figure 12: GMWL, representing the relationship of $\delta^{18}O$ and δ^2H (modified from Rosanski et al., 1993)

Inversely, warmer climates have more enriched values on the GMWL. Secondary evaporation during precipitation affects equilibrium fractionation factors of ^{18}O and ^2H and defines the slope of the GWML. The y-intercept represents the humidity levels during the formation of the vapor mass and therefore kinetic fractionation. The GMWL assumes a humidity level of 85% with local humidity changes altering it through evaporation by shifting values to the right of the line.

The kinetic effects during evaporation when the initial vapor is formed produce excess deuterium in the precipitation, known as *d*-excess. This parameter was originally defined by Dansgaard (1964) and can be differentiated through a calculation relating isotopic signatures of water to the meteoric line slope of 8 (Eqn 2).

$$d = \delta^2H - 8\delta^{18}O \qquad \text{(Eqn 2)}$$

Variations in *d*-excess are due to the humidity and temperature at the source of the air mass formation, evaporation, and therefore the prevailing season of recharge; higher *d*-excess values

result from recharge by snow melt. These effects by *d*-excess are seen within the slope of the linear relationship between δ^2H_{H2O} and $\delta^{18}O_{H2O}$. The GMWL line uses an overall humidity level of 85%, corresponding to *d*-excess of 10‰. As humidity increases, the relative *d*-excess lowers. The *d*-excess composition can be used to track sources of the original vapor mass through humidity levels and isotopic signatures.

Different water sources show unique δ^2H_{H2O} and $\delta^{18}O_{H2O}$ isotope signatures due to variations in origin, time of recharge, and/or salinity. Mixing between several aquifers can also be seen within the fractionation of δ^2H_{H2O} and $\delta^{18}O_{H2O}$. The time and season of recharge can also result in isotopic variation. In aquifers consisting of sedimentary rocks, minerals within clays and carbonates drive the reactions for altering the composition of δ^2H and $\delta^{18}O$ in formation waters. Applicable mechanisms include the hydration of silicates in the numerous clay lithologies and water-rock exchange (Figure 13). Sampled lithologies in this study do not reach depths of high temperature exchange, but will exchange more shallowly to potentially deviate to the right of the GMWL. In areas where surface contamination of disposed flowback is an issue, $\delta^{18}O$ and δ^2H can be used to establish if surface water infiltrating groundwater wells. Mineral formation and reactions alter the isotopic composition of water depending on the minerals present, proportions, and the aquifer

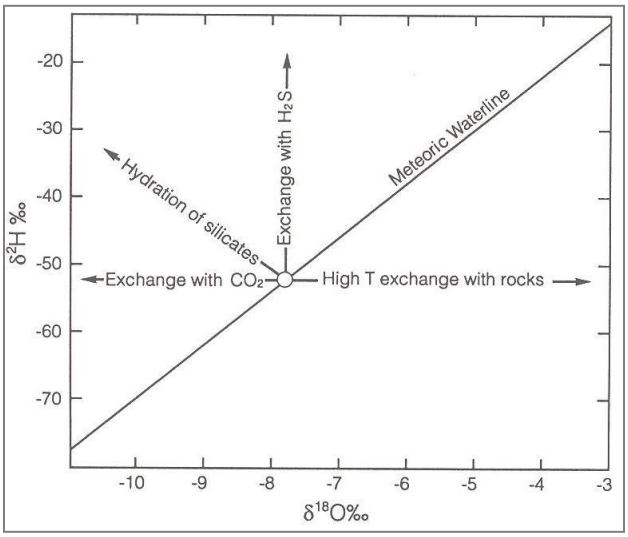

Figure 13: Deviation from the GMWL from water-rock interaction (Clark and Fritz, 1997)

temperature. Examples of such studies include Blasch et al., 2007; Bouchaou et al., 2009; Hunt et al., 2005; Kharaka et al., 1973; Land et al., 1987.

Specific to the north central West Virginia area, oil and gas fields and their formation waters have been studied extensively by Kharaka and Thordsen (1992) in terms of isotopes of water, geochemistry, and water origin. The isotopic composition within the formation waters has been shown to intersect the GMWL and can be used in conjunction with TDS to determine the origin. The water isotopes alone can indicate an age prior to the Holocene from meteoric input if the values are significantly lower on the GMWL (Kharaka et al., 1973). Hydrogen isotopes within formation waters can fractionate (enrich or deplete) with surrounding clays, as clay structures contribute most of the total hydrogen in the reservoir. δ^2H_{H2O} and $\delta^{18}O_{H2O}$ can be used as fingerprints for petroleum production and contamination from formation waters with their isotopic signature shown to be unique for individual aquifers. This allows the ability to use these isotopes as tracers to distinguish formation fluids of different formations and depths for contamination purposes, applicable to the Marcellus Formation. Studies highlighting this include Kharaka et al., 1973; Kharaka et al., 1986; Rostron et al., 2000; and Wittrup et al., 1987.

2.3.4 Carbon Isotopes in Dissolved Inorganic Carbon

Carbon in groundwater evolves through the diffusion of meteoric water through soil. As CO_2 is produced through carbonate and silicate weathering, dissolved inorganic carbon (DIC) accumulates. Simultaneously,

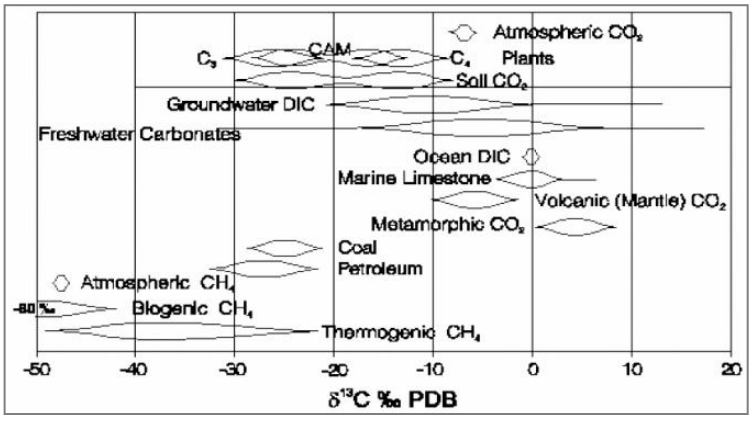

Figure 14: Natural variation of carbon isotope values in the environment (Clark and Fritz, 1997)

anaerobic bacteria within the soil can oxidize organic matter, adding dissolved organic matter/carbon (DOC) to groundwaters. If DOC in groundwater exceeds atmospheric O_2 levels, anaerobic bacteria will mediate methanogenic reactions (discussed in Section 2.3.6). These processes of carbon evolution affect the distribution of specific carbon species and isotopic distributions in nature (Figure 14). This study focuses on the isotopic fractionation of carbon in DIC of groundwaters.

As $CO_{2(g)}$ diffuses through soil and into groundwater, it hydrates and dissociates to form the four species that comprise total DIC:

$$CO_{2(g)} + H_2O \leftrightarrow H_2CO_3 \leftrightarrow H^+ + HCO_3^- \leftrightarrow 2H^+ + CO_3^{2-}$$

Carbonic acid, H_2CO_3, is the most abundant natural acid, controlling alkalinity and therefore pH. The equilibrium constants and temperature associated with each reaction correspond to the pH distribution in a Bjerrum plot, with $CO_{2(aq)}$ at low pH, HCO_3^- at mid-pH, and CO_3^{2-} at higher pH. The primary sources of carbon in DIC include the decay of organic matter in soil and soil carbonates. These endmembers have distinct isotopic compositions of carbon, with C_3 vegetation more depleted and carbonates more enriched. The produced bicarbonate with these contributions will have a $\delta^{13}C$ of approximately -12‰. In most natural pH waters, bicarbonate is the main component of DIC, leading to a predicted range for $\delta^{13}C_{DIC}$ of -11 to -16‰, depending on the relative contributions from the varying carbon sources (Figure 15). The exact composition of $\delta^{13}C_{DIC}$ depends on multiple factors including temperature, pH, CO_2 endmembers, and parent material of silicate or carbonate (Figure 16). Fractionation associated with different CO_2 endmembers and carbonate dissolution have corresponding effects.

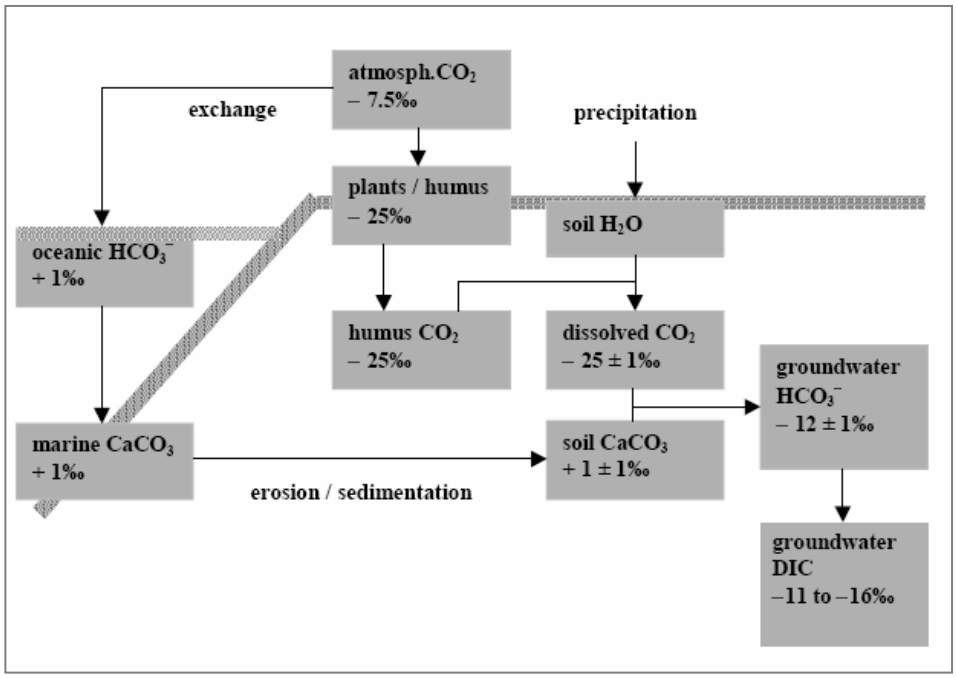

Figure 15: Groundwater DIC endmembers and associated $\delta^{13}C$ effects (Mook et al., 2001)

Carbonate weathering is seen through calcite and/or dolomite dissolution, respectively:

$$CO_{2(g)} + H_2O + CaCO_3 \rightarrow Ca^{2+} + 2HCO_3^- \quad \text{(Eqn 3)}$$

$$Ca^{2+} + HCO_3^- + CaMg(CO_3)_2 + H_2O \rightarrow Ca^{2+} + Mg^{2+} + 2HCO_3^- + CaCO_3 + OH^- \quad \text{(Eqn 4)}$$

Throughout these geochemical reactions, the $\delta^{13}C$ signature can be used as a tracer within numerous hydrological situations. Applications include carbon sources, water recharge sources, and determining water-rock interactions. The linear relationship of $\delta^{13}C$ and 1/DIC can be used to evaluate sources of carbon to the system. Local effects on $\delta^{13}C$ applicable to

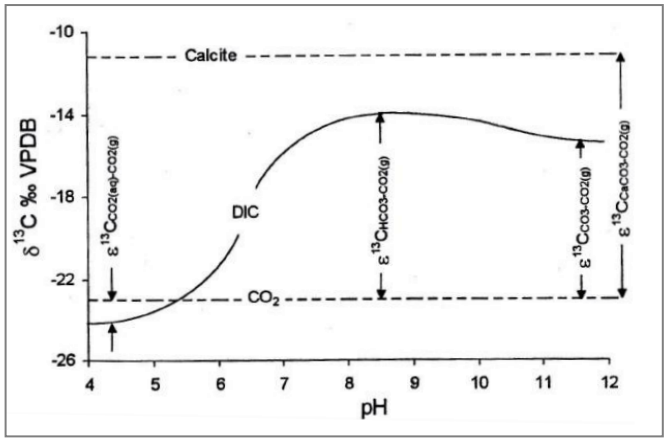

Figure 16: Evolution of $\delta^{13}C$ from DIC contributions according to pH (Clark and Fritz, 1997)

this study may include dissolved organic carbon from shallow and deep coal beds, soil organic matter oxidation, carbonate rock dissolution, carbon in methane produced through biogenic pathways (methanogenesis), and carbon in bicarbonate through the oxidation of methane via oxygen or sulfate (methanotrophy).

The biological production of methane, also known as methanogenesis, occurs through acetate fermentation (Eqn 5) or CO_2 reduction pathways (Eqns 6-7). This instigates isotope discrimination for lighter carbon due to biological preferences, leading to an accumulating carbon pool of heavier ^{13}C. The carbon pool is represented by the residual DIC, with enriched $\delta^{13}C_{DIC}$ signatures ranging from +10 to +30‰, providing evidence of biological methane production (Whiticar et al. 1986; Simpkins and Parkin, 1993; Scott et al., 1994; Botz et al., 1996; Maritini et al., 1998; Whiticar,1999; Hellings et al., 2000; Aravena et al., 2003; McIntosh et al., 2008; Sharma and Frost, 2008; Sharma and Baggett, 2011; McLaughlin et al., 2011). Hence, corresponding changes in the composition of $\delta^{13}C_{DIC}$ can provide a proxy with $\delta^{13}C_{CH4}$ to evaluate if methanogenesis is occurring.

$CH_3COOH \rightarrow CH_4 + CO_2$ (Eqn 5)

$CO_2 + 4H_2 \rightarrow CH_4 + 2H_2O$ (Eqn 6)

$HCO_3^- + 4H_2 \rightarrow CH_4 + 2H_2O + OH^-$ (Eqn 7)

The oxidation of methane in groundwaters in the presence of O_2 or SO_4^{2-} is known as methanotrophy. The reduced carbon in methane is oxidized and produces reduced bicarbonate, which contributes to the total DIC pool (Eqns 8-9). With an isotopically depleted carbon source i.e. CH_4, the produced HCO_3 added to the DIC pool will be depleted resulting in a decrease of the $\delta^{13}C_{DIC}$ signatures. This will be reflected in very negative $\delta^{13}C_{DIC}$ compositions reaching up to -60‰ (Alperin and Hoehler, 2009; Assayag et al., 2008).

$CH_4 + 2O_2 \rightarrow HCO_3^- + H_2O + H^+$ (Eqn 8)

$CH_4 + SO_4^{2-} \rightarrow HCO_3^- + HS^- + H_2O$ (Eqn 9)

Mineral dissolution and rock weathering can also be dominant sources of carbon in total DIC within the aquifer formations (Eqns 3-4). These reactions can be discerned from analyzing isotopic variations in combination with hydrochemistry. High TDS values corresponding with the enrichment of $\delta^{13}C_{DIC}$ and increasing DIC concentrations can indicate carbonate dissolution. Other geochemical influences for the enrichment of $\delta^{13}C_{DIC}$ may result from calcite formations with high Mg^{2+} concentrations or dolomite dissolution (Eqn 4), which may translate to gypsum dissolution. Dolomite dissolution can also be seen in a positive correlation of Mg^{2+} with $\delta^{13}C_{DIC}$, and gypsum dissolution with SO_4^{2-} and $\delta^{13}C_{DIC}$. If an inverse relationship between $\delta^{13}C_{DIC}$ and DIC is present, it can indicate bacterial activity in the groundwater system. As a result, the bacteria will metabolize and produce isotopically depleted organic carbon to be added to total DIC. Examples of studies highlighting these relationships include Atekwana et al., 2004; Jiráková et al., 2010; Marfia et al., 2003; Spence et al., 2005; and Tweed et al., 2005.

2.3.5 Sulfur and Oxygen Isotopes in Dissolved Sulfate

Sulfur can be found in numerous forms in groundwater: minerals, dissolved sulfate, dissolved sulfide, and hydrogen sulfide gas. The sulfur isotope, ^{34}S, can play a key part in tracing the origin of waters due to fractionation within biological reactions, introducing a wide range of isotopic compositions (Figure 17). These

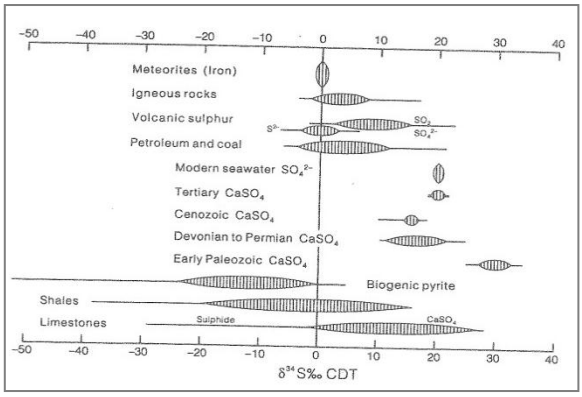

Figure 17: Natural variation of sulfur isotope values in the environment (Clark et al, 1997)

geochemical pathways introduce fractionation through the dissolution of sulfate minerals, sulfate reduction, sulfide oxidation, and the general exchange of isotopes (Eqns 10-15) as summarized by Krouse et al. (1991) and Clark and Fritz (1997). Sulfide oxidation may be catalyzed biologically or abiologically in low pH settings. These reactions may proceed abiologically or catalyzed by bacteria such as *Thiobacillus thiooxidans*, *Thiobaciullus ferrooxidans*, and *Desulfovibrio desulfuricans* (Krouse et al., 1979).

Sulfide oxidation:

$$FeS_2 + 3.5O_2 + H_2O \rightarrow Fe^{2+} + 2SO_4^{2-} + 2H^+ \quad \text{(Eqn 10)}$$

$$FeS_2 + 14Fe^{3+} + 8H_2O \rightarrow 15Fe^{2+} + 2SO_4^{2-} + 16H^+ \quad \text{(Eqn 11)}$$

$$Fe^{2+} + 0.25O_2 + H^+ \rightarrow Fe^{3+} + 0.5H_2O \quad \text{(Eqn 12)}$$

Sulfate reduction – fixed carbon oxidation and reduced carbon oxidation:

$$2CH_2O + SO_4^{2-} \rightarrow 2HCO_3^- + H_2S \quad \text{(Eqn 13)}$$

$$CH_4 + SO_4^{2-} \rightarrow HCO_3^- + HS^- + H_2O \quad \text{(Eqn 14)}$$

Exchange of isotopes in sulfate:

$$SO_4^{2-} + 2H^+ \leftrightarrow HSO_4^- + H^+ \leftrightarrow H_2SO_4 \leftrightarrow SO_{3(aq)} + H_2O \quad \text{(Eqn 15)}$$

The depleted source of ^{34}S in pyrite during oxidation reactions (Eqn 10-12) will result in depleted sulfur in SO_4^{2-}, seen in depleted $\delta^{34}S_{SO4}$ signatures. This depletion has been seen to reach -20‰ in biologically mediated reactions and -2‰ abiotically (Kaplan and Rittenberg, 1964; Fry et al. 1986). The presence of bacteria to facilitate reduction reactions introduces the preference for lighter sulfur, accumulating enriched sulfur in the residual sulfate. Hence, enriched $\delta^{34}S_{SO4}$ signatures are seen in both forms of sulfate reduction (Eqns 13-14), ranging typically from 9 to 45‰ (Clark and Fritz, 1997; Fritz, 1989; Krouse and Mayer, 2000).

Oxygen in sulfate can be used as an additional proxy to understand sulfate sources. The ^{18}O signature in SO_4^{2-} can be formed from isotopic exchange in two sources: oxygen within the water molecule of the original water source and back with the oxygen in sulfate (Eqn 15). These endmembers introduce complications when attempting to tease apart $^{18}O_{SO4}$ sources. Similar to ^{34}S, ^{18}O will also become enriched during sulfate reduction due to microbial preferences. The enrichment follows Rayleigh distillation and the exact isotopic composition will depend on the oxygen isotope composition within the original water source and the fraction of $^{18}O_{H2O}$ and $^{18}O_{SO4}$ in the sulfate molecule (Mizutani and Rafter, 1973). However, estimations predict the enrichment of ^{18}O during reduction is 2.5 to 4 times less than that of ^{34}S, but the enrichment increases throughout the reaction until it plateaus (Fritz et al. 1989; Pierre, 1989).

Using the isotopic signatures of $\delta^{34}S_{SO4}$ and $\delta^{18}O_{SO4}$ in conjunction with one another can provide evidence of sulfate reduction. With the bacterial preference of lighter isotopes in both species, enrichment in both signatures is indicative of reduction.

Relevant anthropogenic effects on sulfate isotope compositions may include acid mine drainage (AMD) and surface mining. The prevalent reaction mechanism resulting from AMD is the oxidation of pyrite. Pyrite in coals has been shown to range from -50 to +34‰ in sulfur isotope compositions (Smith et al., 1974; Hackley et al., 1986), more commonly between -10 and 0 ‰ (Figure 17). During pyrite oxidation, ^{34}S will lack reasonable fractionation but ^{18}O will undergo enrichment, more so in the presence of bacteria. Low sulfur isotope compositions have been shown to correspond with pyrite oxidation and oxidation of organic sulfur compounds from soils (Krouse et al., 1996; Taylor et al. 1984; Van Stempvoort et al., 1994). As a result, $\delta^{34}S$ and $\delta^{18}O$ isotope signatures can be used to evaluate the oxidation of pyrite in association with AMD (i.e. Gammons et al., 2010). Surface mining pits can result in the mixing of natural sulfate with

sulfide of biogenic sources, with depleted $\delta^{34}S$ signatures of ~ -30‰ and $\delta^{18}O$ ~ -30‰ (i.e. Krouse et al., 2000). Examples studies include Berner et al., 2002; Lewica-Szczebak, 2009; Trembaczowki et al., 2004; Van Donkelaar et al., 1995; and Van Stempvoort et al., 1994.

Isotopes of dissolved sulfate have been used to differentiate sources and explain variations in groundwaters due to its stability and conservative nature through redox reactions. Sulfate isotopes can be used to distinguish water horizons and sources of sulfate. These sources may include precipitation, runoff, and groundwater infiltration (Van Stempvoort et al., 1994). Other causes in enrichment of oxygen isotopes in sulfate can be due groundwater recharge leaning towards enriched signatures from precipitation, atmospheric oxygen at +23‰, or carbonate dissolution. Carbonate minerals are enriched in ^{18}O, resulting in the final enriched groundwater during dissolution (Van Donkelaar et al., 1995).

2.3.6 Carbon and Hydrogen Isotopes in Dissolved Methane

One of the concerns associated with Marcellus Formation drilling is that stray methane can contaminate shallow groundwater aquifers of the area. However, high methane concentrations in groundwaters cannot solely be used as indicators of methane contaminations from shale gas development. This is because methane can be produced in geological formations by three sources, namely biogenic, thermogenic, and abiogenic/mantle. However, methane produced by these different processes has very distinct C and H isotopic signatures and can be used to fingerprint sources of methane leaks into groundwater. Higher chain hydrocarbons, such as ethane and propane, can be used to further constrain formation pathways in addition to other isotopic proxies.

Biogenic methane is produced in an anaerobic setting by the metabolizing of bacteria, most commonly in shallow groundwaters. Fermenting bacteria break down organic compounds into molecules such as acetate, fatty acids, CO_2 gas, or H_2 gas. Specific bacteria use these molecules and gases to produce methane through acetate fermentation, also known as methyl type fermentation, or CO_2 reduction (Eqns 5-7). Methanogenic bacteria will preferentially metabolize lighter carbon in the system, resulting in highly depleted $\delta^{13}C_{CH4}$ signatures in dissolved methane with a range from -50 to -110‰ (Schoell, 1980; Whiticar, 1999). These high fractionation factors are due to lower amounts of energy required, kinetic effects, and the source material compositions. The kinetic effects are seen within faster diffusion rates in molecules with lower mass; ^{12}C molecules in comparison to ^{13}C based molecules. This microbial preference also corresponds to the enrichment in $\delta^{13}C_{DIC}$ during the production of methane (Section 2.3.4). Biogenic methane can be further analyzed into formation from freshwater or saline (marine) environments, with increased depletion in $\delta^{13}C_{CH4}$ and enrichment in $\delta^{2}H_{CH4}$ from saline environments. This generalization arises from the dominant methane forming process occurring; acetate pathways in freshwater and carbonate reduction in marine environments (Whiticar, 1999).

Abiogenic methane, on the other hand, is produced in low redox groundwaters, without the presence of organic matter and in much deeper settings of high pressure and temperature. This methane is formed through the reaction of mafic minerals with CO_2. These settings are not present and abiogenic methane is not expected to be seen.

Thermogenic methane is indicative of natural gas residing in sedimentary basins through thermally modifying organic matter. This methane is sought after by industry, as it is cracked thermally from the original high mass hydrocarbons. The general range for thermogenic methane

is -100 to -275‰ in δ^2H_{CH4} and -20 to -50‰ in $\delta^{13}C_{CH4}$ (Whiticar, 1999). More specifically, this methane can be in the form of wet gas associated with crude oil or dry gas not in association with petroleum. The high hydrocarbon chains of wet gas are found to have δ^2H_{CH4} and $\delta^{13}C_{CH4}$ compositions up to -250‰ and -50‰, respectively (Schoell, 1980). Dry gas, from marine or humic sources, is less depleted; up to ≈ -175‰ in δ^2H_{CH4} and -45‰ in $\delta^{13}C_{CH4}$ (Schoell, 1980).

These differences in isotopic compositions between biogenic and thermogenic methane are due to parent material, maturation factors, kinetic effects, temperature differences, and the hydrocarbon generation itself. These fractionation factors allow for the ability to distinguish these pathways. Studies such as Whiticar (1999) and Coleman (1994) have well-defined these boundaries for sourcing methane as biogenic or thermogenic and demonstrates the use of stable isotopes of methane as fingerprints to trace dissolved methane through waters for contamination purposes (Figure 18).

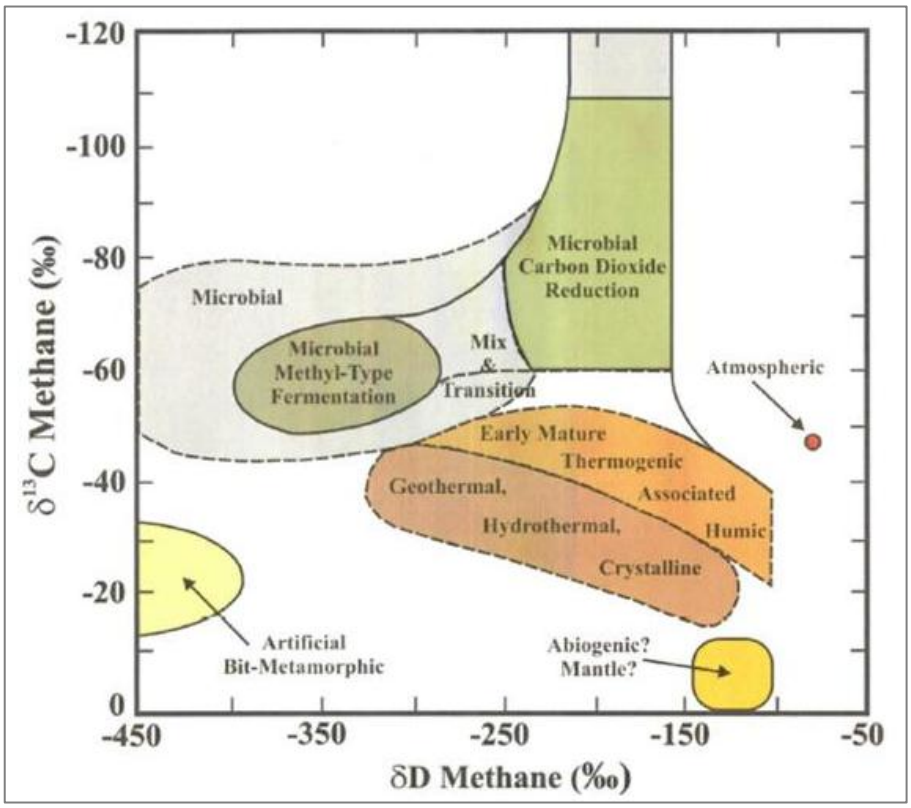

Figure 18: Formation pathways of methane (Whiticar, 1999)

A recent study by Osborn et al. (2011) in northeast Pennsylvania and upstate New York utilized these isotope proxies to distinguish contributions of biogenic methane from deeper thermogenic shale gases like the Marcellus Formation and/or Utica. However, there could be several potential sources of biogenic/thermogenic methane in groundwaters. For example, biogenic methane can originate in landfills or from microbial processes in shallow coal beds. On the other hand, there are several sources of thermogenic methane such as abandoned oil and gas wells, gas storage fields, and thermally mature coal beds. Further, mixing of methane from several sources can modify/overprint these isotopic signatures. Hence, in order to clearly identify sources of methane contamination in north central West Virginia, different end members need to be identified. In addition, the isotopic composition of associated molecules such as carbon dioxide and water, and the proportion of ethane, propane and other natural gas liquids to the methane needs to be taken into account.

Additional analysis can be done to further constrain methane sources by analyzing the percentage of higher chain hydrocarbons and their isotopic compositions. This is plausible because natural gas produced by microbial processes is dominantly composed of methane. These proxies can better delineate the origin, potential mixing, and migration of natural gas (i.e. Atekwana, 1996; Börjesson et al., 2007; Cheung et al., 2010; Laughrey et al., 1998; Kinnon et al., 2010; Osborn et al., 2011; Sharma et al., 2008; Shengfei et al., 2006; Zhang et al., 2001). However, these detailed analyses are out of the scope of this study.

3.0 – Methodology

3.1 – Sample Collection

Water samples were collected from 41 groundwater wells of both private and public supply, accessed through permissions of the USGS WV Water Science Center (Figure 11). Each well was purged following the EPA Code 540/S-95/504 (Puls et al., 1996) through a hose line. Water samples were collected after 2-3 casing volumes were removed using Teflon sampling line connected to the well plumbing at a rate of less than 1 L/min.

Samples were collected after field parameters i.e. temperature, conductivity, pH, dissolved oxygen were stabilized to ±10% using a 650MDS YSI meter (Appendix A, Table 1). Isotope samples personally collected at each groundwater well site included one sample for $\delta^{13}C_{DIC}$, duplicate samples for $\delta^{2}H_{H2O}$ and $\delta^{18}O_{H2O}$, one sample for $\delta^{13}C_{CH4}$ and $\delta^{2}H_{CH4}$ at selected sites, and one for $\delta^{34}S_{SO4}$ and δO_{SO4}. The USGS scientists sampled each well for major cations and anions, trace elements, dissolved gases, and radiochemistry. All samples were collected wearing nitrile gloves and were refrigerated until analysis was completed or shipped to the appropriate laboratory.

The $\delta^{13}C_{DIC}$ samples were collected through a 60 mL syringe (pre-rinsed 3 times with sample water) with a Lueur-Lok tip. The water was filtered through a Cameo 0.45 μm nylon pre-filter into a 10 mL Wheaton serum vial with no headspace. 2-3 drops of benzalkonium chloride (17% w/w) were added to the vial as an astringent. A 20 mm Teflon septa was placed on the top and sealed with Al caps using a crimper. Samples were refrigerated and stored for analysis. Duplicate samples for $\delta^{2}H_{H2O}$ and $\delta^{18}O_{H2O}$ were taken by filling a pre-rinsed 8 mL glass threaded vial, with no headspace. Parafilm was wrapped around the lid of the vial and refrigerated until analysis. Sulfate samples were collected in a pre-rinsed 1 L polyethylene bottle with no

headspace. Each sample was filtered back into the rinsed bottle through a 45 mm diameter, 0.4 μm PCM filter. During the filtering process, a glass petri dish was used to cover the filtering sample to prevent the oxidation of sulfide to sulfate. Further sample preparation at Isotech Laboratory includes precipitating $BaSO_4$ powder for the isotopic analysis of sulfate. Numerous duplicate samples were taken to ensure quality control. Samples for dissolved methane were collected in a rinsed 5 gallon bucket. The bucket was filled with sample water through Teflon tubing connected to the groundwater sampler so that the water line was above the height of the sample bottle. The sampling tube was inserted into the pre-rinsed methane sample bottle and fully submerged in the filled bucket. After the duration of approximately 3 sample bottle fills, the sample hose was quickly removed underwater and the sample bottle was capped underwater. Extra care was taken not to expose the sample to air, fully underwater, with no air bubbles present after being capped.

Major cations and anions were analyzed at the National Water Quality Laboratory (NWQL). Calcium, magnesium, potassium, sodium and iron were filtered in the field through a 0.45 μm filter. Analysis is completed using inductively coupled plasma atomic emission spectroscopy (ICP-AES). Chloride and sulfate are analyzed using a Dionex DX-120 ion chromatography (IC) system. Relative standard deviations are reported from NWQL in terms of percent and are 3% (sulfate and chloride) and 11% (calcium, iron, potassium, magnesium, and sodium). Dissolved gases are analyzed at NWQL, concentrations calculated following Wiesenburg and Guinasso (1979).

A field titration was done at each sample site to determine alkalinity as total $CaCO_3$ (mg/L). The field titrator was out of service for 14 sites; the subsequent samples were analyzed for alkalinity at the NWQL. When alkalinity was titrated, HCO_3^- concentrations subsequently

were determined, and used for calculating DIC. Total DIC is calculated as the total of the carbon species from the dissociation of H_2CO_3 through the dissolving of CO_2 in water. Therefore, total DIC is the sum total of $H_2CO_3^*$, HCO_3^-, and CO_3^{2-} concentrations. As mentioned, HCO_3^- concentrations were determined in the field, but $H_2CO_3^*$ and CO_3^{2-} are calculated the Van't Hoff equation. Variables in the Van't Hoff equation include literature K_{CO2}, K_1, and K_2 values and the each site's field temperature and pH data, providing the ability to calculate site specific values of K_{CO2}, K_1, and K_2. Each concentration of H_2CO_3 is back-calculated using the field determined concentration of HCO_3^- and site specific K_1 value. Concentrations of CO_3^{2-} are calculated using the site specific K_2 and the concentration of H^+ from pH.

3.2 – Analytical Techniques

Stable isotopes of water and DIC were analyzed within the West Virginia Stable Isotope Laboratory (WVSIL) using a Finnigan Delta Advantage continuous flow isotope ration mass spectrometer (IRMS) with the ThermoQuest Finnigan GasBench II device. Each sample is flushed using the PAL autosampler system, equilibrated for 24 hours, and then sampled with PAL system. The headspace is analyzed using a double-needle; while the carrier gas is being injected continuously into the sample vial through one slit, the other removes headspace evacuated by the gas. Duplicate samples of 10.0 µL are taken over the course of 60 seconds with a total 10 replications for each sample. From there, the head space sample is carried through the components of the IRMS via the carrier gas through the GasBench. Any water present is first removed from the sample and gas mixture through a NAFION™ tube, removing any vapor by the pressure of the gas. The remaining dried sample gas passes through a sample loop via the Valco valve, removing a set volume of sample to send through the isothermal gas chromatograph

(GC). In the GC, the specific isotope-containing gas is separated from the blend to be analyzed for the desired isotopic composition. Finally, a second NAFION™ tube is employed and the isotope is separated by mass in the IRMS. These components are highlighted within Figure 19 (Thermo Finnigan, 2001; Torres et al., 2005). The IRMS software, ISODAT 3.0, produces a sample chromatogram with 5 reference standard peaks and 10 sample peaks displayed. The peaks are analyzed and processed with respect to the corresponding lab standard derived from the original IAEA reference standard. Internal lab standards are incorporated in triplicates in the beginning, middle (if a high number of samples), and end of each run sequence for QA/QC checks. These internal standards are calibrated against the respective IAEA international standard.

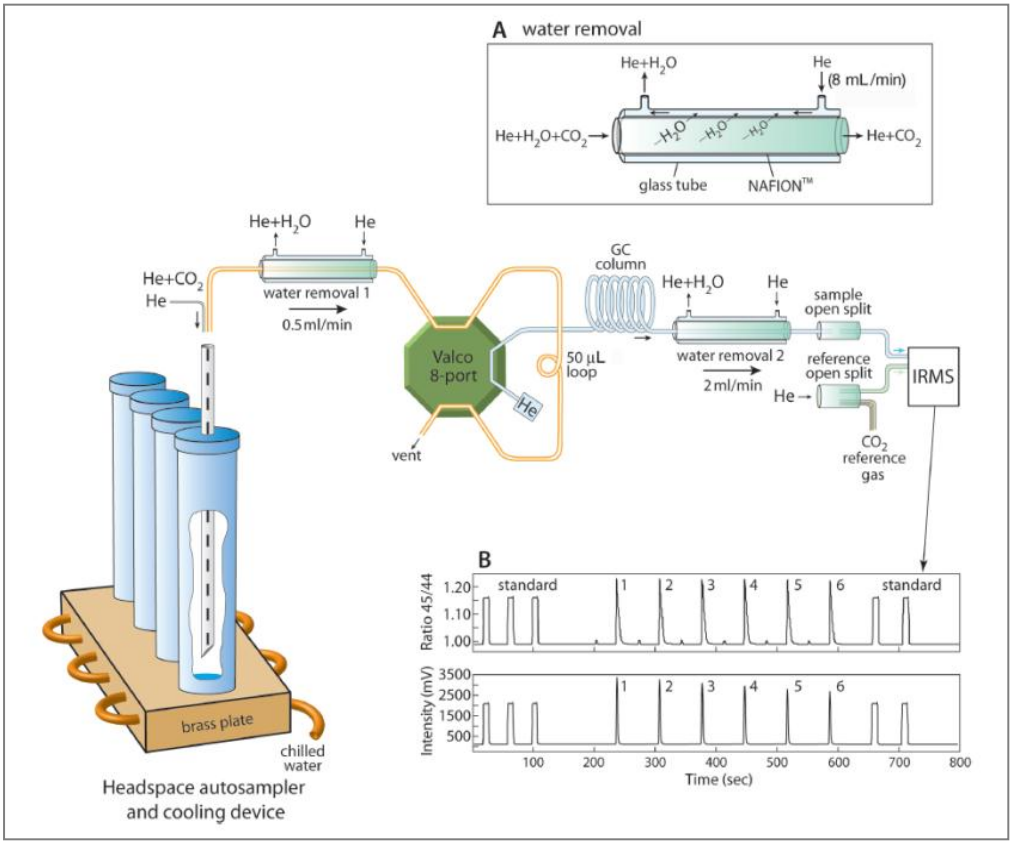

Figure 19: Analysis pathway and components of the GasBench and IRMS system (Torres et al., 2005)

A minimum of 3 sample duplicates were also included in each analysis. However, specific lab preparation, reference gas blend, and lab standards differ for each isotopic analysis.

The $\delta^{18}O$ and $\delta^{2}H$ signatures of waters are analyzed individually, with different carrier gases. Sample aliquots of 0.5 mL are injected into a flat bottom vial for the analysis of $\delta^{18}O$, and flushed using a blend of CO_2 and He gases and CO_2 as a reference gas during analysis. The analysis of $\delta^{2}H_{H2O}$ requires a blend of H_2 and He gas during flushing, with H_2 as a reference gas for analysis. Additional, platinum catalysts are employed through the flushing, equilibration, and analysis processes. Specific internal lab standards used in these analyses are Hawaiian Spring, Eldorado, and Morgantown tap waters; calibrated against the IAEA standard of V-SMOW. Precision rates are $\delta^{18}O_{H2O} \pm 0.02‰$ and $\delta^{2}H_{H2O} \pm 1‰$.

The sample vials for $\delta^{13}C_{DIC}$ analysis are flushed prior to analysis with only 60 µL of phosphoric acid in a round bottom vial using He gas. After flushing, 650 µL of the sample water is added, shaken, and equilibrated for 24 hours. Analysis is completed using CO_2 as the reference gas. Carbonate normalization standards of $CaCO_3$ and pure ground "Le Grand" limestone are used as internal standards, but have 100 µL of phosphoric acid added and shaken after flushing for the 24 hour equilibration. Additionally, Morgantown tap water is used as an internal standard for carbon analysis of DIC in addition to isotopes of water. Internal carbonate standards are calibrated against the IAEA V-PDB standard. The precision for $\delta^{13}C_{DIC}$ is $\pm 0.02‰$.

Groundwater analyses for stable isotopes of dissolved methane and dissolved sulfate were completed at Isotech Laboratory. A dual-inlet IRMS is predominantly used for analysis of isotopes in dissolved methane. Specific models are Delta S for $\delta^{13}C_{CH4}$and Delta Plus XL for $\delta^{2}H_{CH4}$. This is a high precision, offline preparation system where the pure sample gas is compared directly to the reference gas. An online gas chromatography – combustion – isotope

ratio mass spectrometer (GC-C-IRMS) system is used when the samples contain low concentrations of dissolved methane, employed for a total of 4 samples. The setup for a GC-C-IRMS is similar to that of a continuous flow except that the carrier gas containing sample passes through a GC column first to separate and then is combusted via oxidation in a reactor. Water is then removed via NAFION™ tubes and isotopes separated within the mass spectrometer. Duplicate samples consist of 10% of the total samples in smaller analysis sets and every 10^{th} analysis is a duplicate sample within larger sets of analyses.

Analysis of methane isotopes is completed through gas extraction from water by headspace equilibration. The internal check standards for methane isotopes cover a wide range of natural gas samples contained in high volumes at Isotech. Precision rates for dissolved methane isotopes at Isotech are $\delta^{13}C_{CH4}$-offline ± 0.1‰, $\delta^{13}C_{CH4}$-online ± 0.4, $\delta^{2}H_{CH4}$-offline ± 2‰ and $\delta^{2}H_{CH4}$-online ± 5‰.

Sulfate isotopes are analyzed through the precipitation of $BaSO_4$ from the sampled groundwater. Each sample is acidified with HCl^- to a pH or approximately 3-4 and heated for 45-60 minutes. Immediately after heating, 20% $BaCl_2$ solution is added to the acidified and heated sample to precipitate $BaSO_4$. The entire solution is cooled to room temperature, filtered using pre-weighed 0.2 µm filters and dried overnight at a temperature around 90°C. The precipitated $BaSO_4$ is scraped from the filter, homogenized, and sealed in a vial until analysis (Révész and Qi, 2007). This solid sample is analyzed for $^{18}O_{SO4}$ using a temperature conversion elemental analysis - IRMS system (TC/EA-IRMS), in which gas is produced from the sample in the TC/EA and isotopically analyzed with the IRMS. The analysis of $^{34}S_{SO4}$ is performed with an elemental analyzer-IRMS (EA-IRMS). The sample is combusted with a flow of helium gas, forming SO_2. A continuous flow carries the sample through the system to the IRMS. Dissolved sulfate isotope

standards include by normalization and check standards. For $\delta^{18}O_{SO4}$, these standards include IAEA (No-3) and USGS (34 and 35) standards. Sulfanilic acid (Merck brand) and NBS-123, NBC-127, IAEA S-1, and IAEA S-3 are used for $\delta^{34}S_{SO4}$. Precision rates are ± 0.5‰ for both $\delta^{34}S_{SO4}$ and $\delta^{18}O_{SO4}$.

4.0 – Results & Discussion

4.1 Major Hydrochemistry

In order to delineate the variations in groundwater geochemistry within the study area, the 9 aquifer formations were grouped together by geologic period of deposition (Figure 10). Routine hydrochemistry was collected at each of the groundwater sites (Appendix A, Table 2), and a piper plot was created to determine the hydrochemical facies throughout the study area. Generally speaking, the groundwater chemistry differs significantly not only between lithologies, but greatly between periods of deposition as well (Figure 20). The dominant facies include calcium, sodium or potassium, and bicarbonate types with local areas of sulfate and chloride type waters.

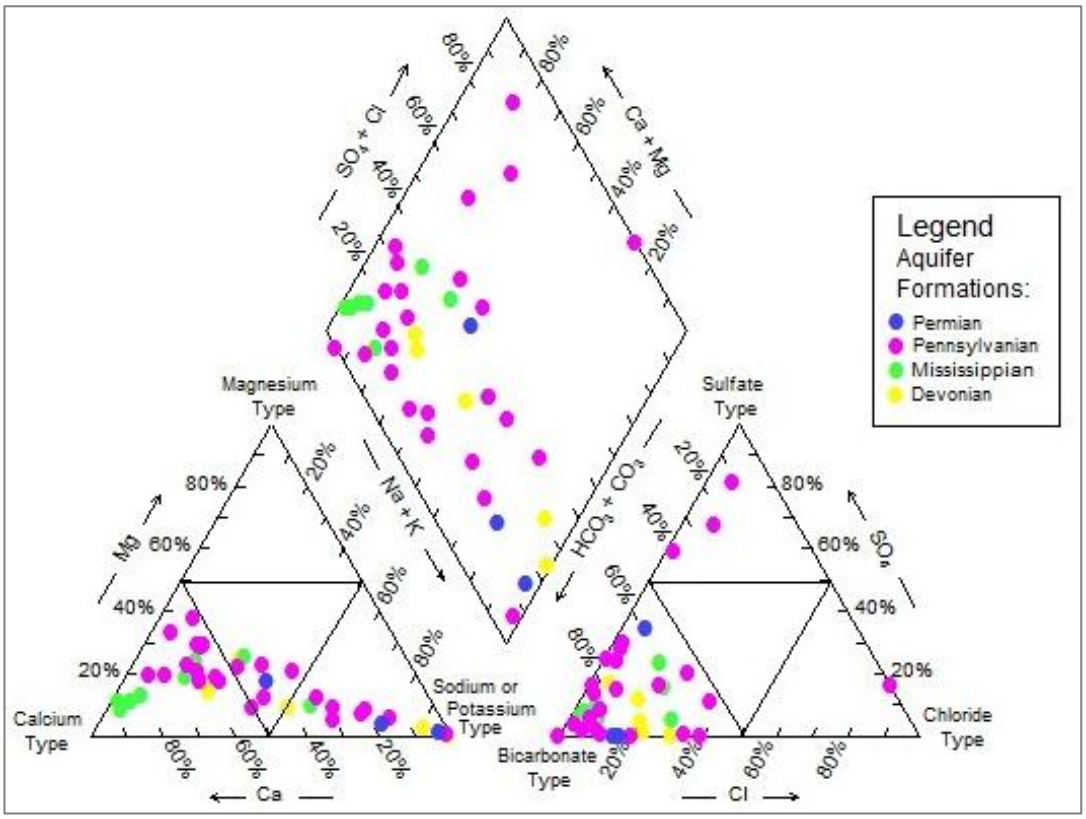

Figure 20: Piper plot designating hydrochemical facies

The greatest variation in major cation and anion distribution is within the Pennsylvanian, which is expected with the cyclical changes in lithology through changing depositional environments. Rock weathering and dissolution causes increased dissolving and suspension of cations and anions in the groundwater. Initial causes for such variation were examined through common types of rock weathering and mineral dissolutions correlations. With the extreme variations seen within hydrochemistry and the lack of knowing the exact lithology accessed through the well screens, analysis for this research is grouped into geologic ages of formation deposition. This grouping into age series allows analysis of groundwaters of similar depths and environments of deposition.

With the abundance of shales and coals in the majority of the study lithologies, pyrite oxidation (Eqn 10-12) is expected to be the dominant source of iron and sulfate, with gypsum dissolution potential but in minor quantities. Based on simple molar plots, half of the formations appear to show evidence of pyrite oxidation and gypsum dissolution (Figures 21-22). However, there are multiple sources that can produce iron and sulfate through the study area (Chapter 2.2). These include evaporite dissolution, gypsum dissolution, oxidation of other sulfate bearing minerals, sulfate reduction, weathering or oxidation of iron bearing minerals and acid mine drainage related reactions. As a result, trends within molar ratios are preliminary indicators but cannot be used as definite conclusions for pyrite and gypsum as iron and sulfate sources.

Carbonate rocks are not widespread through many of the aquifers aside from the Greenbrier Formation of Mississippian age except locally from cyclical deposition stages. Carbonaceous shales are also common throughout most of the lithologies (USGS, 2012). Mineral dissolution of calcite and dolomite is common within carbonates (Eqns 3-4), and is evident in aquifers with limestone zones; Devonian, Pennsylvanian, and Permian (Figure 23). Calcite

dissolution is not directly evident with in the Mississippian formations, but it is the only age series with indications of dolomite dissolution (Figure 24b). Dolomite dissolution may also account for ~50% of the variation in the Pennsylvanian (Figure 24c).

Sources of these cations and anions extend beyond that of lithology, including coal mining, acid mine drainage and previously drilled wells. Additional geochemical reactions can introduce changes in concentrations of cations and anions, including precipitation of minerals i.e. the production of bicarbonate through sulfate reduction instigating calcite precipitation, lowering calcium concentrations. Ions can also exchange with adjacent aquifer compositions and on potential cation exchange sites on clays in shale lithologies. As a result, hydrochemistry alone cannot distinguish geochemical pathways accounting for the variation in cation and anion concentrations. Hence, stable isotopes were used to discern the variation in geochemical pathways for the remaining analyses, with hydrochemistry data as an aid in the interpretation of isotopic signatures.

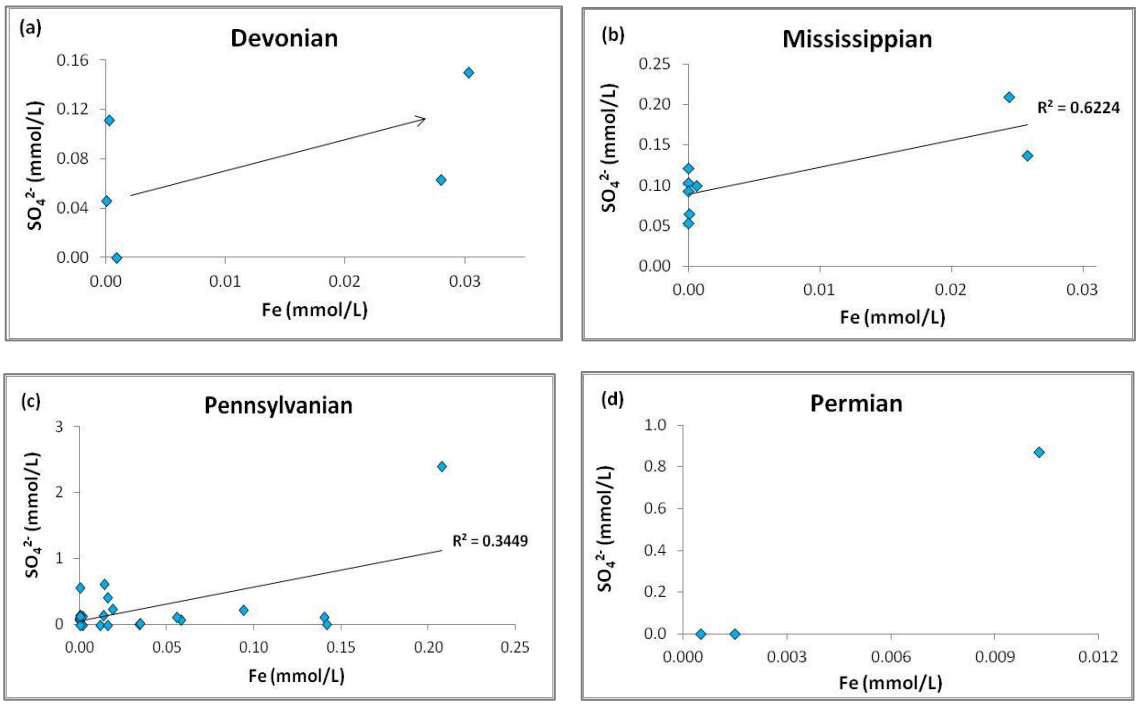

Figure 21a-d: Pyrite oxidation within regional groundwaters

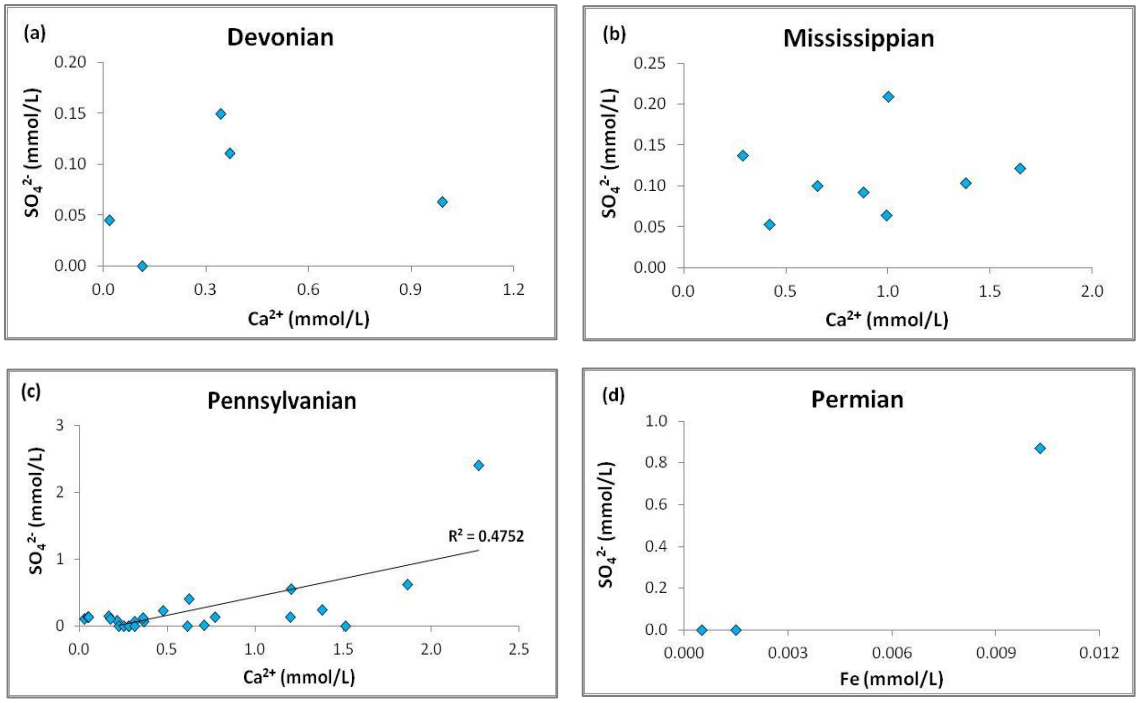

Figure 22a-d: Gypsum dissolution within study area groundwaters

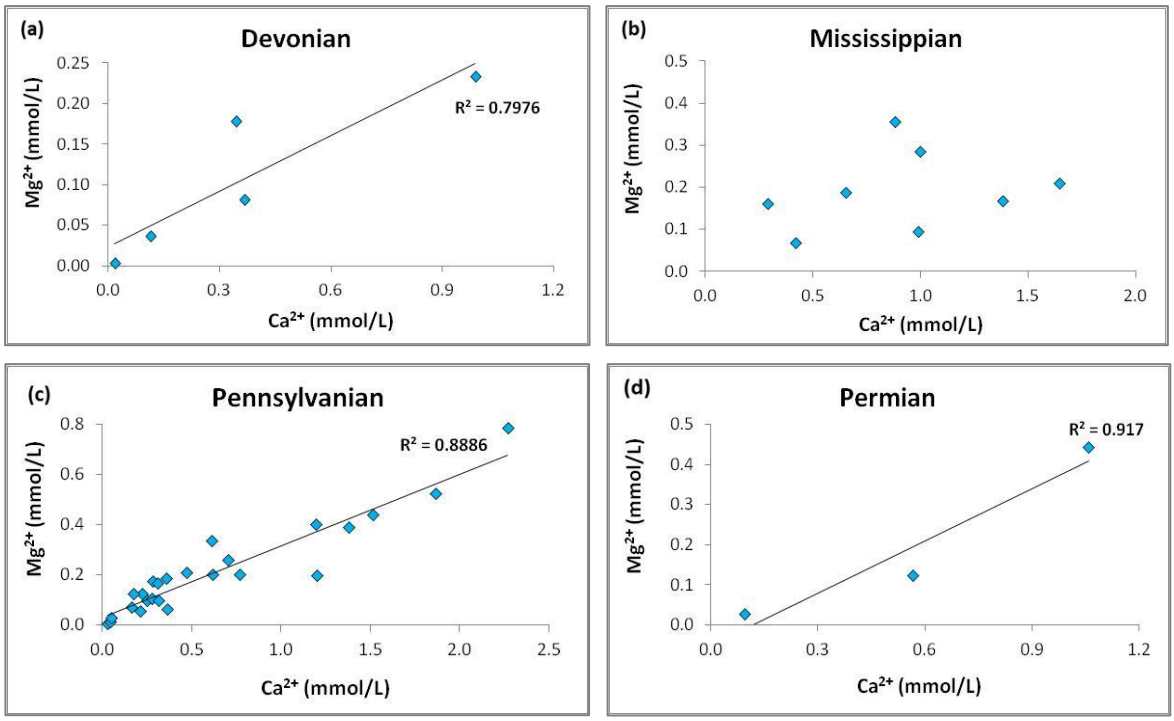

Figure 23a-d: Calcite dissolution within study area groundwaters

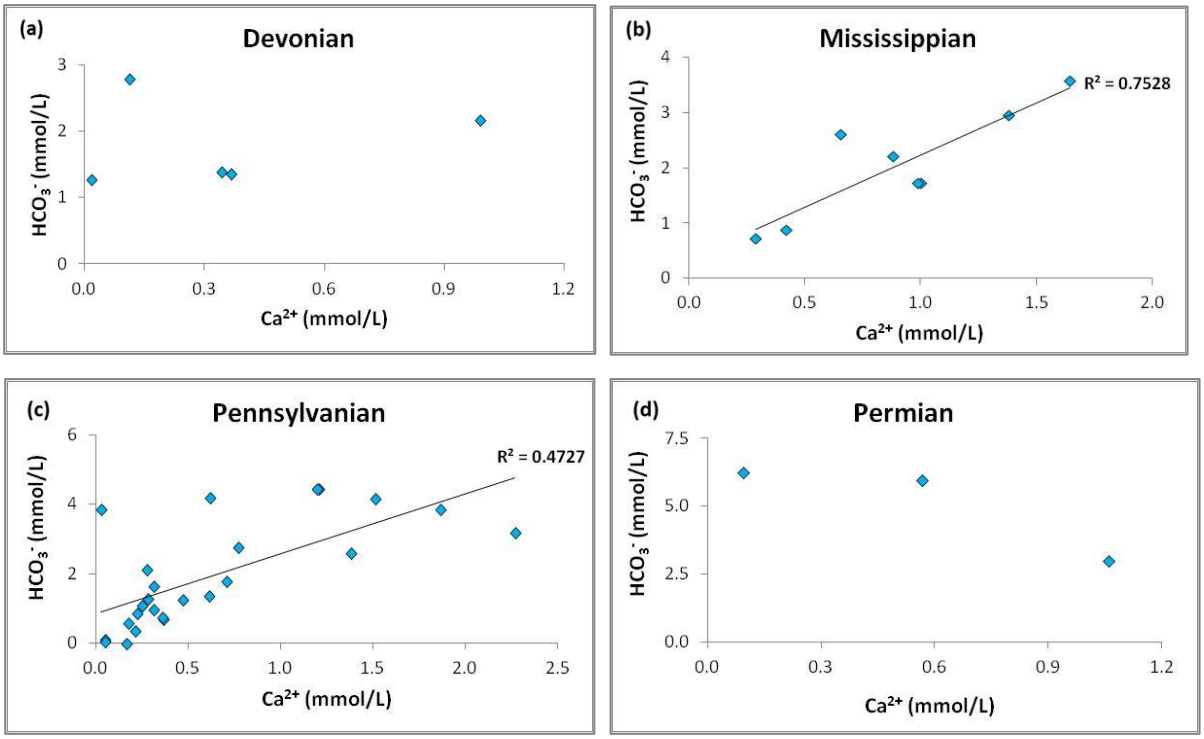

Figure 24a-d: Dolomite dissolution within study area groundwaters

4.2 – Isotopes of Hydrogen and Oxygen in Water

The groundwater samples collected in the Monongahela river basin have negative δ^2H compositions ranging from -50.08 to -67.77‰ V-SMOW, with negative ^{18}O compositions from -7.98 to -10.33‰ V-SMOW (Appendix A, Table 3). These values were plotted against the GMWL, originally established by Craig (1961), to determine if

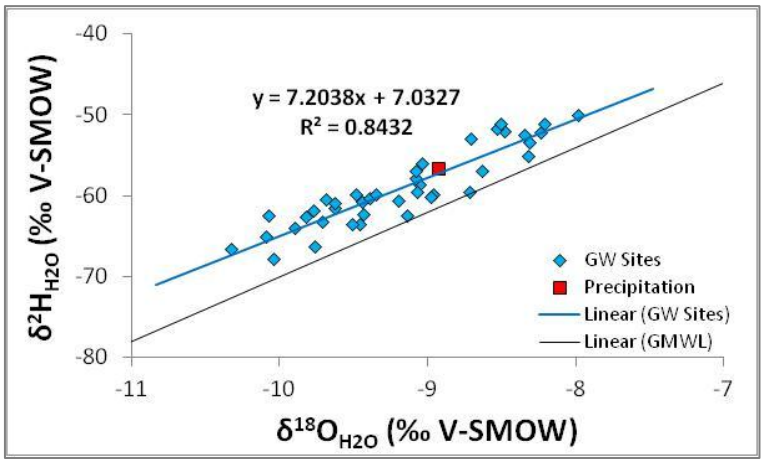

Figure 25: Origin of isotopes in water with reference to the GWML

recharge conditions are dominated by precipitation (Figure 25). The linear correlation of hydrogen and oxygen shows the groundwaters plotting above and just above the central area of the GMWL. The basic, preliminary observation with the GMWL plot indicates a consistent warm region in higher altitudes with the vapor mass originating from an arid source (Chapter 2.3.3, Figure 12). However, a more detailed analysis for vapor and recharge sources can be done with literature studies and *d*-excess.

To further evaluate this vapor source, the humidity at the time for formation is examined through *d*-excess values. The GMWL assumes a humidity of 85%, correlating to *d*–excess values of 10‰. Assuming precipitation dominated recharge, the *d*-excess values of an arid source would be significantly higher than 10‰. The groundwater sites show *d*-excess values ranging from 10.3 to 18.1‰, with of average at 14.41‰ (Appendix A, Table 3). These values correspond with a humidity level of ≈75% which doesn't correspond with an arid climate source for vapor mass. To examine additionally, these groundwater signatures are compared with predicted rainfall signatures using the Water Resources Research by Bowen et al. (2012). Using specific latitude, longitude, and altitude values, $\delta^{2}H_{H2O}$ and $\delta^{18}O_{H2O}$ signatures can be predicted at specific locations across the United States. Comparisons of the sampled groundwater signatures with the predicted precipitation signatures (at the same latitude and longitude locations) show an overlap of isotopic compositions (Figure 26). This detailed analysis provides a more accurate conclusion of recharge by local precipitation, in which the calculated d-excess compositions of precipitation correspond with the groundwaters (Appendix A, Table 4). To further confirm, the collected rain water precipitation sample also falls amidst both linear trends.

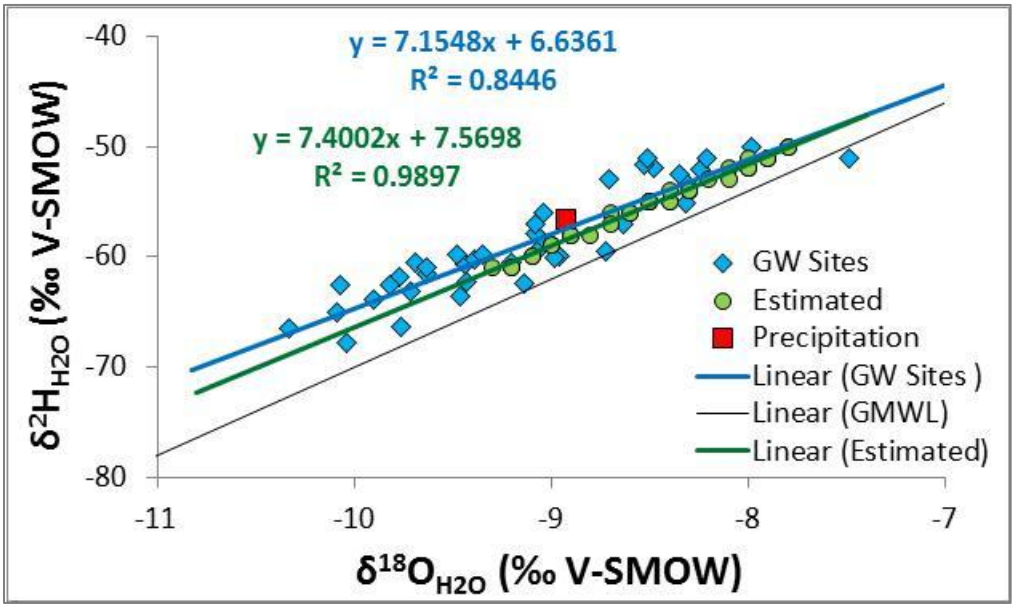

Figure 26: Groundwater compositions compared with estimated area precipitation compositions. Estimated precipitation data from Bowen, 2012

Numerous studies have been done to analyze national and global trends in ^{18}O and ^{2}H in precipitation and rivers. A study by the USGS (Kendall and Coplen, 2001) correlated areas across the United States using $\delta^{18}O_{H2O}$, $\delta^{2}H_{H2O}$, *d*-excess, and the corresponding LMWL slope. The study area groundwater results fall within the range of the central east coast data for all mentioned parameters. Signatures of $\delta^{18}O_{H2O}$ and $\delta^{2}H_{H2O}$ are comparable with signatures of precipitation and rainwater with the study area region along the east coast. Topography, latitude, and temperature are shown to influence the composition of $\delta^{18}O_{H2O}$ on the east coast and therefore the study area. The composition of $\delta^{2}H_{H2O}$ is also affected by latitude changes but also with the type of precipitation i.e. snowfall vs. rain (Bowen and Wilkinson, 2002; Dutton et al., 2005; Kendall and Coplen, 2001). However, extrapolated contours for ^{18}O, ^{2}H in the eastern states show sudden southern curvature occurring in West Virginia, resulting in higher *d*-excess

values (Kendall and Coplen, 2001). This dipping trend in $\delta^{18}O_{H2O}$ contours generally matches up with the jet stream wind pattern originating from the Great Lakes region (Figure 27).

The high levels of evaporation in the area of the Great Lakes can introduce additional (recycled) water vapor into the atmosphere. Fractionation during evaporation results from the introduced kinetic effects, leading to isotopic depletion in the vapor mass and consequently higher *d*-excess values. The evaporation of Lake Michigan comprises between 4-16% of the total vapor in the atmosphere, and can increase *d*-excess values of downwind areas by an average of 3.5‰ (Gat et. Al, 1994; Machavarma and Krishnamurthy, 1995). This increase in *d*-excess from the evaporation of the Great Lakes corresponds with the slightly higher *d*-excess values calculated from the groundwater samples. The correlation with meteoric waters further confirms groundwater recharge by precipitation.

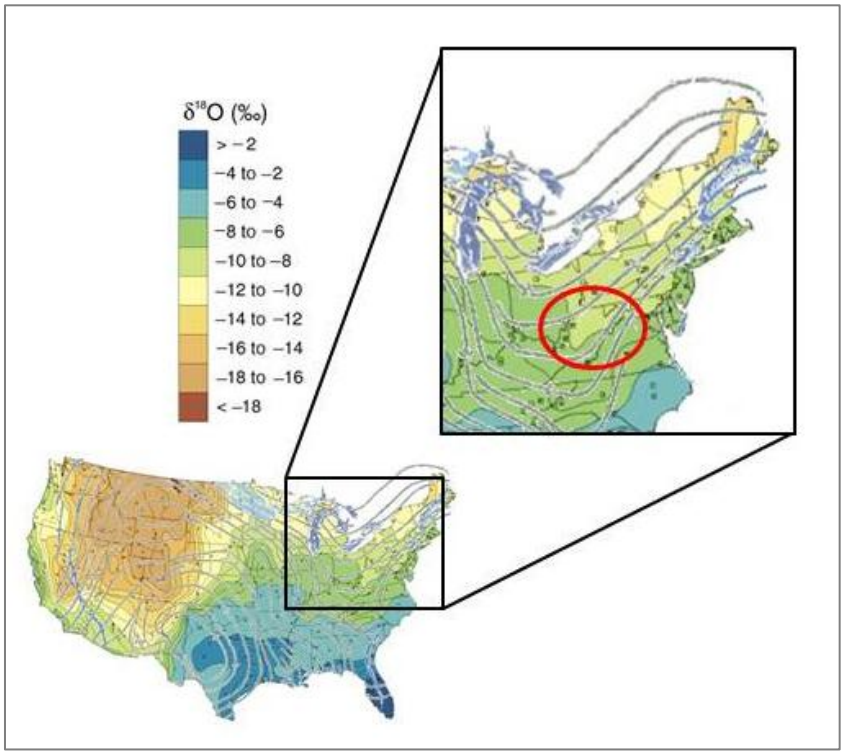

Figure 27: Correlation of ^{18}O isopachs with jet stream contours (modified from Kendall and Coplen, 2001; intellecast.com, 2012)

The overall signatures of the study area groundwaters demonstrate a combination of local effects with processes moving downwind from the Great Lakes affecting precipitation and *d*-excess, and therefore groundwater recharge. The processes may include that of elevation,

topography, temperature, and humidity levels, with the cluster of data points within the GMWL implying steady vapor mass sources. The positioning on the GMWL indicates a deceivingly arid source but is the result of a mixed vapor mass of evaporative and atmospheric moisture originating from the Great Lakes.

4.3 – Carbon Isotopes of DIC

Sources of dissolved inorganic carbon (DIC) can be determined through the analysis of $^{13}C_{DIC}$ using hydrochemistry and isotopic proxies. As mentioned in Chapter 2.3.4, the range for $\delta^{13}C$ in natural waters is between -11 and -16‰ pending on the contribution of carbon from the diffusion of $CO_{2(g)}$ through soil and carbonate weathering. The isotopic composition of DIC ranges from -23.4 to -1.1‰, with the majority of samples more depleted or enriched in comparison to the normal range of carbon isotopes in natural waters (Appendix A, Table 3). Hydrochemistry showed evidence of carbonate weathering happening within each age group of aquifers, showing a weak association of depleted $\delta^{13}C$ with high DIC concentrations through all of the groundwater samples (Figure 28). Carbonate dissolution will enrich $\delta^{13}C_{DIC}$ signatures from adding ^{13}C from an enriched carbonate source (0 ± 2‰). Biologic methanogenesis will also enrich $\delta^{13}C_{DIC}$ signatures by the preferential removal of ^{12}C, leaving $\delta^{13}C_{DIC}$ enriched by greater than 10‰. All groundwater

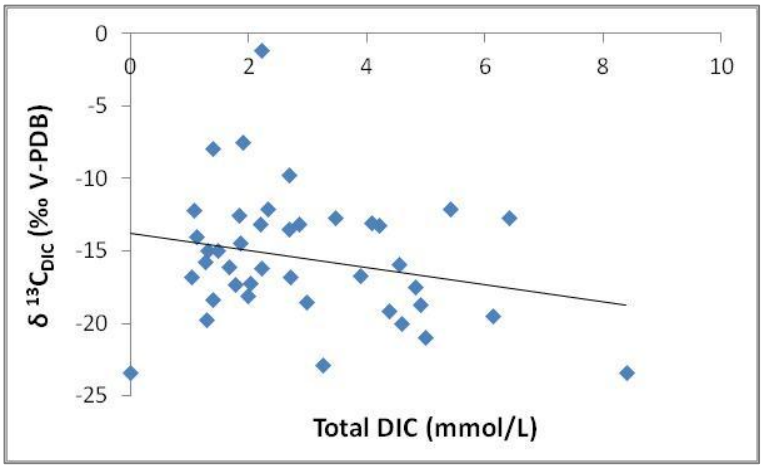

Figure 28: Overall DIC variations within $\delta^{13}C_{DIC}$ of West Virginia groundwaters

samples have $\delta^{13}C_{DIC}$ signatures below 0‰, suggesting that biogenic methanogenesis is not playing a dominant role in controlling the isotopic evolution of DIC. It is hypothesized that the dissolution or weathering of carbonates and/or carbonaceous shales is causing the enrichment of $\delta^{13}C_{DIC}$. To further evaluate the geochemical cause for such variations in $\delta^{13}C$ and deviation from natural water signatures, the aquifer formations are grouped together by geologic period of deposition and analysis will continue in this form for the remainder of this study.

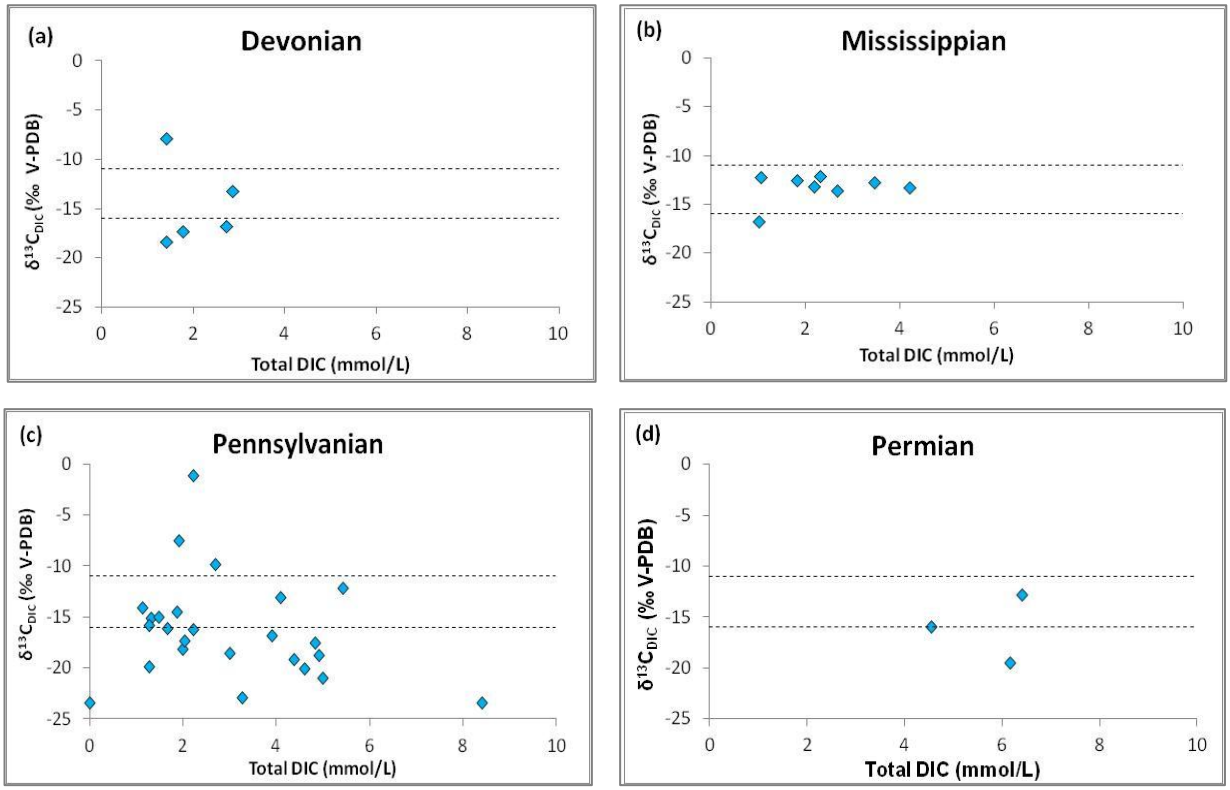

Figure 29a-d: Correlation of total DIC with $^{13}C_{DIC}$.
Dashed lines indicate theorized boundary of $^{13}C_{DIC}$ in natural waters

With the exception of the Mississippian age aquifers with dominantly limestone lithologies, most samples groundwaters did not fall within the natural water range (Figure 29a-d). The Devonian, Mississippian, and Permian waters were primarily within the expected range of natural waters, with several outliers throughout. The scatter of data may be the result of the cyclical deposition throughout the Pennsylvanian with varying sources of carbon. It is of note that each site with increased enrichment of $\delta^{13}C$ past the range of natural waters had associated methane in concentrations greater than 2 mg/L, but additional methane concentrations also accompany depleted carbon isotope signatures.

When comparing total DIC with carbon isotope compositions, no direct correlations are evident for distinguishing the waters from one another. However, HCO_3^- can be used as a proxy by the direct linear trends seen in Devonian, Mississippian, and Pennsylvanian waters, or the lack thereof within Permian aged waters. More specifically, specific aquifer formations show individual relationships of the input of HCO_3^- affecting carbon isotope signatures and can be distinguished in more detail than by formation age (Figure 30a-d). Specific outliers in visible trends or age series that lack trends have the highest concentrations of methane, ranging from 12.84 to 48.20 mg/L.

Within the Devonian, a linear relationship is evident within the sampled sites in the Chemung Group, with one Hampshire Formation site confirming the trend and the second as an outlier (Figure 30a). The linear relationship in the Chemung Group is hypothesized to be similar to that of the Hampshire Formation; the lithologies are of similar origin with clay and siltstone, with the Hampshire Formation has gas zones present through deposition which may be confirmed in the dissolved methane data. One Hampshire Formation sampled site falls along the linear regression for the Chemung Group, with the other (outlier) sample the only site with

dissolved methane present and at a high level of having 48.20 mg/L. This methane can potentially be of biogenic origin, in which enrichment of the outlier compared to the other Chemung Group sample is due to the biological preference for lighter carbon. However, the $\delta^{13}C_{DIC}$ is not enriched beyond +10‰ (indicative of methanogenesis) and the methane may simply be the result of migration from a thermogenic origin.

The carbon isotope signatures within the Mississippian are that of natural waters, which is expected with the dominant lithology being carbonate (Figure 30b). With only 2 sample sites within the Pocono formation, additional sampling will be necessary to confirm the proposed trend.

The cyclic deposition and the multiple lithologies that result within the Pennsylvanian are seen in the scatter and distinct correlations of HCO_3^- and carbon isotopes (Figure 30c). The Pottsville and Monongahela Groups are greatly distinguished by their distinctive correlations between HCO_3^- and $\delta^{13}C_{DIC}$. The lack of correlation in the Pottsville Group and range of $\delta^{13}C_{DIC}$ values shows evidence of multiple carbon inputs and/or geochemical reactions. The single sample location for the Allegheny Formation does not allow for correlations to be made, but does plot at the extreme low end of the positive trend within the Pottsville Group. Several samples fall below the $\delta^{13}C_{DIC}$ range of natural waters. This addition of depleted carbon may be the result of the oxidation of isotopically depleted organic matter (-25‰) in the presence of oxygen or via sulfate reduction (Eqn 5).

There are no evident trends within the Dunkard Group of Permian age. This may be the result of high concentrations (12.26 to 17.84 mg/L) of dissolved methane in two of the three sample sites (Figure 30d) and additional chemical reactions.

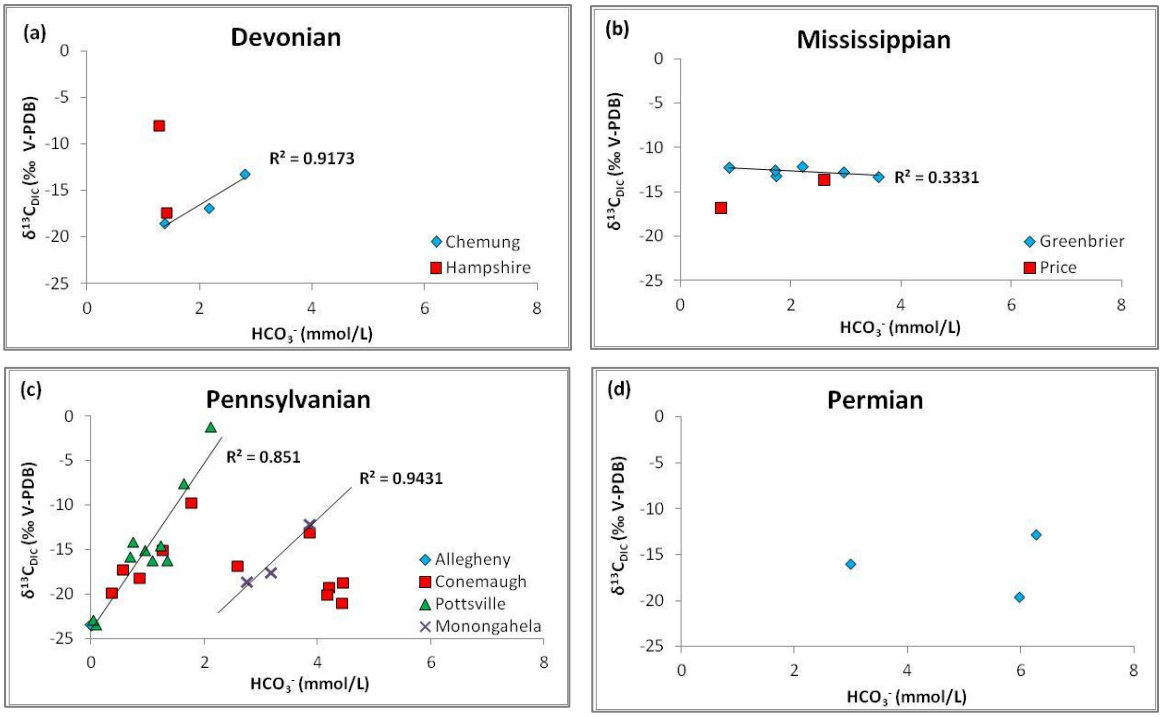

Figure 30a-d: Using HCO_3^- as a proxy for carbon isotope variations

Overall, with a form of carbonate dissolution present within each age series, enriched carbon is added to total DIC throughout the study area. The enrichment of ^{13}C does not extend past 0‰, indicating excess carbonate/carbonaceous formations are the dominant cause of the enrichment. The geochemical reactions occurring throughout these formations allow for distinct trends to be used as proxies to distinguish these groundwaters. Locally, high levels of sulfate (up to 231 mg/L) within the waters can instigate the formation of sulfuric acid, which can cause the dissolution of carbonates and enrich the $\delta^{13}C_{DIC}$ signatures. On the other hand, sulfate reduction will add depleted carbon to the DIC pool, decreasing the DIC signatures.

4.4 – Isotopes of Dissolved Sulfate

The spread of sulfur isotope compositions, -17.1 to +17.1‰, falls within the literature range of biogenic pyrite, shales, limestones, and coal (Appendix A, Table 3). This is expected due to the large amount of shales and pyrite within the study formations. Dr. Sharma's stable isotope research group collected shale and coal samples from the Pittsburgh coal seam, showing sulfur isotope signatures of 1 to 3‰, which can be used as a partial datum for comparison as an origin for the sulfur in dissolved sulfate in the groundwaters. Additional isotopic studies performed in the Upper Freeport coal (found in the study area) show positive ^{34}S signatures up to 15‰ for pyritic sulfur (Spiker et al., 1994). The sampled $^{34}S_{SO4}$ signatures represent bulk sulfate from sulfate dissolution, pyrite, and organic sources, resulting in wide variation. There are multiple geochemical reactions that can result in such depleted or enriched sulfur isotope compositions; depletion by oxidation, enrichment by sulfate weathering and reduction, and atmospheric invasion.

The oxidation of pyrite commences with a depleted pyrite source (-25 to 0‰), which will consequently have depleted ^{34}S signatures in the produced sulfate (Eqns 10-12). However, the depleted values of up to -20‰ may preliminary indicate oxidation. The oxygen composition in the molecule is a factor of the atmospheric input as well as the oxygen in the water molecule during formation. Atmospheric invasion, with $\delta^{18}O_{O2}$ having a more positive composition of 23.5‰, will complicate the oxidation signatures by enriching the values. Sulfate within the atmosphere also shows enriched signatures in both ^{18}O and ^{34}S. Sulfate weathering and dissolution also produces enriched sources through the weathering of minerals and limestones with signatures ranging from 0 to 30‰. Marine environments produce the signatures on the more enriched end of that range. With precipitation being the dominant form of recharge in these

aquifers and underlying dissolution producing enriched sources of ^{34}S and ^{18}O, it is difficult to delineate oxidation within the waters. The oxidation of pyrite also produces significant concentrations of iron and sulfate. No correlations between the increase in concentration and sulfate isotopes is present, but again could be due to the multiple geochemical pathways for the production and consumption of iron and sulfate.

Sulfate reduction, via oxidation of fixed carbon or oxidation of reduced carbon, introduces enriched compositions of $\delta^{34}S_{SO4}$. The enrichment of both ^{34}S and ^{18}O is present during reduction as the result of bacterial preferences for lighter isotopes. This relationship can be used as a proxy for determining if sulfate reduction is occurring; it's not expected to occur in a 1:1 relationship due to the multiple inputs and sources of sulfate. The general trend in enrichment is seen within Mississippian and Pennsylvanian age series (Figure 31a-d). The lack of sulfate concentrations within two of the three samples of Permian age constrained the data to a single point. These signatures can also be affected by different sources of sulfate introduced into the system through the open recharge of the aquifers via precipitation and surficial influences.

A large range in $\delta^{34}S_{SO4}$ and $\delta^{18}O_{SO4}$ is evident; -17.1 to +17.1‰ and -3.3 to +10.9‰, respectively. This is indicative of multiple processes occurring from sources of pyrite, coal, and shales with atmospheric influence, overprinted with the occurrence of sulfate reduction.

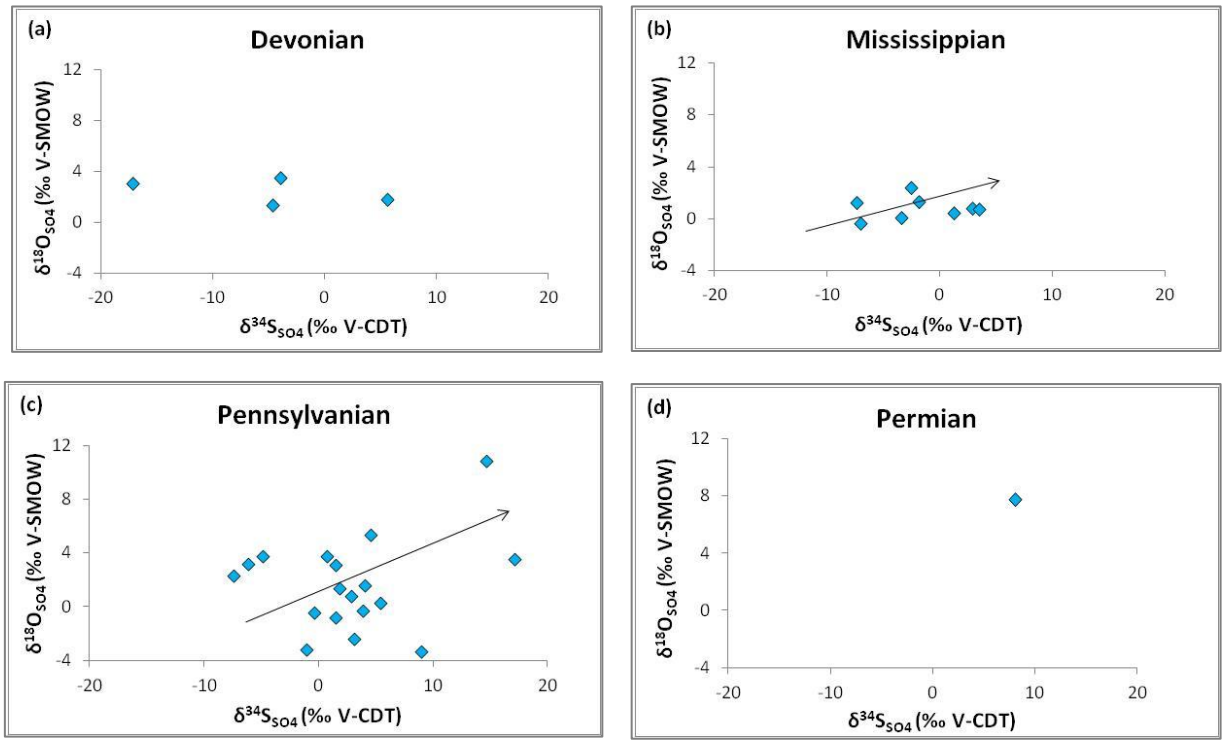

Figure 31a-d: Isotopes of sulfate for evidence of sulfate reduction

4.5 – Determining the Source of Dissolved Methane

The vital information derived from the isotopic analysis of dissolved methane is determining the source of methane as biogenic or thermogenic. Multiple studies have determined boundaries for these origins (Chapter 3.2d), but the end member limits differ for interpretation. Ranges for distinguishing biogenic from thermogenic methane have been determined in multiple studies (Figure 32). These limits show an inconsistent consensus of biogenic, thermogenic, and/or mixed origin of the dissolved methane in the sampled groundwaters; the result of compiling past data of significantly different geologic areas and formations. The major difference between these studies lies within the extension of thermogenic methane past -50‰ in Schoell (1980), Ryder et al. (2003), and Molofsky et al. (2011). This demonstrates the inability

to consistently report isotopic methane sourcing of dissolved methane within current literature. Clark and Fritz (1997), Whiticar (1999), and Schoell (1980) are the most referenced in the literature, and each has distinctly different conclusions about biogenic and thermogenic boundaries. The introduction of Ryder et al. (2003) and Molofsky et al. (2011) for Appalachian Basin methane further complicates this issue. Previous and current studies that apply these conclusions in attempt to isotopically determine the source of methane fail to acknowledge the conflicting outcomes that would result from comparing these literature variations. Future work needs to be done to address this issue in order to accurately determine methane sources that will be agreeable between all reporting authors.

Author	Biogenic (approx.)		Thermogenic (approx.)	
	‰ $\delta^{13}C_{CH4}$	‰ $\delta^{2}H_{CH4}$	‰ $\delta^{13}C_{CH4}$	‰ $\delta^{2}H_{CH4}$
Clark et al. (1997)	-40 to -90	-150 to -300	-35 to -50	-150 to -185
Whiticar (1999)	-45 to -80	-140 to < -450	-20 to -50	> -100 to -340
Osborn et al. (2011)	-64 to < -80	-158 to < -300	> -20 to -50	> 0 to < -300
Schoell (1980)	-64 to < -90	-149 to < -300	-20 to -56	-125 to -275
Ryder et al. (2003)	-65 to < -80	-160 to < -325	> -20 to -63	-160 to < -325
Molofsky et al. (2011)	-63 to < -80	-200 to < -325	> -20 to -64	> -100 to -255

Figure 32: Comparison of literature endmembers for determining sources of methane

Using three commonly reference plots in current literature, the groundwater isotopic signatures (Appendix A, Table 3) indicates all possible sources from thermogenic, biogenic, or mixed (Figure 33a-c). Dominantly deep microbial stimulated methane with mixing is seen in Coleman (1994). Methane originating from biogenic, thermogenic, and a mix is shown in Whiticar (1999) and dominantly thermogenic via Molofsky et al. (2011). These plots demonstrate the variety in conclusions that can be interpreted from conflicting reports. Even though the dissolved methane measured in these groundwaters can be difficult to classify based

on the conflicting endmembers, distinctions can still be made using these diagrams. It is important to note that all samples lie in a cluster, distinct from the Marcellus Formation gas collected from Greene County as well as from Ordovician, Silurian and Devonian gases collected by other researchers in WV and PA. This dissimilarity demonstrates the ability to use carbon and hydrogen isotopes of dissolved methane as a proxy to distinguish natural gas leakage into the groundwater from deeper thermogenic sources. It is also of note that the coalbed methane sample, of the Pittsburgh coalbed, plots amongst the groundwater samples. This suggests overlap between biogenic and thermogenic – coalbed methane compositions. There are additional complications that arise to complicate these methane sourcing plots, including introduction of methane from other sources (i.e. landfills, septic tanks). If the oxidation of biogenic methane is occurring, the signatures become more enriched and appear to have thermogenic signatures, despite their microbial origin (shown in Figure 33a). With the extreme history of natural gas drilling and coal mining in the study area, a more detailed examination of land use is necessary to examine potential methane sources.

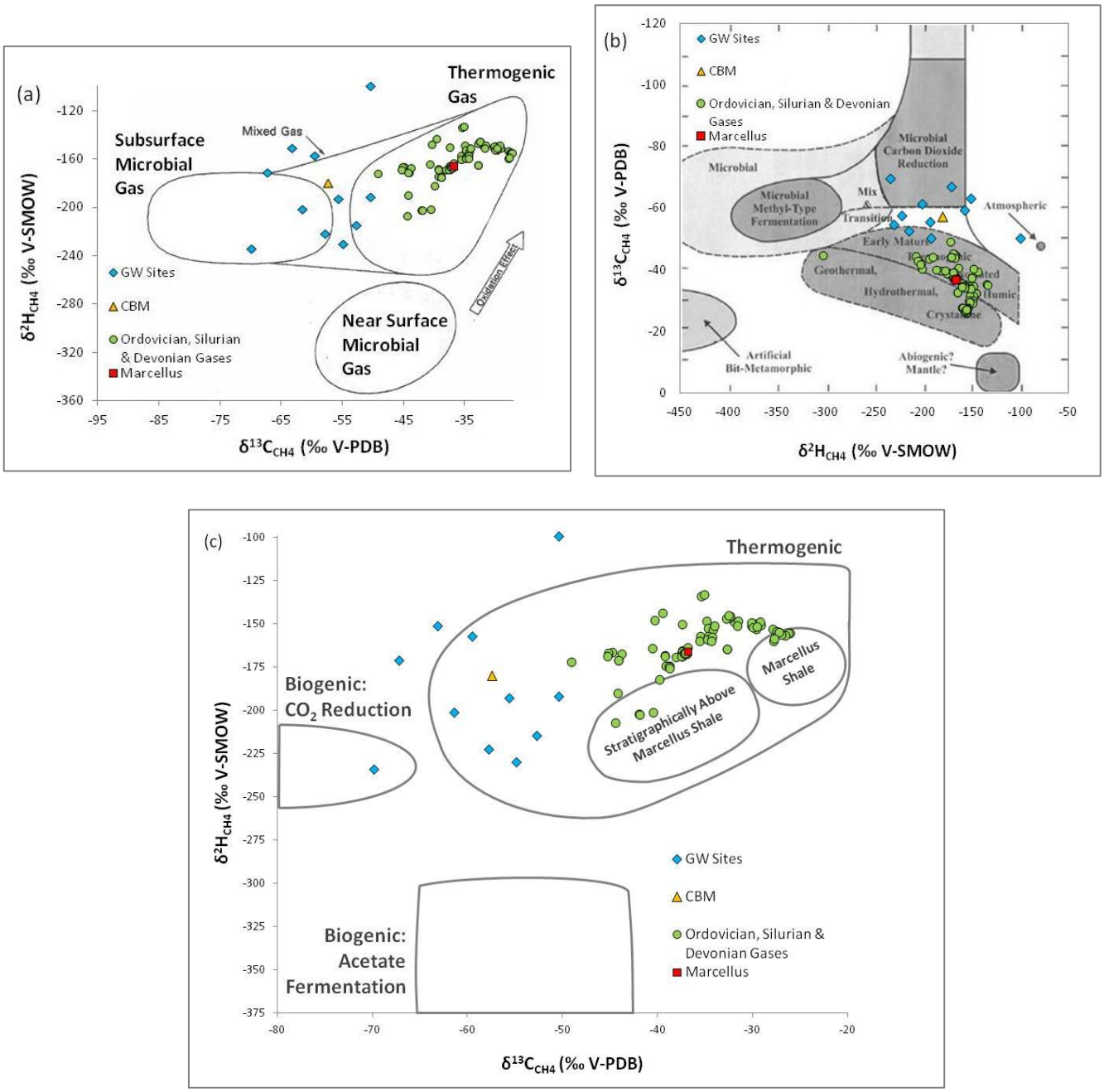

Figure 33a-c: Isotopically distinguishing between biogenic and thermogenic methane in groundwater site modified from a – Coleman (1994); b – Whiticar (1999); c – Molofsky et al. (2011). Thermogenic endmembers plotted as reference through WVU stable isotope research group: CBM – coalbed methane; Marcellus – dissolved methane flowback sample.
Regional natural gas studies plotted as reference: Ordovician, Silurian – Burruss and Laughrey (2010); Lower Silurian, Upper Devonian – Laughrey et al. (2004); Upper Silurian, Devonian – Breen et al. (2007)

Thermogenic methane can be derived from natural gas fields, abandoned oil and gas wells, and/or shallow and deep coalbeds. Coalbed methane is shown to be distinguishable from deeper natural gas using literature studies (Figure 33a-c); land use in terms of mining and drilling can further confirm these graphical observations. Using data provided from the West Virginia Geological and Economic Survey, abandoned or previously drilled gas wells (APG) and coalbed methane wells (CBM) were spatially examined with reference to the groundwater wells. Osborn et al. (2011) researched natural gas contamination resulting from Marcellus Formation drilling in surrounding groundwaters, emphasizing a spatial component. Their results showed the significant methane concentrations within ~5,000 feet of each Marcellus Formation well. Translating their findings to this study, APG well data was buffered to within 1 mile of each sampled groundwater well containing methane concentrations greater than 1mg/L. This buffer narrowed down the estimated 30,000+ APW wells across the study area to 635.

Dissolved methane concentrations vary with the number of APG wells, no direct connection is apparent (Figure 34). The number of APG wells within 1 mile range from 0 to 118, with methane concentrations from 0 to 48.20 mg/L. Of the 21 wells with detectable methane concentrations and therefore isotopic signatures of $^{13}C_{CH4}$ and $^{2}H_{CH4}$, 7 have concentrations greater than 1 mg/L and will be of focus. As a result, data is evaluated in terms of methane with no APW or methane with APW.

There are 2 groundwater wells (Ran-0276, Ran-0278) with methane concentrations and no APG wells within 1 mile, both of Devonian age. Isotopes indicate thermogenic origin for Ran-0276 and biogenic for Ran-0278 (Figure 34). The remaining 5 groundwater wells (Ran-0282, Mar-0300, Tay-0130, Lew-0221, Har-0173) have methane concentrations greater than 1 mg/L with surrounding APG wells. These aquifers are of Pennsylvanian age with the exception

of one Permian aquifer (Mar-0300). These waters all show thermogenic origin and between 4 and 118 surrounding APG wells. This evidence indicates the vertical migration of natural gas, but not distinguishable from deeper sources. These groundwater wells are located across the study area, specifying vertical migration in specific areas and not widespread.

Available plugging data for these wells could potentially further confirm this. However, plugging data is only available (through the WV-GES) for 103 of the 635 surrounding APG wells. Including the plugged wells (assuming to completely prevent natural gas migration) does not appear to significantly affect any individual groundwater site in terms of lowering the potential exposure to APG well migration (Figure 35). Availability of total well plugging data is needed to further explore APG migration.

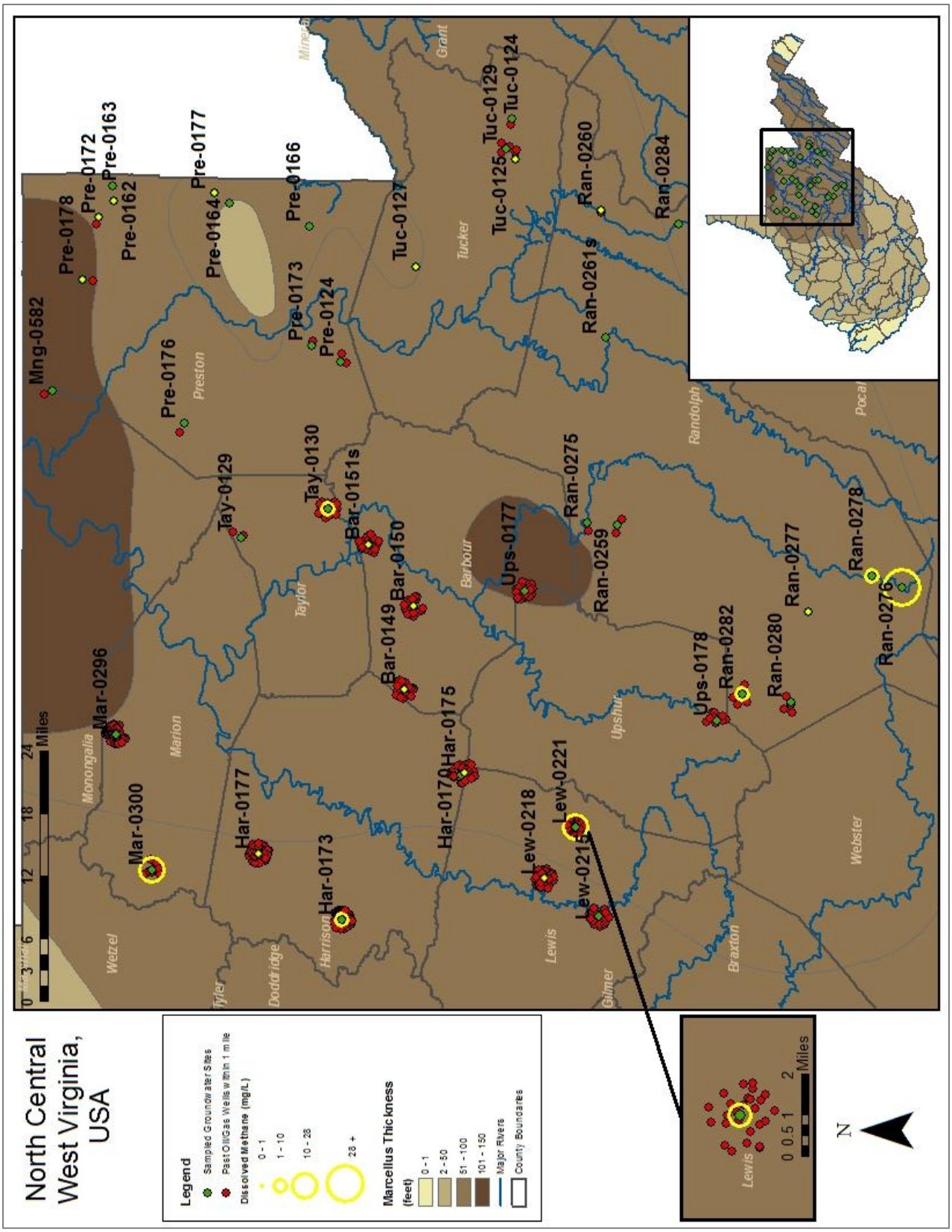

Figure 34: Land use analysis of adjacent APG wells within 1 mile of sampled groundwater sites

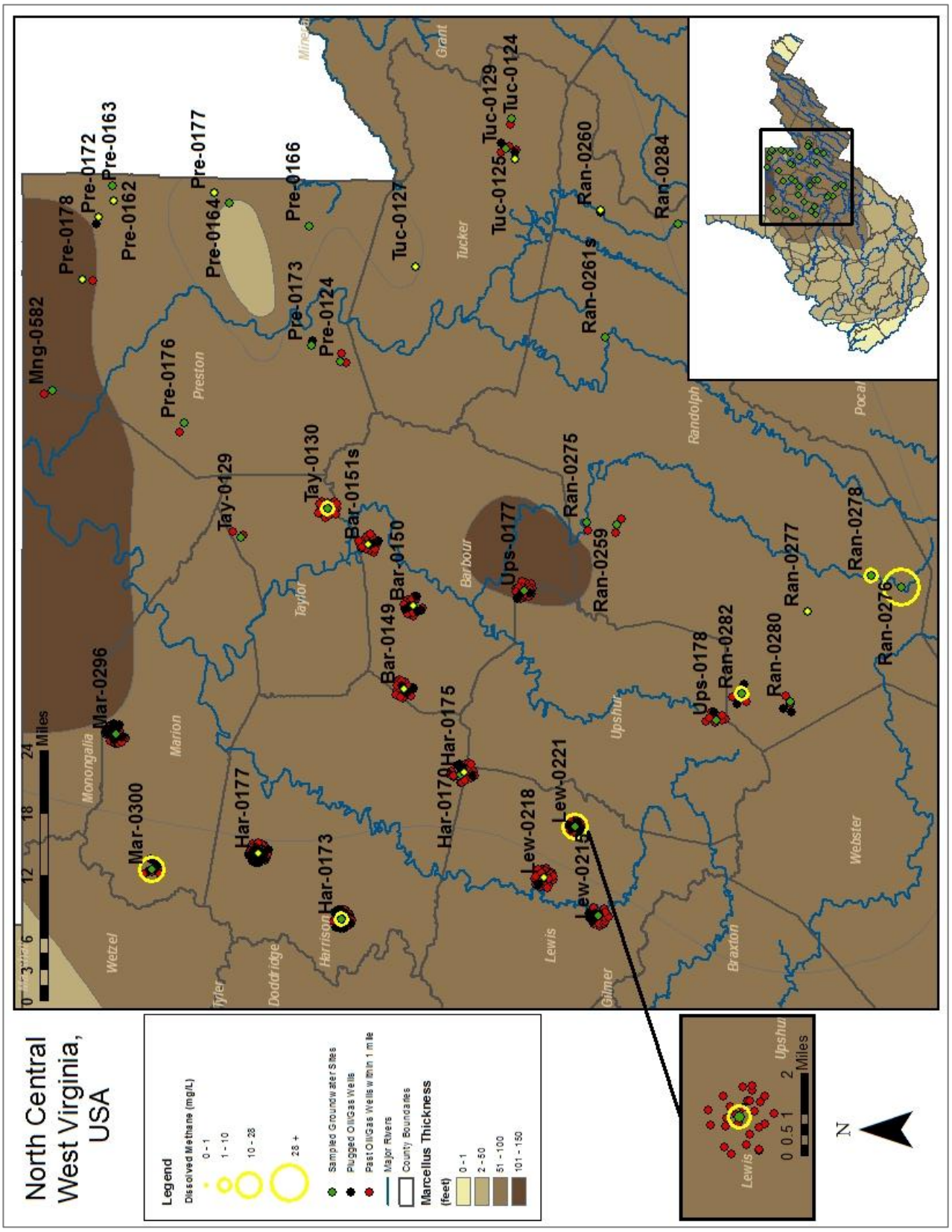

Figure 35: Land use analysis of adjacent APG wells within 1 mile of sampled groundwater sites – incorporating available plugging data of APG wells

CBM is another predominant source of thermogenic methane in West Virginia. CBM wells are not as widespread across the study area, unlike APG wells (Figure 36). None of the groundwater sites have surface CBM wells within 1 mile, and only two have CBM wells within 5 miles (Bar-0149 and Bar-0150). However, these 2 groundwater sites did not have significant methane concentrations. There is also a significant amount of abandoned mines throughout the study area; however none of the higher dissolved methane concentrations correspond to those areas. The physical evaluation of land use for surface coalbed methane drilling and coal mining does not appear to explain higher methane levels in the groundwaters of the study area. However, there may be deeper and unmineable coal sources (not mapped) that may introduce methane to groundwaters.

Contradictory conclusions can be drawn regarding the biogenic vs. thermogenic origin of the dissolved methane in the study area. However, it is noted that isotopic signatures of the dissolved methane in the groundwaters of the study area are different from the Silurian, Ordovician and Devonian aged natural gases throughout the region. As discussed above, difficulties arise when classifying the source of the methane as biogenic vs thermogenic due to discrepancies in the boundaries assigned to these sources in literature. Carbon isotopes of DIC demonstrate that biogenic methanogenesis is not dominantly occurring in any sampled groundwaters in the study area. It is interpreted that the dissolved methane isotopic signatures represent thermogenic sources overprinted by biological processes occurring in the groundwaters. The methane in groundwaters could be originating from the large numbers of coal beds and abandoned oil and gas wells that exist in the area. In conjunction, the complex geology of the area could also create preferential flow paths of methane migration and accumulation.

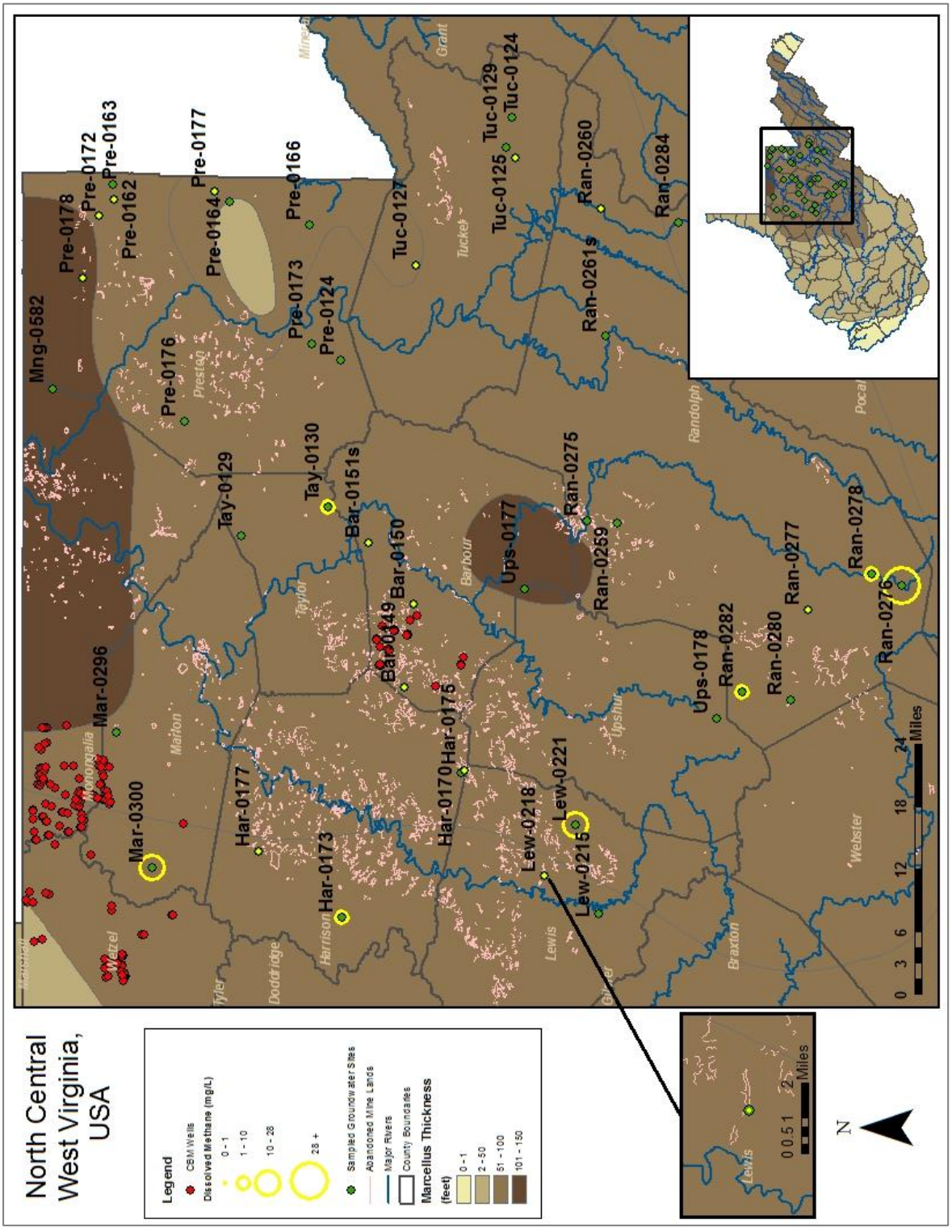

Figure 36: Land use analysis of abandoned coal mines and adjacent CBM wells within 1 mile of sampled groundwater sites

In an area of accelerating shale gas development, the concerns of methane contamination can be addressed by determining the source of methane in the groundwater. Methane concentrations have also shown to be correlated with land topography, showing near surface geologic features and downward gradients as means for migration (Molofsky et al., 2011). This correlation of higher concentrations in low-lying areas is very generally occurring throughout the study area, with methane highest in the western area of the study area in lower topographies (Figure 37). The highest methane concentration, in Randolph county, is in an area lacking in previous coal and gas development. It is, however, in an area within the low-lying river valley. Structural deformation combined with the low topography in the area could introduce means of geologic migration. Additional explanations include CBM migrating from unmineable coal formations throughout in the lithologies.

Despite the challenges associated with assigning the exact source of groundwater methane as biogenic vs thermogenic, this study shows that methane in groundwaters across north central West Virginia have very different isotopic signatures compared to the deeper thermogenic natural gases in the area. These baseline isotopic signatures can be used to identify sources of any increase in dissolved methane concentrations in the future. Hence this study demonstrates the use of stable isotopes to identify methane leaks associated with shale gas development.

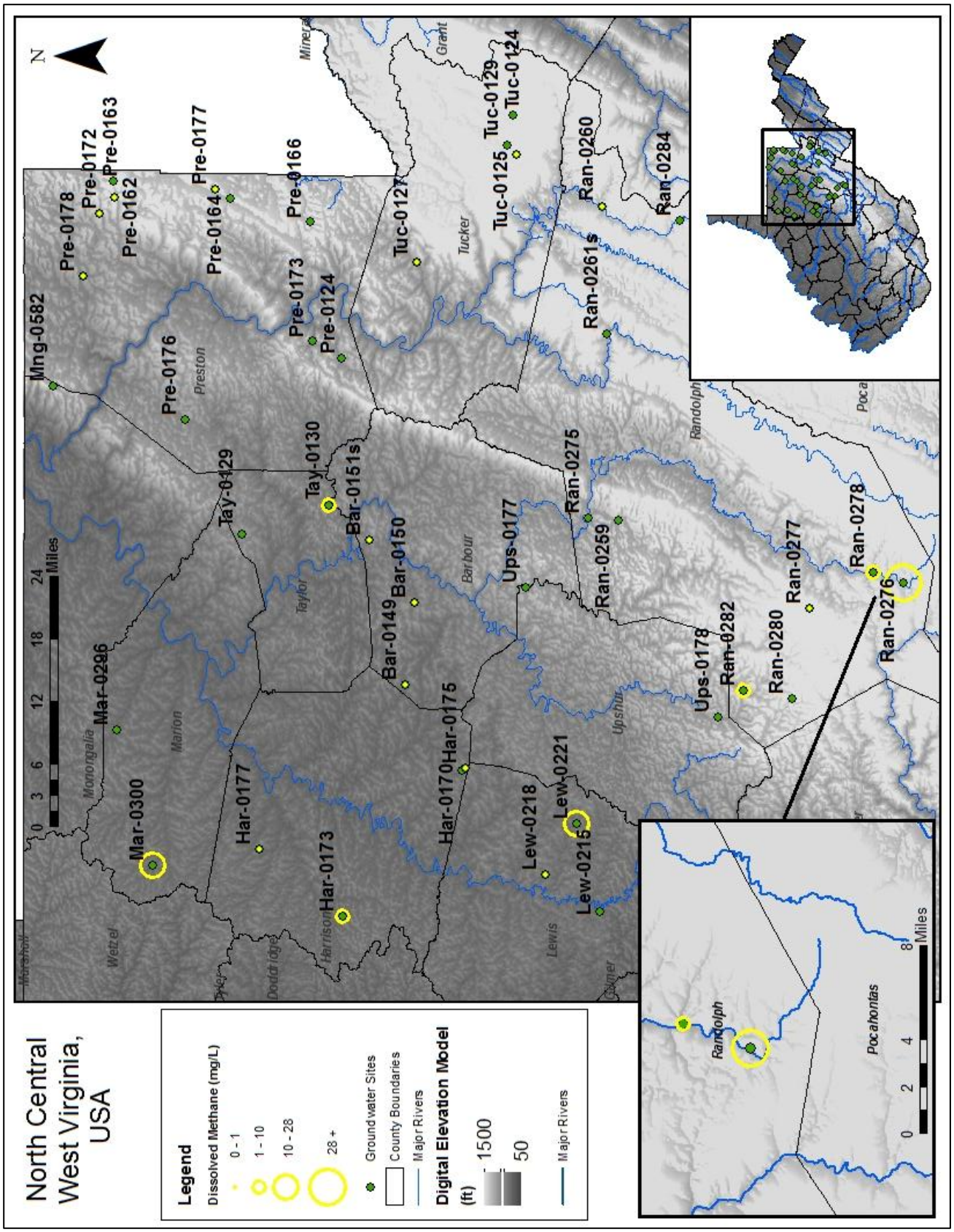

Figure 37: Analysis of topographical effects on methane concentrations for geologic paths of migration

5.0 – Conclusions

A basic Piper Plot shows the wide variation in hydrochemistry of the waters across the study area. This variation is present not only overall, but within individual formations. Analyses were grouped by age of formation to include the Devonian, Mississippian, Pennsylvanian, and Permian. Hydrochemistry shows that a form of carbonate dissolution is occurring within each series of ages, and pyrite oxidation or weathering may be the source of iron and sulfate in the waters. However, due to multiple inputs, cation exchange, and mineral precipitation that can affect concentrations of major cations and anions, a multi-proxy isotopic analysis was used to discern the cause of variations.

The composition of hydrogen and isotope isotopes in water show similar signatures to that of precipitation and river water of the area. The higher *d*-excess values in the groundwaters are interpreted to be a result of dominant recharge being sourced by recycled moisture in air masses originating above the Great Lakes area. The original air masses are subjected to high rates of evaporation over the water bodies, of which the evaporative vapor is mixed with atmospheric. In conjunction with local processes such as altitude and latitude, the isotopic signatures of $\delta^{2}H_{H2O}$ and $\delta^{18}O_{H2O}$ plot above the GMWL in the area of an arid vapor mass.

Carbon isotopes of DIC show deviation from the range of natural waters. Enriched values of $\delta^{13}C_{DIC}$ are predominantly the result of carbonate and carbonaceous shale weathering, evident through hydrochemical relationships. Dissolved methane is present throughout the groundwaters with the highest concentration of 48.20 mg/L, and isotopically plots amongst the signature of local CBM. The associated isotopic signatures of dissolved methane are distinguishable from natural gases of Silurian, Ordovician, and Devonian age. The isotopic signatures of methane characterize its source as thermogenic with an overprint of biological processes. Sulfur isotope

compositions in dissolved sulfate can indicate the source of sulfur, shown to be ranging from coals, shales, and pyrite. The depleted carbon signatures may be indicative of sulfate reduction, but was not confirmed through the isotopic analysis of $\delta^{34}S_{SO4}$ with $\delta^{18}O_{SO4}$ or $\delta^{13}C_{DIC}$ due to the origin of the oxygen atom and variations in carbon input in DIC. The depletion seen in $\delta^{34}S_{SO4}$ is a preliminary indication of sulfide oxidation.

Overall variation, both in hydrochemistry and isotopic signatures, differed widely between and within age series. Specifically, samples collected from Pennsylvanian aged aquifers had more variation than between samples of Permian, Mississippian, and Devonian aquifer ages. The variability may be due to a larger sample pool taken from Pennsylvanian aged aquifers or it may be the result of higher heterogeneity in the Pennsylvanian systems compared to the other age series. More sampling will be necessary in the other systems to confirm the heterogeneity or homogeneity in the aquifer age systems.

In order to fully verify these findings, future temporal studies need to be done to monitor any potential decrease in cation and anion concentrations to analyze in conjunction with stable isotopes. This data establishes the foundation for future temporal studies to evaluate trends in geochemical pathways. The lack of complete well logs for all study sites prevented interpreting the exact lithology was accessed through the well screen during sampling. Depending on the exact lithology accessed, the hydrochemistry and isotopic signatures may shift. Knowing the exact lithology and mineralogy would provide a better foundation for the precise source of ions and potential reactions occurring.

The ambient hydrochemical and isotopic variations in the area groundwaters in this study provide the basis for prospective studies regarding the water quality of north-central West Virginia as shale gas exploration is expanding. Flowback water originates from a different

lithological source in extreme depths; it will have undergone different water rock interactions than what is being seen in these shallow groundwater aquifers. If these aquifers are exposed to significant contributions of flowback/produced water from natural gas drilling, the established baseline isotopic signatures will dramatically change. This occurrence will distinctly shift the ambient signatures and hence serve as a natural fingerprint to determine if aquifers are receiving significant contribution from flowback waters. Accordingly, this study provides the foundation for geochemical assessment of water quality issues related to Marcellus Formation gas development in the study area.

6.0 – Appendix A

Table 1: Physical parameters of groundwater sites.
First three letters of 'Site Names' refers to state county of sampling.

Site Name	Aquifer Formation/ Group	Geologic Age	Date	Time	Temp (^{0}C)	pH	Land Alt. (ft)	Well Depth (ft)
Pre-0124	Chemung	Devonian	8/11/2011	1020	15.5	7	1880	205
Ran-0278	Chemung	Devonian	8/23/2011	0930	13.7	8.7	2380	100
Tuc-0127	Chemung	Devonian	8/8/2011	1420	13.6	8.2	1700	60
Ran-0276	Hampshire	Devonian	7/5/2011	1330	13.4	9.4	2620	320
Ran-0284	Hampshire	Devonian	8/22/2011	1330	11.9	7	2810	200
Pre-0164	Greenbrier	Mississippian	8/30/2011	1005	12.2	7	2480	207
Pre-0177	Greenbrier	Mississippian	8/29/2011	1500	12.1	7.6	2505	145
Ran-0261	Greenbrier	Mississippian	8/3/2011	0920	11.9	7.1	2242	nd
Tuc-0124	Greenbrier	Mississippian	8/9/2011	0920	10.9	7.2	3270	100
Tuc-0125	Greenbrier	Mississippian	8/10/2011	1400	10.6	7.8	3240	250
Tuc-0129	Greenbrier	Mississippian	8/9/2011	1155	10.5	7.2	3230	45
Pre-0166	Price	Mississippian	8/11/2011	1500	12.8	6.8	2630	100
Ran-0260	Price	Mississippian	8/10/2011	0940	11.7	8	2380	222
Pre-0172	Allegheny	Pennsylvanian	8/30/2011	1325	14.4	4.5	2310	65
Bar-0149	Conemaugh	Pennsylvanian	8/25/2011	0940	15.3	7.4	1160	180
Bar-0150	Conemaugh	Pennsylvanian	9/19/2011	1220	15.7	6.7	1345	52
Bar-0151s	Conemaugh	Pennsylvanian	9/21/2011	1145	15.4	6	1610	nd
Har-0170	Conemaugh	Pennsylvanian	8/1/2011	1700	15.5	7.3	1124	75
Har-0175	Conemaugh	Pennsylvanian	8/24/2011	1405	14.8	7.8	1160	45
Lew-0221	Conemaugh	Pennsylvanian	8/23/2011	1445	13.8	7.4	1110	100
Pre-0173	Conemaugh	Pennsylvanian	8/12/2011	1000	13.3	7.9	1560	57
Pre-0176	Conemaugh	Pennsylvanian	6/30/2011	1030	13.1	9.2	1710	200
Pre-0178	Conemaugh	Pennsylvanian	8/31/2011	1005	11.7	6.3	1585	nd
Tay-0129	Conemaugh	Pennsylvanian	7/27/2011	1005	13.7	6	1530	113
Tay-0130	Conemaugh	Pennsylvanian	9/20/2011	1300	13.6	6.7	1290	160
Ran-0275	Kanawha	Pennsylvanian	8/2/2011	1410	15.5	6.7	1870	500
Ran-0280	Kanawha	Pennsylvanian	7/6/2011	1410	14.8	6.5	2710	80
Ran-0282	Kanawha	Pennsylvanian	7/7/2011	1430	12.6	6.7	2190	105
Ups-0178	Kanawha	Pennsylvanian	7/7/2011	1100	12.5	7.8	1920	158
Har-0177	Monongahela	Pennsylvanian	9/19/2011	1645	14.5	6.8	1090	150
Lew-0215	Monongahela	Pennsylvanian	8/24/2011	1010	14	7.5	1130	100
Lew-0218	Monongahela	Pennsylvanian	8/1/2011	1140	14.1	6.7	1080	60
Ran-0277	New River	Pennsylvanian	7/6/2011	1030	11.4	6.7	3220	220
Mng-0582	Pottsville	Pennsylvanian	6/28/2011	1355	15.6	6.6	2230	190
Pre-0162	Pottsville	Pennsylvanian	6/29/2011	1355	10.6	4.5	2610	145
Pre-0163	Pottsville	Pennsylvanian	6/29/2011	1035	11	4.5	2660	179
Ran-0259	Pottsville	Pennsylvanian	8/2/2011	1020	13.1	6.7	2160	155
Ups-0177	Pottsville	Pennsylvanian	8/3/2011	1410	14.1	7.2	1740	120
Har-0173	Dunkard	Permian	7/28/2011	0945	14.7	8.2	1080	70
Mar-0296	Dunkard	Permian	7/25/2011	1450	13.4	6.7	1050	107
Mar-0300	Dunkard	Permian	7/26/2011	1100	16.4	8	1040	70

Table 2: Field and calculated hydrochemistry of groundwater sites.
All units in mmol/L unless designated otherwise.
Fe – total Fe, DIC – calculated total DIC.
SO_4^{2-}, Cl^- ± 3%; Ca^{2+}, Fe, K^+, Mg^{2+}, Na^+ ± 11%

Site Name	Aquifer Formation/ Group	Geologic Age	Ca^{2+}	Mg^{2+}	K^+	Na^+	Cl^-	SO_4^{2-}	Fe	CH_4^+ mg/L	CH_4^+	HCO_3^-	DIC
Pre-0124	Chemung	Devonian	0.99	0.23	0.02	0.84	0.59	0.06	0.03	1.63	0.10	2.16	2.71
Ran-0278	Chemung	Devonian	0.11	0.04	0.03	3.36	1.28	0.00	0.00	8.38	0.52	2.79	2.85
Tuc-0127	Chemung	Devonian	0.37	0.08	0.01	0.91	0.31	0.11	0.00	0.32	0.02	1.37	1.40
Ran-0276	Hampshire	Devonian	0.02	0.00	0.03	8.09	1.91	0.05	0.00	48.20	3.01	1.27	1.40
Ran-0284	Hampshire	Devonian	0.34	0.18	0.03	0.40	0.11	0.15	0.03	0.01	0.00	1.39	1.77
Pre-0164	Greenbrier	Mississippian	1.00	0.28	0.05	0.48	0.60	0.21	0.02	0.00	0.00	1.74	2.20
Pre-0177	Greenbrier	Mississippian	0.99	0.09	0.02	0.07	0.08	0.06	0.00	0.00	0.00	1.72	1.84
Ran-0261	Greenbrier	Mississippian	0.42	0.07	0.01	0.07	0.06	0.05	0.00	0.00	0.00	0.88	1.07
Tuc-0124	Greenbrier	Mississippian	1.38	0.17	0.01	0.06	0.09	0.10	0.00	0.00	0.00	2.97	3.47
Tuc-0125	Greenbrier	Mississippian	0.88	0.36	0.02	0.50	0.09	0.09	0.00	0.00	0.00	2.21	2.31
Tuc-0129	Greenbrier	Mississippian	1.65	0.21	0.01	0.21	0.34	0.12	0.00	0.00	0.00	3.59	4.21
Pre-0166	Price	Mississippian	0.29	0.16	0.03	0.35	0.20	0.14	0.03	0.00	0.00	0.72	1.02
Ran-0260	Price	Mississippian	0.65	0.19	0.06	2.09	1.15	0.10	0.00	0.96	0.06	2.61	2.69
Pre-0172	Allegheny	Pennsylvanian	0.17	0.07	0.04	1.20	1.51	0.15	0.00	0.00	0.00	0.00	0.00
Bar-0149	Conemaugh	Pennsylvanian	1.21	0.20	0.02	5.22	1.39	0.56	0.00	0.41	0.03	4.44	4.90
Bar-0150	Conemaugh	Pennsylvanian	1.38	0.39	0.03	0.41	0.29	0.24	0.02	0.00	0.00	2.59	3.90
Bar-0151s	Conemaugh	Pennsylvanian	0.21	0.05	0.02	0.02	0.02	0.08	0.00	0.00	0.00	0.36	1.28
Har-0170	Conemaugh	Pennsylvanian	1.20	0.40	0.03	1.06	0.31	0.14	0.01	2.11	0.13	4.43	4.99
Har-0175	Conemaugh	Pennsylvanian	0.62	0.20	0.03	4.10	0.06	0.41	0.02	0.01	0.00	4.20	4.38
Lew-0221	Conemaugh	Pennsylvanian	1.51	0.44	0.04	1.02	0.76	0.00	0.01	21.92	1.37	4.16	4.60
Pre-0173	Conemaugh	Pennsylvanian	0.28	0.18	0.03	0.75	0.16	0.00	0.00	3.16	0.20	1.26	1.31
Pre-0176	Conemaugh	Pennsylvanian	0.03	0.01	0.02	5.09	0.14	0.11	0.00	0.39	0.02	3.85	4.09
Pre-0178	Conemaugh	Pennsylvanian	0.22	0.12	0.02	0.38	0.09	0.01	0.03	0.39	0.02	0.85	1.99
Tay-0129	Conemaugh	Pennsylvanian	0.18	0.12	0.03	0.04	0.03	0.11	0.14	0.00	0.00	0.57	2.04
Tay-0130	Conemaugh	Pennsylvanian	0.71	0.26	0.04	0.32	0.11	0.02	0.03	3.07	0.19	1.77	2.69
Ran-0275	Kanawha	Pennsylvanian	0.47	0.21	0.06	0.52	0.59	0.23	0.09	0.14	0.01	1.24	1.86
Ran-0280	Kanawha	Pennsylvanian	0.37	0.06	0.02	0.57	0.48	0.07	0.00	0.00	0.00	0.69	1.26
Ran-0282	Kanawha	Pennsylvanian	0.25	0.10	0.03	0.88	0.58	0.00	0.14	2.35	0.15	1.09	1.67
Ups-0178	Kanawha	Pennsylvanian	0.28	0.11	0.07	3.06	1.37	0.00	0.00	7.31	0.46	2.11	2.21
Har-0177	Monongahela	Pennsylvanian	1.87	0.53	0.04	1.26	0.05	0.62	0.01	0.00	0.00	3.85	5.42
Lew-0215	Monongahela	Pennsylvanian	0.77	0.20	0.03	1.40	0.24	0.13	0.00	0.00	0.00	2.75	2.98
Lew-0218	Monongahela	Pennsylvanian	2.27	0.79	0.04	1.39	0.18	2.40	0.21	0.08	0.00	3.18	4.82
Ran-0277	New River	Pennsylvanian	0.31	0.17	0.04	0.16	0.04	0.08	0.06	0.04	0.00	0.96	1.48
Mng-0582	Pottsville	Pennsylvanian	0.61	0.34	0.04	0.08	0.00	0.00	0.00	0.00	0.00	1.35	2.22
Pre-0162	Formation	Pennsylvanian	0.05	0.02	0.01	0.04	0.04	0.14	0.00	0.00	0.00	0.10	8.40
Pre-0163	Pottsville	Pennsylvanian	0.05	0.03	0.01	0.02	0.03	0.14	0.00	0.00	0.00	0.04	3.26
Ran-0259	Pottsville	Pennsylvanian	0.36	0.19	0.07	0.13	0.04	0.12	0.06	0.35	0.02	0.74	1.13
Ups-0177	Pottsville	Pennsylvanian	0.31	0.10	0.04	1.34	0.41	0.00	0.02	12.84	0.80	1.64	1.90
Har-0173	Dunkard	Permian	0.10	0.03	0.02	7.05	1.10	0.00	0.00	12.26	0.76	6.26	6.40
Mar-0296	Dunkard	Permian	1.06	0.44	0.04	1.97	0.34	0.87	0.01	0.00	0.00	2.98	4.54
Mar-0300	Dunkard	Permian	0.57	0.12	0.03	5.13	1.21	0.00	0.00	17.84	1.11	5.97	6.14

Table 3: Isotopic signatures of groundwaters sites. All units in ‰ (per thousand). Associated *d*-excess calculated from δ^2H_{H2O} and δ^2O_{H2O}. nd – not determined; * – not enough analyte present for analysis. $\delta^{13}C_{DIC}$, $\delta^{18}O_{H2O}$ ± 0.06‰; δ^2H_{H2O} ± 1‰; $\delta^{34}S_{SO4}$, $\delta^{18}O_{H2O}$ ± 0.5‰; $\delta^{13}C_{CH4}$ ± 0.1,0.4‰; δ^2H_{CH4} ± 0.2‰; ± 2,5‰.

Site Name	Aquifer Formation/ Group	Geologic Age	$\delta^{13}C_{DIC}$	$\delta^{34}S_{SO4}$	$\delta^{18}O_{SO4}$	$\delta^{13}C_{CH4}$	δ^2H_{CH4}	δ^2H_{H2O}	δ^2O_{H2O}	*d*-excess
Pre-0124	Chemung	Devonian	-16.8	-3.9	3.5	nd	nd	-60.7	-9.4	14.8
Ran-0278	Chemung	Devonian	-13.2	*	*	-69.9	-233.9	-62.4	-9.1	10.7
Tuc-0127	Chemung	Devonian	-18.4	-4.6	1.3	-63.1	-151.0	-60.6	-9.2	13.0
Ran-0276	Hampshire	Devonian	-7.9	5.6	1.8	-57.8	-222.1	69.1	-9.0	11.7
Ran-0284	Hampshire	Devonian	-17.3	-17.1	3.0	nd	nd	-65.1	-10.1	15.7
Pre-0164	Greenbrier	Mississippian	-13.2	-7.0	-0.4	nd	nd	-62.5	-10.1	18.1
Pre-0177	Greenbrier	Mississippian	-12.6	-2.5	2.4	*	*	-59.8	-9.5	16.1
Ran-0261	Greenbrier	Mississippian	-12.2	2.9	0.8	nd	nd	-56.0	-9.0	16.3
Tuc-0124	Greenbrier	Mississippian	-12.8	-3.4	0.1	nd	nd	-61.6	-9.6	15.5
Tuc-0125	Greenbrier	Mississippian	-12.1	3.5	0.7	*	*	-63.2	-9.7	14.5
Tuc-0129	Greenbrier	Mississippian	-13.2	1.3	0.4	nd	nd	-62.3	-9.4	13.1
Pre-0166	Price	Mississippian	-16.8	-7.4	1.2	nd	nd	-66.6	-10.3	16.1
Ran-0260	Price	Mississippian	-13.6	-1.8	1.3	-59.5	-157.0	-62.6	-9.8	16.00
Pre-0172	Allegheny	Pennsylvanian	-23.4	1.8	1.4	*	*	-61.9	-9.8	16.3
Bar-0149	Conemaugh	Pennsylvanian	-18.7	4.5	5.4	-50.4	-99.2	19.5	-8.0	8.8
Bar-0150	Conemaugh	Pennsylvanian	-16.8	-6.2	3.2	*	*	-55.1	-8.3	11.5
Bar-0151s	Conemaugh	Pennsylvanian	-19.8	-0.4	-0.4	*	*	-59.9	-9.0	11.8
Har-0170	Conemaugh	Pennsylvanian	-20.9	14.6	10.9	nd	nd	-52.0	-8.5	15.9
Har-0175	Conemaugh	Pennsylvanian	-19.2	-4.9	3.8	*	*	-53.0	-8.7	16.7
Lew-0221	Conemaugh	Pennsylvanian	-20.0	8.9	-3.3	-52.7	-214.5	-51.1	-8.2	14.6
Pre-0173	Conemaugh	Pennsylvanian	-15.0	*	*	nd	nd	-60.5	-9.7	17.0
Pre-0176	Conemaugh	Pennsylvanian	-13.0	3.8	-0.3	nd	nd	-58.5	-9.1	13.9
Pre-0178	Conemaugh	Pennsylvanian	-18.1	*	*	-67.2	-171.0	-57.8	-9.1	14.8
Tay-0129	Conemaugh	Pennsylvanian	-17.3	0.7	3.8	nd	nd	-57.0	-9.1	15.7
Tay-0130	Conemaugh	Pennsylvanian	-9.8	17.1	3.6	-50.4	-191.7	-59.5	-8.7	10.3
Ran-0275	Kanawha	Pennsylvanian	-14.5	1.5	3.1	nd	nd	-60.3	-9.4	14.8
Ran-0280	Kanawha	Pennsylvanian	-15.8	3.1	-2.4	nd	nd	-57.0	-8.6	12.1
Ran-0282	Kanawha	Pennsylvanian	-16.1	*	*	-61.4	-201.1	-59.5	-9.1	13.0
Ups-0178	Kanawha	Pennsylvanian	-1.1	*	*	nd	nd	-59.9	-9.4	14.9
Har-0177	Monongahela	Pennsylvanian	-12.2	-1.1	-3.2	*	*	-50.0	-8.0	13.8
Lew-0215	Monongahela	Pennsylvanian	-18.5	-7.5	2.3	nd	nd	-53.3	-8.3	13.2
Lew-0218	Monongahela	Pennsylvanian	-17.5	5.4	0.3	-42.0	*	-52.1	-8.2	13.8
Ran-0277	New River	Pennsylvanian	-15.0	4.0	1.6	*	*	-67.8	-10.0	12.6
Mng-0582	Pottsville	Pennsylvanian	-16.2	2.8	0.8	nd	nd	-63.5	-9.5	12.2
Pre-0162	Pottsville	Pennsylvanian	-23.4	1.5	-0.8	*	*	-63.5	-9.5	12.6
Pre-0163	Pottsville	Pennsylvanian	-22.9	*	*	nd	nd	-66.3	-9.8	11.8
Ran-0259	Pottsville	Pennsylvanian	-14.1	nd	nd	nd	nd	-64.0	-9.9	15.3
Ups-0177	Pottsville	Pennsylvanian	-7.5	*	*	-54.9	-229.9	-61.0	-9.6	16.1
Har-0173	Dunkard	Permian	-12.7	*	*	nd	nd	-51.7	-8.5	16.6
Mar-0296	Dunkard	Permian	-15.9	8.1	7.8	nd	nd	-51.1	-8.5	17.0
Mar-0300	Dunkard	Permian	-19.5	*	*	-55.6	-192.8	-52.5	-8.4	14.3

Table 4: Estimated compositions of water isotopes in precipitation. Signatures estimated from Water Resources Research by Bowen et al. (2012). Latitude and longitude in decimal degrees. Alt. – Altitude, Est. – Estimated.

Site Name	Latitude	Longitude	Land Altitude (m)	Est. δ^2H_{H2O} (‰)	Est. $\delta^{18}O_{H2O}$ (‰)	Est. *d*-excess
Bar-0149	39.19	-80.19	353.57	-51	-8.0	13.0
Bar-0150	39.18	-80.08	409.96	-52	-8.1	12.8
Bar-0151s	39.24	-79.99	490.73	-54	-8.3	12.4
Har-0170	39.11	-80.31	342.60	-51	-7.9	12.2
Har-0173	39.28	-80.51	329.18	-51	-7.9	12.2
Har-0175	39.11	-80.31	353.57	-51	-7.9	12.2
Har-0177	39.39	-80.42	332.23	-52	-8.0	12.0
Lew-0215	38.92	-80.51	344.42	-50	-7.8	12.4
Lew-0218	39.00	-80.45	329.18	-50	-7.8	12.4
Lew-0221	38.95	-80.38	338.33	-50	-7.8	12.4
Mar-0296	39.59	-80.25	320.04	-52	-8.0	12.0
Mar-0300	39.54	-80.44	316.99	-52	-8.0	12.0
Mng-0582	39.68	-79.78	679.70	-58	-8.8	12.4
Pre-0124	39.28	-79.74	573.02	-55	-8.5	13.0
Pre-0162	39.60	-79.51	795.53	-60	-9.1	12.8
Pre-0163	39.60	-79.49	810.77	-60	-9.1	12.8
Pre-0164	39.43	-79.52	755.90	-58	-8.9	13.2
Pre-0166	39.32	-79.55	801.62	-59	-9	13.0
Pre-0172	39.62	-79.54	704.09	-58	-8.9	13.2
Pre-0173	39.32	-79.72	475.49	-54	-8.3	12.4
Pre-0176	39.50	-79.82	521.21	-55	-8.5	13.0
Pre-0177	39.46	-79.50	763.52	-59	-9	13.0
Pre-0178	39.64	-79.62	483.11	-55	-8.5	13.0
Ran-0259	38.90	-79.96	658.37	-55	-8.5	13.0
Ran-0260	38.92	-79.53	725.42	-56	-8.7	13.6
Ran-0261s	38.91	-79.70	683.36	-56	-8.6	12.8
Ran-0275	38.94	-79.96	569.98	-54	-8.3	12.4
Ran-0276	38.50	-80.05	798.58	-56	-8.6	12.8
Ran-0277	38.63	-80.08	981.46	-59	-9	13.0
Ran-0278	38.54	-80.04	725.42	-55	-8.4	12.2
Ran-0280	38.66	-80.21	826.01	-57	-8.7	12.6
Ran-0282	38.72	-80.20	667.51	-55	-8.4	12.2
Ran-0284	38.81	-79.55	856.49	-58	-8.9	13.2
Tay-0129	39.42	-79.98	466.34	-54	-8.3	12.4
Tay-0130	39.30	-79.94	393.19	-53	-8.1	11.8
Tuc-0124	39.04	-79.40	996.70	-61	-9.3	13.4
Tuc-0125	39.04	-79.46	987.55	-61	-9.2	12.6
Tuc-0127	39.18	-79.61	518.16	-54	-8.4	13.2
Tuc-0129	39.05	-79.44	984.50	-61	-9.2	12.6
Ups-0177	39.03	-80.06	530.35	-54	-8.3	12.4
Ups-0178	38.76	-80.24	585.22	-53	-8.2	12.6

7.0 – References

M.J. Alperin and T.M. Hoehler, Anaerobic Methane Oxidation By Archaea/Sulfate-Reducing Bacteria Aggregates: 2. Isotopic Constraints, *American Journal of Science*, 2009, **309**, 958-984.

R.M. Anderson, K.M. Beer, T.F. Buckwalter, M.E. Clark, S.D. McAuley, J.I. Sams III and D.R. Williams, Water Quality in the Allegheny and Monongahela River Basins, Pennsylvania, West Virginia, New York, and Maryland, 1996-98, *U.S. Geological Survey, Circular 1202*, 2000, 1-41.

A. Andrews, C. Copeland, P. Folger, M. Humphries, R. Meltz and M. Tieman, *Congressional Research Service Memorandum*: Natural Gas Drilling in the Marcellus Shale, 2009, 1-39.

A. Andrews, P. Folger, M. Humphries, C. Copeland, M. Tieman, R. Meltz and C. Brougher, *Congressional Research Service Report for Congress*: Unconventional Gas Shales: Development, Technology, and Policy Issues, 2009, 1-53.

Appendix C Regional Setting Supporting Information, Mountain Mining Valley Fill in Appalachia EIS, United States Environmental Protection Agency, 1-54, www.epa.gov/region3/mtntop/pdf/appendices/c/appc.pdf

Application Flash Report No. G 30, *Thermo Finnigan MAT*, 2001, 1-12.

R. Aravena, S. M. Harrison, J. F. Barker, H. Abercrombie and D. Rudolph, 2003, Origin of Methane in the Elk Valley Coal Field, Southeastern British Columbia, Canada, *Chemical Geology*, **195**, 219–227.

J.D. Arthur, B. Bohm and M. Layne, Hydraulic Fracturing Considerations For Natural Gas Wells of the Marcellus Shale, *Ground Water Protection Council presentation*, 2008, 1-17.

J.D. Arthur, B. Bohm, B.J. Coughlin and M. Layne, Evaluating the Environmental

Implications of Hydraulic Fracturing in Shale Gas Reservoirs, ALL Consulting, 2008, 1-17.

N. Assayag, D. Jézéquel, M. Ader, E. Viollier, G. Michard, F. Prévot and P. Agrinier, Hydrological Budget, Carbon Sources and Biogeochemical Processes in Lac Pavin (France): Constraints From $\delta^{18}O$ of Water and $\delta^{13}C$ of Dissolved Inorganic Carbon, *Applied Geochemistry*, 2008, **23**, 2800-2816.

E.A. Atekwana, Hydrogeology and Stable Isotope Investigations of a Landfill Impacted Site in Southwest Michigan, *Western Michigan University*, 1996, 1-197.

E.A. Atekwana and D.S. Richardson, Geochemical and Isotopic Evidence of a Groundwater Source in the Corral Canyon Meadow Complex, Central Nevada, USA, *Hydrological Processes*, 2004, **18**, 2801-2815.

K.L. Avary, Overview of Gas and Oil Resources in West Virginia, *West Virginia Geological and Economic Survey*, 1-31.

K.L. Avary, Geology of the Marcellus Shale and Current Activity in West Virginia, *West Virginia Geological and Economic Survey*, 1-38.

F.J. Baldassare and C.D. Laughrey, Identifying the Sources of Stray Methane by Using Geochemical and Isotopic Fingerprinting, *Environmental Geoscience*, 1997, **4**, 85-94.

Z.A. Berner, D. Stüben, M.A. Leosson and H. Klinge, S- and O-Isotopic Character of Dissolved Sulphate in the Cover Rock Aquifers of a Zechstein Salt Dome, *Applied Geochemistry*, 2002, **17**, 1515-1528.

K.W. Blasch and J.R. Bryson, Distinguishing Sources of Ground Water Recharge by Using $\delta^{2}H$ and $\delta^{18}O$, *Ground Water*, 2007, **45**, 294-308.

G. Börjesson, J. Samuelsson and J. Chanton, Methane Oxidation in Swedish Landfills

Quantified with the Stable Carbon Isotope Technique in Combination with an Optical Method for Emitted Methane, *Environmental Science Technology*, 1997, **41**, 6684-6690.

R. Botz, H. D. Pokojski, M. Schmitt and M. Thomm, Carbon Isotope Fractionation during Bacterial Methanogenesis by CO2 Reduction, *Organic Geochemistry*, 1996, **25**, 255–262.

L. Bouchaou, J.L. Michelot, M. Qurtobi, N. Zine, C.B. Gaye, P.K. Aggarwal, H. Marah, A. Zerouali, H. Taleb and A.Vengosh, Origin and Residence Time of Groundwater in the Tadla Basin (Morocco) Using Multiple Isotopic and Geochemical Tools, *Journal of Hydrology*, 2009, **379**, 323-338.

G.J. Bowen, The Online Isotopes in Precipitation Calculator, version 2.2, 2012, http://www.waterisotopes.org

G.J. Bowen and J. Revenaugh, Interpolating the Isotopic Composition of Modern Meteoric Precipitation, *Water Resources Research*, 2003, **39.** 1-13.

G.J. Bowen and B. Wilkinson, Spatial Distribution of $\delta^{18}O$ in Meteoric Precipitation, *Geological Society of America*, 2002, **30**(4), 315-318.

K.J. Breen, K. Révész, F.J. Baldassare and S.D. McAuley, Natural Gases in Ground Water Near Tioga Junction, Tioga County, North-Central Pennsylvania-Occurrence and Use of Isotopes to Determine Origins, 2005, *U.S. Geological Survey*, Scientific Investigations Report Series 2007-5085, 2007, 1-75.

K.R. Bruner and R. Smosna, A Comparative Study of the Mississippian Barnett Shale, Forth Worth Basin, and Devonian Marcellus Shale, Appalachian Basin, *URS Corporation*, DOE/NETL, 2011, 1478, 1-118.

R.S. Burruss and C.D. Laughrey, Carbon and Hydrogen Isotopic Reversals in Deep Basin Gas:

Evidence for Limits to the Stability of Hydrocarbons, *Organic Geochemistry*, 2010, **41**, 1285-1296.

D.H. Cardwell, Geologic History of West Virginia, *West Virginia Geological and Economic Survey*, 1975, 1-74.

I. Cartwright, K. Hannam and T.R. Weaver, Constraining Flow Paths of Saline Groundwater at Basin Margins Using Hydrochemistry and Environmental Isotopes: Lake Cooper, Murray Basin, Australia, *Australian Journal of Earth Sciences*, 2007, **25**, 1103-122.

K. Cheung, P. Klassen, B. Mayer, F. Goodarzi and R. Aravena, Major Ion and Isotope Geochemistry of Fluids and Gases From Coal Bed Methane and Shallow Groundwater Wells in Alberta, Canada, *Applied Geochemistry*, 2010, **25**, 1307-1329.

I.D. Clark and P. Fritz, *Environmental Isotopes in Hydrogeology*, CRC Press, 1997, 1-328.

D.D. Coleman, Advances in the Use of Geochemical Fingerprinting for Gas Identification, *Isotech Laboratories, Inc.*, at American Gas Association Operations Conference, 1994, 1-10.

T. Considine, R. Watson, R. Entler and J. Sparks, An Emerging Giant: Prospects and Economic Impacts of Developing the Marcellus Shale Natural Gas Play, *Pennsylvania State University*, 2009, 1-39.

H. Craig, Isotopic Variations in Meteoric Waters, *Science*, 1961, **133**, 1702-1703.

R.E. Criss and M.L. Davisson, Isotopic Imaging of Surface Water/Groundwater Interactions, Sacramento Valley, California, *Journal of Hydrology*, 1996, **178**, 205-222.

W. Dansgaard, Stable Isotopes in Precipitation, *Tellus*, 1964, **16**, 436-468.

J. Demchak, J.G. Skousen, P.F. Ziemkiewicz and G. Bryant, Comparison of Water Quality from Fifteen Underground Coal Mines 1968 and 1999, *ICARD*.

DOE and NETL, Modern Shale Gas Development in the United States: A Primer, 2009, 1-116.

J.J. Donovan and B.R. Leavitt, The Future of Mine-Water Discharges from Underground Coal Mines of the Pittsburgh Coal Basin, WV-PA, *National Meeting of the American Society of Mining and Reclamation and the 25th West Virginia Surface Mine Drainage Task Force*, 2004, *ASMR*, 1-11.

J.J. Donovan, B.R. Leavitt and E. Werner, Long-Term Changes in Water Chemistry as a Result of Mine Flooding in Closed Mines of the Pittsburgh Coal Basin, USA, *Calms, QLD*, 2003, 1-7.

A. Dutton, B.H. Wilkinson, J.M. Welker, G.J. Bowen and K.C. Lohmann, Spatial Distribution and Seasonal Variation in $^{18}O/^{16}O$ of Modern Precipitation and River Water Across the Conterminous USA, *Hydrological Processes*, 2005, **19**, 4121-4146.

E&P Focus, NETL, Appalachian Shale Gas, The Energy Lab, *Oil & Natural Gas Program Newsletter*, 2009, 1-20.

S. Eckel, Protecting New York's Air, Land, Water, and People, Citizens Campaign for the Environment, *Citizens Campaign for the Environment*, 2010, 1-20.

Enerdynamics, The Rise of Unconventional Gas, *The Energy Insider*, 2007, 1-4.

I. Friedman and G.I. Smith, Deuterium Content of Snow Cores from Sierra Nevada Area, *Science*, 1970, **169**, 467-470.

P. Fritz, G.M. Basharmal, R.J. Drimmie, J. Ibsen and R.M. Qureshi, Oxygen Isotope Exchange Between Sulphate and Water During Bacterial Reduction of Sulphate, *Chemical Geology*, 1989, **79**, 99-105.

B. Fry, J. Cox, H. Gest and J.M. Hayes, Discrimination Between ^{34}S and ^{32}S During Bacterial

Metabolism of Inorganic Sulfur Compounds, *Journal of Bacteriology*, 1986, **165**, 328-330.

C.H. Gammons, T.E. Duaime, S.R. Parker, S.R., Poulson and P. Kennelly, Geochemistry and Stable Isotope Investigation of Acid Mine Drainage Associated With Abandoned Coal Mines in Central Montana, USA, *Chemical Geology*, 2009, **269**, 100-112.

J.R. Gat, C.J. Bowser, C. Kendall, The Contribution of Evaporation from the Great Lakes to the Continental Atmosphere: Estimate Based on Stable Isotope Data, *Geophysical Research Letters*, 1994, **21**(7), 557-560.

Geologic Units in West Virginia (State in United States), Mineral Resources On-Line Spatial Data, *USGS*, 2012, http://tin.er.usgs.gov/geology/state/fips-unit.php?state=WV

M. Gibson, How Will Marcellus Shale Drilling Impact West Virginia Rivers?, West Virginia Rivers Coalition, *Headwaters*, 2008, **18**, 3-5.

R. Gonfiantini, Environmental Isotopes in Lake Studies, in *Handbook of Environmental Isotope Geochemistry*, ed. P. Fritz, 1986, **2**, pp. 113-168.

K.C. Hackley and T.F. Anderson, Sulfur Isotopic Variations in Low-Sulfur Coals From the Rocky Mountain Region, *Geochimica et Cosmochimica Acta*, 1986, **50**, 1703-1713.

Hazen and Sawyer Environmental Engineers & Scientists, Rapid Impact Assessment Report: Impact Assessment of Natural Gas Production in the New York City Water Supply Watershed, *New York City Department of Environmental Protection*, 2009, 1-87.

L.K Hellings, K. van den Driessche, W. Baeyens, E. Keppens and F. DeHairs, Origin and Fate of Dissolved Inorganic Carbon in Interstitial Waters of Two Freshwater Intertidal Areas: A case study of the Scheldt Estuary, Belguim: *Biogeochemistry*, 2000, **51**, 141–160.

W.J. Herb, L.C. Shaw and D.E. Brown, Hydrology of Area 5, Eastern Coal Province,

Pennsylvania, Maryland, and West Virginia, U.S. Geological Survey Water-Resources Investigations 81-538, 1981, 1-101.

E.R.C. Hornibrook, F.J. Longstaffe and W.S. Fyfe, Spatial Distribution of Microbial Methane Production Pathways in Temperate Zone Wetland Soils: Stable Carbon and Hydrogen Isotope Evidence, *Geochemicica et Cosmochimica Acta*, 1997, **61**, 745-753.

R.J. Hunt, T.B. Coplen, N.L. Haas, D.A. Saad and M.A. Borchardt, Investigating Surface Water-Well Interaction Using Stable Isotope Ratios of Water, *Journal of Hydrology*, 2005, **302**, 154-172.

N. Ingraham, Hydrogen Isotope Study of Large-Scale Meteoric Water Transport in Northern California, *Journal of Hydrology*, 1986, **85**, 183-197.

Intellicast.com: The Authority in Expert Weather, *WSI Corporation*, 2012, http://www.intellicast.com/National/Wind/JetStream.aspx

H. Jiráková, F. Huneau, Z. Hrkal, H. Celle-Jeanton and P. Le Coustumer, Carbon Isotopes to Constrain the Origin and Circulation Pattern of Groundwater in the Northwestern Part of the Bohemian Cretaceous Basin (Czech Republic), *Applied Geochemistry*, 2010, **25**, 265-1279.

I.R. Kaplan, K.O. Emery and S.C. Rittenberg, The Distribution and Isotopic Abundance of Sulphur in Recent Marine Sediments off Southern California, *Geochimica et Cosmochimica Acta*, 1963, **24**(4), 297-331.

C. Kendall and T.B. Coplen, Distribution of Oxygen-18 and Deuterium in River Waters Across the United States, *Hydrological Processes*, 2001, **15**, 1363-1393.

Y.K. Kharaka and F.A.F. Berry, Isotopic Composition of Oil-Field Brines from Kettleman

North Dome, California, and Their Geologic Implications, *Geochimica et Cosmochimica Acta*, 1973, **37**, 1899-1908.

Y.K. Kharaka, and J. J. Thordsen, Stable Isotope Geochemistry and Origin of Waters in Sedimentary Basins, in *Isotope Signatures and Sedimentary Records*, eds. N. Clauer, and S. Chaudouri, 1992, 441-466.

Y. Kim, K-S. Lee, D-C. Koh, D-H. Lee, S.G. Lee, W-B. Park, G-W. Koh and N-C. Woo, *Journal of Hydrology*, 2003, **270**, 282-294.

E.C.P. Kinnon, S.D. Golding, C.J. Boreham, K.A. Baublys and J.S. Esterle, Stable Isotope and Water Quality Analysis of Coal Bed Methane Production Waters and Gases From the Bowen Basin, Australia, *International Journal of Coal Geology*, **82**, 219-231.

D.L. Klass, Methane From Anaerobic Fermentation, *Science*, 1984, **223**, 1021-1028.

M.D. Kozar and M.V. Mathes, Aquifer-Characteristics Data For West Virginia: Water-Resources Investigations Reports 01-4036, *U.S. Geological Society*, 2001, 1-79.

H.R. Krouse and R.G.L. McCready, Biogeochemical Cycling of Sulfur, in *Biogeochemical Cycling of Mineral Forming Elements*, eds. P.A. Trudinger and D.J. Swaine 1979, **1**, 401-425.

H.R. Krouse, F.D. Cook, A. Sasaki and V. Smejkal, Microbial Isotope Fractionation in Springs in Western Canada, in *Recent Developments in Mass Spectrometry*, International Conference on Mass Spectrometry, K. Ogata, and T. Hayakawa, 1970, 629-639.

H.R. Krouse, W.D. Gould, R.G.L. McCready and S. Rajan, (super 18) O Incorporation into Sulphate During the Bacterial Oxidation of Sulphide Minerals and the Potential for Oxygen Isotope Exchange Between O (sub 2), H (sub 2) O and Oxidized Sulphur Intermediates, *Earth and Planetary Science Letters*, 1991, **107**, 90-94.

H.R. Krouse and B. Mayer, Sulphur and Oxygen Isotopes in Sulphate, in *Environmental Tracers in Subsurface Hydrology*, P. Cook and A. L. Herczeg, 2000, **1**, 195-231.

H.R. Krouse, B. Mayer and J.J. Schoneau, Applications of Stable Isotope Techniques to Soil Sulfur Cycling, in *Mass Spectrometry of Soils*, 1996, **1**, 247-284.

L.S. Land and R.S. Fisher, Wilcox sandstone diagenesis, Texas Gulf Coast: a Regional Isotopic Comparison with the Frio Formation, in *Diagenesis of Sedimentary Sequences*: Geological Society Special Publication, 1987, **36**, 219-235.

C.D. Laughrey and F.J. Baldassare, Geochemistry and Origin of Some Natural Gases in the Plateau Province, Central Appalachian Basin, Pennsylvania and Ohio, *AAPG Bulletin*, 1998, **82**, 317-355.

C.D. Laughrey, D.A. Billman and M.R. Canich, Petroleum Geology and Geochemistry of the Council Run Gas Field, North Central Pennsylvania, *AAPG Bulletin*, 2004, **88**(2), 213-239.

D. Lewicka-Szczebak, A. Trojanowska, W. Drzewicki, M. Górka, M-O. Jędrysek, P. Jezierski, M. Kurasiewicz and J. Krajniak, Sources and Sinks of Sulphate Dissolved in Lake Water of a Dam Reservoir: S and O isotopic Approach, *Applied Geochemistry*, 2009, **24**, 1941-1950.

Marcellus Shale, *SM Group, Inc. Engineering and Environmental Services*, 2001-2011, http://ssmgroup.com/marcellusshale.aspx

A.M. Marfia, R.V. Krishnamurthy, E.A. Atekwana and W.F. Panton, Isotopic and Geochemical Evolution of Ground and Surface Waters in a Karst Dominated Geological Setting: A Case Study from Belize, Central America, *Applied Geochemistry*, 2004, **19**, 937-946.

M.V. Machavaram and R.V. Krishnamurthy, Earth Surface Evaporative Process; A Case Study from the Great Lakes Region of the United States Based on Deuterium Excess in Precipitation, *Geochimica et Cosmochimica Acta*, 1995, **20**, 4279-4283.

A.M. Martini, L. M. Walter, J. M. Budai, T. C.W. Ku, C. J. Kaiser and M. Schoell, Genetic and Temporal Relations Between Formation Waters and Biogenic Methane; Upper Devonian Antrim Shale, Michigan Basin, U.S.A., *Geochimica et Cosmochimica Acta*, 1998, **62**(10), 1699–1720.

J.C. McIntosh, A. M. Martini, S. Petsch and K. Nüsslein, Biogeochemistry of the Forest City Basin Coalbed Methane Play, *International Journal of Coal Geology*, 2008, **76**, 111–118.

J.F. McLaughlin, C.D. Frost and S. Sharma, Geochemical Analysis of Atlantic Rim Water, Carbon County, Wyoming: New Applications for Characterizing Coalbed Natural Gas Reservoirs, *AAPG Bulletin*, 2011, 191-217.

L. Merlivat and J. Jouzel, Global Climatic Interpretation of the Deuterium-Oxygen 18 Relationship for Precipitation, *Journal of Geophysical Research*, **84**, 5029-5033.

G.T. Merovich Jr., J.M. Stiles, J.T. Petty, P.J. Ziemkiewicz and J.B. Fulton, Water Chemistry-Based Classification of Streams and Implications for Restoring Mined Appalachian Watersheds, *Environmental Toxicology and Chemistry*, 2007, **26**(7), 1361-1369.

R.C. Milici and C.S. Swezey, Assessment of Appalachian Basin Oil and Gas Resources: Devonian Shale–Middle and Upper Paleozoic Total Petroleum System, *U.S. Geological Survey*: Open-File Report Series 2006-1237, 2006, 1-70.

Y. Mizutani and T.A. Rafter, Isotopic Behaviour of Sulphate Oxygen in the Bacterial Reduction of Sulphate, *Geochemical Journal*, 1973, **6**, 183-191.

L.J. Molofsky, J.A. Connor, S.K. Farhat, A.S. Wylie Jr. and T. Wagner, Methane in

Pennsylvania Water Wells Unrelated to Marcellus Shale Fracturing, *Oil & Gas Journal*, 2011, 1-13.

Monongahela Basin Mine Pool Project, *West Virginia Water Research Institute*, 2000-2004, http://wvwri.nrcce.wvu.edu/programs/mbmpp/index.cfm

W.G. Mook and J.J. de Vries, *Environmental Isotopes in the Hydrological Cycle: Principles and Application*, 2001, **39**(III), 1-121.

A.J. Morris, J.J. Donovan and J.E. Thies, Reconnaissance Spatial Analysis of the Hydrogeology of Closed Underground Coal Mines, *Environmental Geosciences*, 2008, **15**(4), 183-197.

G.F. Olivero, M. Zauli, G.M. Zuppi and T.E. Ricchiuto, Isotopic Composition and Origin of Sulphur Compounds in Groundwaters and Brines in the Po Valley (Northern Italy), *Studies on Sulphur Isotope Variations in Nature; Proceedings of an Advisory Group Meeting on the Hydrology and Geochemistry of Sulphur Isotopes*, 1987, **1**, 49-64

S.G. Osborn, A. Vengosh, N.R. Warner and R.B. Jackson, Methane Contamination of Drinking Water Accompanying Gas-Well Drilling and Hydraulic Fracturing, *PNAS*, 2011, **108**(20), 1-9.

C. Pierre, Sedimentation and Diagenesis in Restricted Marine Basins, in *Handbook of Environmental Isotope Geochemistry*, eds. P. Fritz and J.-Ch. Fontes, 1989, **3**, 257-316.

R.W. Puls and M.J. Barcelona, Low-Flow (Minimal Drawdown) Ground-Water Sampling Procedures, *United States Environmental Protection Agency: Ground Water Issue*, 2006, 8172-8176.

K.M. Révész, K.J. Breen, A.J. Baldassare and R.C. Burruss, Carbon and Hydrogen Isotopic Evidence for the Origin of Combustible Gases in Water-Supply Wells in North-Central Pennsylvania, *Applied Geochemistry*, 2010, **25**, 1845-1859.

K. Révész and H. Qi, Determination of the δ($^{34}S/^{32}S$) of Sulfate in Water: RSIL Lab Code 1951, in *Book 10, Methods of the Reston Stable Isotope Laboratory*, U.S. Geological Survey, eds. K. Révész and T.B. Coplen, 2007, 1-45.

B.J. Rostron and C. Holmden, Fingerprinting Formation-Waters Using Stable Isotopes, Midale Area, Williston Basin, Canada, *Journal of Geochemical Exploration*, 2000, **69-70**, 219-223.

K. Rozanski, L. Araguás-Araguás and R. Gonfiantini, Isotopic Patterns in Modern Global Precipitation, *Geophysical Monograph*, 1993, **78**, 1-36.

L.F. Ruppert and C.L. Rice, Coal Resource Assessment Methodology and Geology of the Northern and Central Appalachian Basin Coal Regions, *U.S. Geological Survey Professional Paper 1625-C*, 2000, 1-23.

R.T. Ryder, R.D. Crangle Jr., M.H. Trippi, C.S. Swezey, E.E. Lentz, E.L. Rowan and R.S. Hope, Geologic Cross Section *D–D'* through the Appalachian Basin from the Findlay Arch, Sandusky County, Ohio, to the Valley and Ridge Province, Hardy County, West Virginia, *U.S. Geological Survey*, Scientific Investigations Map 3067, 2009, 1-60.

R.T. Ryder and W.A. Zagorski, Nature, Origin, and Production Characteristics of the Lower Silurian Regional oil and Gas Accumulation, Central Appalachian Basin, United States, *AAPG Bulletin*, 2003, **87**(5), 847-872.

SAHRA (Sustainability of Semi-Arid Hydrology and Riparian Areas), Oxygen, 2005, http://web.sahra.arizona.edu/programs/isotopes/oxygen.html

M. Schoell, M., The Hydrogen and Carbon Isotopic Composition of Methane from Natural Gases of Various Origins, *Geochemica et Cosmochimica Acta*, 1980, **44**, 649-661.

A.R. Scott, W. R. Kaiser and W. B. Ayers Jr., 1994, Thermogenic and Secondary Biogenic

Gases, San Juan Basin, Colorado and New Mexico: Implications for Coalbed Gas Producibility, *AAPG Bulletin,* 1994, **78**, 1186–1209.

S. Sharma, and C.D. Frost, Tracing Coalbed Natural Gas-Coproduced Water Using Stable Isotopes of Carbon, *Ground Water*, 2008, **46**, 329-334.

S. Sharma and J.K. Baggett, Application of Carbon Isotopes to Detect Seepage out of Coalbed Natural Gas Produced Water Impoundments, *Applied Geochemistry*, 2011, 1-10.

Q. Shengfei, T. Xiuyi, S. Yan, S and W. Hongyan, Distribution and Fractionation Mechanism of Stable Carbon Isotope of Coalbed Methane, *Science in China Series D: Earth Science*, 2006, **49**(12), 1252-1258.

W.W. Simpkins and T.B. Parkin, Hydrogeology and Redox Geochemistry of CH_4 in a Late Wisconsinan Till and Loess Sequence in Central Iowa, *Water Resources Research*, 1993, **29**(11), 3643-3657.

J.W. Smith and B.D. Batts, The Distribution and Isotopic Composition of Sulfur in Coal, *Geochimica et Cosmochimica Acta*, 1974, **38**, 121-133.

D.J. Soeder and W.M. Kappel, Water Resources and Natural Gas Production from the Marcellus Shale, *U.S. Geological Survey: Fact Sheet 2009-3032*, 2009, 1-6.

B.E. Taylor and M.C. Wheeler, Isotope Composition of Sulphate in Acid Mine Drainage as Measure of Bacterial Oxidation, *Nature*, 1984, **308**, 538-541.

L. Toran and R.F. Harris, Interpretation of Sulfur and Oxygen Isotopes in Biological and Abiological Sulfide Oxidation, *Geochimica et Cosmochimica Acta*, 1989, **53**, 2341-2348.

M.E. Torres, A.C. Mix and W.D. Rugh, Precise $\delta^{13}C$ Analysis of Dissolved Inorganic Carbon in Natural Waters Using Automated Headspace Sampling and Continuous-Flow Mass Spectrometry, *Limnology and Oceanography: Methods*, 2005, **3**, 349-360.

A. Trembaczowski, J. Szaran and H. Niezgoda, Investigating the Provenance and Seasonal Variations in Sulphate Sulphur and Oxygen Isotopes of Central Roztocze River Water, SE Poland, Water, Air, and Soil Pollution, 2004, **157**, 65-84.

R. Trettin, K. Knoller, H.H. Loosli and P. Kowski, Evaluation of the Sulfate Dynamics in Groundwater by Means of Environmental Isotopes, *Isotopes Environ. Health Stud.*, 2002, **38**, 103-119.

S.O. Tweed, T.R. Weaver and I. Cartwright, Distinguishing Groundwater Flow Paths in Different Fractured-Rock Aquifers Using Groundwater Chemistry: Dandenong Ranges, Southeast Australia, Hydrogeology Journal, 2005, **13**, 771-786.

C.V. Van Donkelaar, I.E. Hutcheon and H.R. Krouse, $\delta^{34}S$, $\delta^{18}O$, δD in Shallow Groundwater: Tracing Anthropogenic Sulfate and Accompanying Groundwater/Rock Interactions, *Water, Air, and Soil Pollution*, 1995, **79**, 279-298.

H.R. Van Everdingen and H.R. Krouse, Isotope Composition of Sulphates Generated by Bacterial and Abiological Oxidation, *Nature*, 1985, 315, 395-396.

D.R. Van Stempvoort and H.R. Krouse, Controls of $\delta^{18}O$ in Sulfate, in *Environmental Geochemistry of Sulfide Oxidation*, eds. C.N. Alpers and D.W. Blowes, 1994, 446-480.

D.J. Vesper and M.J. Smilley, Attenuation and Diel Cycling of Coal-Mine Drainage Constituents in a Passive Treatment Wetland: A Case Study from Lambert Run, West Virginia, USA, *Applied Geochemistry*, 2010, **23**(6), 795-808.

J.C. Vogel, Variability of carbon isotope fractionation during photosynthesis, in *Stable Isotopes and Plant Carbon – Water Relations*, eds. J.R. Ehleringer, A.E. Hall and G.D. Farquhar, G.D., 1993, 29-38.

D.A. Wiesenburg and N.L. Guinasso, Jr., Equilibrium Solubilities of Methane, Carbon

Monoxide, and Hydrogen in Water and Sea Water, *Journal of Chemical and Engineering Data*, 1979, **24**(4), 356-360.

R.T. Weston, Development of the Marcellus shale – Water Resource Challenges, *Kirkpatrick & Lockhart Preston Gates Ellis LLP*, 2008, 1-21.

J.S. White and M.V. Mathes, Dissolved-Gas Concentrations in Ground Water in West Virginia, 1997-2005, *U.S. Geological Survey, Data Series 156*, 2006, 1-14.

M.J. Whiticar, Carbon and Hydrogen Isotope Systematic of Bacterial Formation and Oxidation of Methane, *Chemical Geology*, 1999, **161**, 291-314.

M.J. Whiticar, E. Faber and M. Schoell, Biogenic Methane Formation in Marine and Freshwater Environments: CO_2 Reduction vs. Acetate Fermentation – Isotope Evidence, *Geochimica et Cosmochimica Acta*, 1986, **50**(5), 693-709.

M.B. Wittrup, T.K. Kyser and T. Danyluk, The Use of Stable Isotopes to Determine the Sources of Brines in Saskatchewan Potash Mines, *Economic Minerals of Saskatchewan*, 1987, 159-165.

T. Zhang and B.M. Krooss, Experimental Investigation on the Carbon Isotope Fractionation of Methane During Gas Migration by Diffusion through Sedimentary Rocks at Elevated Temperature and Pressure, *Geochimica et Cosmochimica Acta*, 2001, **65**, 2723-2742.